GLYCOSYLATION, ASSEMBLY AND TRAFFICKING OF CARDIAC POTASSIUM CHANNEL COMPLEXES

A Dissertation Presented

By

KSHAMA CHANDRASEKHAR

Submitted to the Faculty of the
University of Massachusetts Graduate School of Biomedical Sciences, Worcester
in partial fulfillment of the requirements for the degree of

DOCTOR OF PHILOSOPHY

May 7th 2010

BIOCHEMISTRY AND MOLECULAR PHARMACOLOGY

GLYCOSYLATION, ASSEMBLY AND TRAFFICKING OF CARDIAC POTASSIUM CHANNEL COMPLEXES

A Dissertation Presented

By

KSHAMA CHANDRASEKHAR

The signatures of the Dissertation Defense Committee signifies completion and approval as to style and content of the Dissertation

William R. Kobertz, Ph.D., Thesis Advisor

Carol J. Deutsch, Ph.D., Member of Committee

Haley E. Melikian, Ph.D., Member of Committee

Mary Munson, Ph.D., Member of Committee

Fumihiko Urano, M.D., Ph.D., Member of Committee

The signature of the Chair of the Committee signifies that the written dissertation meets the requirements of the Dissertation Committee.

Reid Gilmore, Ph.D., Chair of Committee

The signature of the Dean of the Graduate School of Biomedical Sciences signifies that the student has met all graduation requirements of the school.

Anthony Carruthers, Ph.D.
Dean of the Graduate School of Biomedical Sciences

Program in Biochemistry and Molecular Pharmacology
May 7th 2010

DEDICATIONS

This thesis work is dedicated to my mom – the strongest and most positive influence in my life. Thank you for everything you have done to make me the person I am today!

ACKNOWLEDGMENTS

Through the course of graduate school, I have been very fortunate to have a solid support system that made the journey both pleasant and relatively stress-free. Many of you have touched my life in a way I cannot possibly find the words to express. So hopefully I can convey that gratitude in these acknowledgments.

To my mentor, Bill Kobertz - Thank you for taking a chance on me oh-so-many years ago with a novel project that _channeled' your lab research into a new direction. I will always value the freedom for independent thinking and the support, inspiration and constant encouragement that you have given me through the years to grow and develop as a scientist. I have enjoyed every moment I have spent learning from you! A heartfelt thank you for all you have done for me.

To my Thesis Committee – thank you for your support and guidance over the years. I'm grateful for the encouragement to persevere when projects failed and the enthusiasm when the going was good. You have all helped make me a better scientist.

To all my lab mates, past and present – thank you for being there every single day! I appreciate all the discussions, scientific and otherwise that have made working with each of you such a wonderful experience.

In particular, Karen Mruk – you have been a wonderful resource with your wealth of scientific knowledge. I am very grateful for all the advice and encouragement and of course, you are a saint for editing this manuscript! Thank you for being a very important

part of my learning process in grad school. And of course, I will never forget Friday lab dance parties!

Dr. Steve Gage – your tireless efforts were an inspiration during your time in the lab. Thank you for all the scientific advice and support over the years. And of course, thank you for the time and effort in editing this manuscript. You are a gem of a friend.

Dr. Anatoli Lvov – your Adobe Illustrator ® skills are beyond compare! I aspire to make pretty figures like the ones you constantly delight us with in your presentations. Thank you for being an integral part of my projects and bringing your electrophysiological expertise to two of my projects. You are an extraordinary scientist and I am so happy to have worked with you!

My ‗hot' lab mates, Yuan Gao and Tuba Bas - I will never forget our elegantly coordinated pulse chase experiments! Yuan, thank you for all your help with biochemistry, generating constructs, and making sure that the lab had all the necessary stocks to keep running smoothly; Tuba, it has been a pleasure working with you. I've learned as much from you as you have from me. Thanks for being a great friend and colleague!

Haley Melikian and her lab – thank you for all your enthusiastic advice and help for the immunofluorescence and cell surface biotinylation experiments and the use of your microscope.

And last but certainly not the least, my family, spread over many countries. Graduate school is a huge emotional investment and you have always been there for me.

Your love, support and prayers have seen me through the best and worst of times. I am a better person today with your guidance and love. I hope I have made you all proud!

THESIS ABSTRACT

KCNE peptides are a class of type I transmembrane β-subunits that assemble with and modulate the gating and ion conducting properties of a variety of voltage-gated K^+ channels. Accordingly, mutations that affect the assembly and trafficking of K^+ channel/KCNE complexes give rise to disease. The cellular mechanisms that oversee KCNE peptide assembly with voltage-gated K^+ channels have yet to be elucidated. In Chapter II, we show that KCNE1 peptides are retained in the early stages of the secretory pathway until they co-assemble with KCNQ1 K^+ channel subunits. Co-assembly with KCNQ1 channel subunits mediates efficient forward trafficking of KCNE1 peptides through the biosynthetic pathway and results in cell surface expression.

KCNE1 peptides possess two N-linked glycosylation sites on their extracellular N-termini. Progression of KCNE1 peptides through the secretory pathway can be visualized through maturation of N-glycans attached to KCNE1. In Chapter III, we examine the kinetics and efficiency of N-linked glycan addition to KCNE1 peptides. Mutations that prevent glycosylation of KCNE1 give rise to the disorders of arrhythmia and deafness. We show that KCNE1 acquires N-glycans co- and post-translationally. Mutations that prevent N-glycosylation at the co-translational site have a long range effect on the disruption of post-translational glycosylation and suggest a novel biogenic mechanism for disease.

In Chapter IV, we determine the presence of an additional post-translational modification on KCNE1 peptides. We define specific residues as sites of attachment of this modification identified as sialylated O-glycans and show that it occurs in native cardiac tissues where KCNE1 plays a role in the maintenance of cardiac rhythm.

Taken together, these observations demonstrate the importance of having correctly assembled K^+ channel/KCNE complexes at the cell surface for their proper physiological function and define a role for the posttranslational modifications of KCNE peptides in the proper assembly and trafficking of K^+ channel/KCNE complexes.

TABLE OF CONTENTS

LIST OF TABLES

LIST OF FIGURES

LIST OF ABBREVIATIONS

α-subunit	pore-forming subunit
β-subunit	accessory subunit
E1, E2, E3, E4, E5	KCNE1, KCNE2, KCNE3, KCNE4, KCNE5
EKG	electrocardiogram
ER	endoplasmic reticulum
HA	hemagglutinin A
hERG	voltage-gated potassium channel, subfamily H (eag-related)
I_{Ks}	delayed rectifying cardiac potassium current
I_{Kr}	rapid cardiac potassium current
I_{to}	transient outward potassium current
JLNS	Jervell and Lange-Nielsen syndrome
K^+	potassium
K_v channel	voltage-gated potassium channel
LQTS	long QT syndrome
N-glycosylation	asparagine-linked glycosylation
N-terminal	amino-terminal
O-glycosylation	threonine- or serine-linked glycosylation
Q1	KCNQ1 voltage-gated potassium channel
RWS	Romano-Ward syndrome
TM	transmembrane domain
WT	wild-type

PREFACE

The work presented in Chapter II has been published in a peer-reviewed journal (Chandrasekhar et al. 2006). Tuba Bas generated the C-terminal HA-tagged construct of KCNE1 that was used in the whole cell immunofluorescence studies examining intracellular localization of KCNE1 peptides.

The experimental work in Chapter III has been written up as a manuscript for publication at the time of this thesis preparation. I performed the initial biochemical investigation to determine the contribution of N-linked glycosylation on the stability and expression of KCNE1 peptides. I examined protein expression and stability of several glycosylation-deficient mutations of KCNE1, in particular T7I that is associated with Long QT syndrome presentation. Chapter III describes the elegant kinetic studies of N-linked glycosylation of KCNE1 peptides executed by Tuba Bas that were based on my preliminary biochemical observations. Tuba Bas is credited with first authorship on the manuscript for her significant work characterizing the process of N-glycosylation of KCNE1 and describing a novel mechanism for the biogenesis of Long QT syndrome. Authorship is also credited to Dr. Anatoli Lvov for the electrophysiological characterizations of the N-glycosylation deficient mutant E1 peptides.

In Chapter IV, the electrophysiological studies investigating the contribution of KCNE1 O-glycans to the function of KCNQ1/KCNE1 channel complexes were performed by Dr. Anatoli Lvov.

CHAPTER I

INTRODUCTION

Potassium channels are involved in many functional aspects of human physiology in excitable and non-excitable cells – from the maintenance of cardiac rhythm, to salt-water homeostasis in epithelial tissues, to neuronal action potential repolarization. The breadth of biological K^+ channel function stems from the diversity of K^+ channel complexes which is further increased by the association of channel subunits with soluble and transmembrane accessory proteins that modulate channel function.

Since a gene encoding a K_v channel was first cloned from Drosophila *Shaker* (Papazian et al. 1987; Tempel et al. 1987), over 40 voltage gated K^+ (K_v) channels have been identified and studied extensively (Wulff et al. 2009). The *Shaker*-like channels have similar structural characteristics to *Shaker* and include the KCNQ family, hERG, the *Shaker*-related channels and Ca^{2+}-activated K^+ channels. The channels assemble as tetramers to generate the ion-conducting pore subunit of a K^+ channel (MacKinnon 1991). Each channel monomer is composed of six transmembrane-spanning α-helices (S1-S6) with the voltage-sensing domain located in helices S1-S4 and the pore domain situated in S5-S6 with a pore loop (P-loop) between helices S5 and S6 (Fig. 1.1).

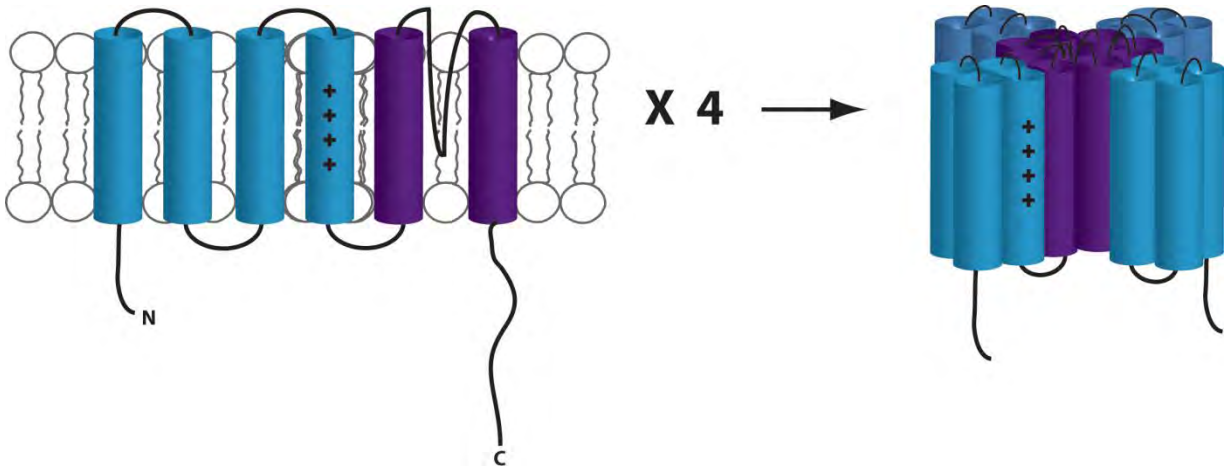

Figure 1.1 Cartoon representation of a *Shaker*-like K^+ channel, KCNQ1. **Left**, schematic of *Shaker*-like K^+ channel KCNQ1 based on the canonical transmembrane structure of a single *Shaker* subunit as viewed through the plane of the plasma membrane. The S1-S4 helices constitute the voltage sensing domain indicated in light blue. The S5 and S6 helices connected with the pore loop make up the pore domain of the channel (purple). The N- and C-termini are shown as facing the intracellular cytoplasm. **Right**, schematic of tetrameric assembly of KCNQ1 K^+ channel monomers to generate the pore-forming subunit of the K^+ channel.

Schematic generated by K. Mruk.

KCNQ K^+ channels

The gene for one *Shaker*-like channel, KCNQ1 (Q1), was identified by positional cloning of locus 11p15.5 on chromosome 11 from a family of individuals exhibiting the phenotype of elongated QT intervals on recorded EKGs and fainting episodes related to ventricular fibrillations (Wang et al. 1996). The KCNQ channel family was established with the discovery of KCNQ2-5 (Q2-Q5) channels (Charlier et al. 1998; Singh et al. 1998; Wang et al. 1998; Yang et al. 1998; Kubisch et al. 1999; Lerche et al. 2000; Schroeder et al. 2000). Q1 channels are distributed throughout the body but are absent in the nervous system where Q2-Q5 are predominantly localized (Cooper and Jan 2003). Q2-Q5 channel subunits can assemble as homo- or heteromeric K^+ channels (Schroeder et al. 1998; Wang et al. 1998; Kubisch et al. 1999; Schroeder et al. 2000; Bal et al. 2008).

On the other hand, Q1 subunits assemble only as a homotetramer forming rapidly activating K^+ channels that achieve maximal conductance but also undergo channel inactivation in short periods of time (Barhanin et al. 1996; Sanguinetti et al. 1996; Pusch et al. 1998). Q1 currents have never been observed in native tissues such as cardiac myocytes and the epithelial cells of the lung, stomach, cochlea, intestine and kidney (Jespersen et al. 2005). *In vivo*, Q1 associates with small regulatory accessory proteins (β-subunits) of the KCNE family to generate the β-subunit specific current characteristics that are observed physiologically (Barhanin et al. 1996; Sanguinetti et al. 1996; Schroeder et al. 2000; Tinel et al. 2000; Angelo et al. 2002; Grunnet et al. 2002).

KCNE peptides

The KCNE peptides are a β-subunit family of small type I single-transmembrane spanning proteins with an extracellular N-terminus. KCNE1 (E1) was the first cloned member of this family and had initially been assumed to be the K^+ channel responsible for the cardiac delayed rectifier current (I_{Ks}) based on observations in *Xenopus* oocytes where injection of E1 RNA gave rise to I_{Ks}-like currents (Takumi et al. 1988). It was after the discovery of Q1 as the ion-conducting subunit of the I_{Ks} channel that E1 was designated the role of an accessory subunit in the I_{Ks} channel complex. Association of Q1 with E1 alters the biophysical properties of the Q1 channel resulting in an increase in macroscopic current amplitude and slowed channel activation with a loss of channel inactivation (Barhanin et al. 1996; Sanguinetti et al. 1996; Splawski et al. 1997) (Fig. 1.2). These characteristic biophysical properties of the Q1/E1 K^+ channel complex are crucial to its role in cardiac myocytes where Q1/E1 channels generate I_{Ks} current for the repolarization of the action potential and in the inner ear where Q1/E1 complexes are involved in the regulation of salt-water homeostasis (Barhanin et al. 1996; Sanguinetti et al. 1996; Vetter et al. 1996; Lee et al. 2000; Wangemann 2002).

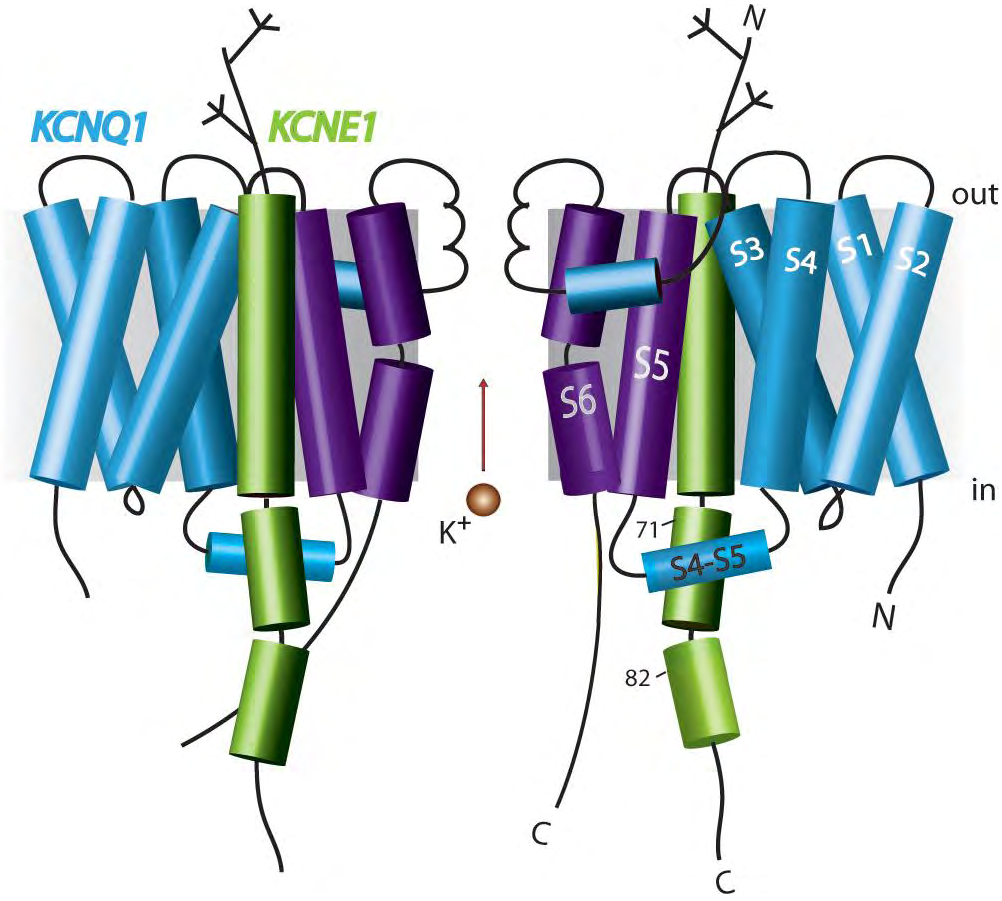
KCNQ1
KCNE1
N
out
S3
S4
S1
S2
S5
S6
in
K+
71
S4-S5
N
82
C
C

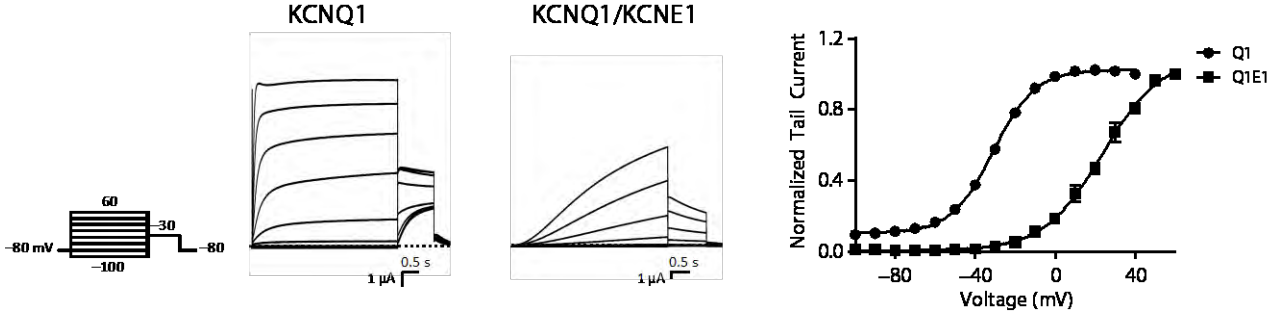
KCNQ1
KCNQ1/KCNE1
60
30
-80 mV
-80
-100
0.5 s
1 µA
0.5 s
1 µA
Normalized Tail Current
1.2
0.8
0.4
0.0
-80
-40
0
40
Voltage (mV)
Q1
Q1E1

Figure 1.2 KCNQ1/KCNE1 channel complex. Transmembrane topology diagram of the KCNQ1/KCNE1 channel complex. For clarity, only two subunits of the Q1 tetramer are shown. Voltage-sensing and pore-forming domains, are colored cyan and purple, respectively; E1 is colored green. Extracellular and intracellular faces of the membrane are indicated as _out' and _in'. KCNQ1 helices are numbered S1-S6 with the C-terminal S4-S5 linker shown interacting with a C-terminal helix of KCNE1. Branched structures on KCNE1 N-terminus indicate positions of N-glycan attachments. K^+ flow (brown) denotes location of ion conducting pore within the fully assembled complex. Stoichiometry of the fully assembled complex is 4 KCNQ1 monomers with 2 KCNE1 peptides. **Bottom**, families of currents recorded from *Xenopus* oocytes expressing KCNQ1 channels alone or KCNQ1/ KCNE1 channel complexes. Currents were elicited by a pulse protocol of 4 s step test potentials from –80 to +60 mV in 10 mV increments from a holding potential of –80 mV followed by a tail pulse to –30 mV (**left**). Dashed line indicates zero current. Scale bars represent 1 μA and 0.5 s. KCNQ1 channels undergo rapid activation and inactivation in the time period shown. KCNQ1/KCNE1 channel complexes are slowly activating with increasing amounts of current conducted over time. The I/V curve illustrates a right shift in voltage activation of KCNQ1 upon association with KCNE1 (**right**).

Schematic adapted with permission from Lvov, A., Gage, S.D., Berrios, V.M. and Kobertz, W.R., *Identification of a protein-protein interaction between KCNE1 and the activation gate machinery of KCNQ1*. J. Gen. Physiol., 2010. **135**(6): 607.

Current traces adapted with permission from Mruk , K. and Kobertz, W.R., *Discovery of a novel activator of KCNQ1/KCNE1 K^+ channel complexes.* PLoS ONE, 2009. **4**(1): e4236.

Cardiac action potential

The propagation of an action potential in cardiac myocytes requires the exquisite interplay between numerous Na^+, Ca^{2+} and K^+ channels. The timing and duration of the cardiac action potential is tightly regulated resulting in rapid depolarization and slow repolarization of cardiac myocytes (Roden et al. 2002). The length of an action potential is on the order of ~200-300 milliseconds, a necessary delay that allows for the normal excitation-contraction phase in myocytes and renders them insensitive to premature excitatory signals. K^+ conducting channels such as Q1 and hERG generate I_{Ks} and I_{Kr} currents respectively and are involved in the long ventricular repolarization phase which allows for the re-equilibration of myocytes to their resting potentials in preparation for the next action potential depolarization (Fig. 1.3). A prolongation or delay in the ventricular repolarization phase is associated with a class of inherited genetic disorders, the Long QT syndromes (LQTS). This delay is measured as an elongation in the QT interval on an EKG, and leads to early-after-depolarizations that can trigger syncopal attacks and ventricular tachycardia causing arrhythmias and sudden death (Ackerman and Clapham 1997; Sanguinetti and Spector 1997; Chiang and Roden 2000). Congenital LQTS is associated with mutations in a variety of ion channels that affect their normal functioning and is characterized as LQT1 through LQT6 based on the ion channel genes involved. Mutations in the Q1 channel and E1 peptides that reduce channel current are associated with LQT1 and LQT5, respectively.

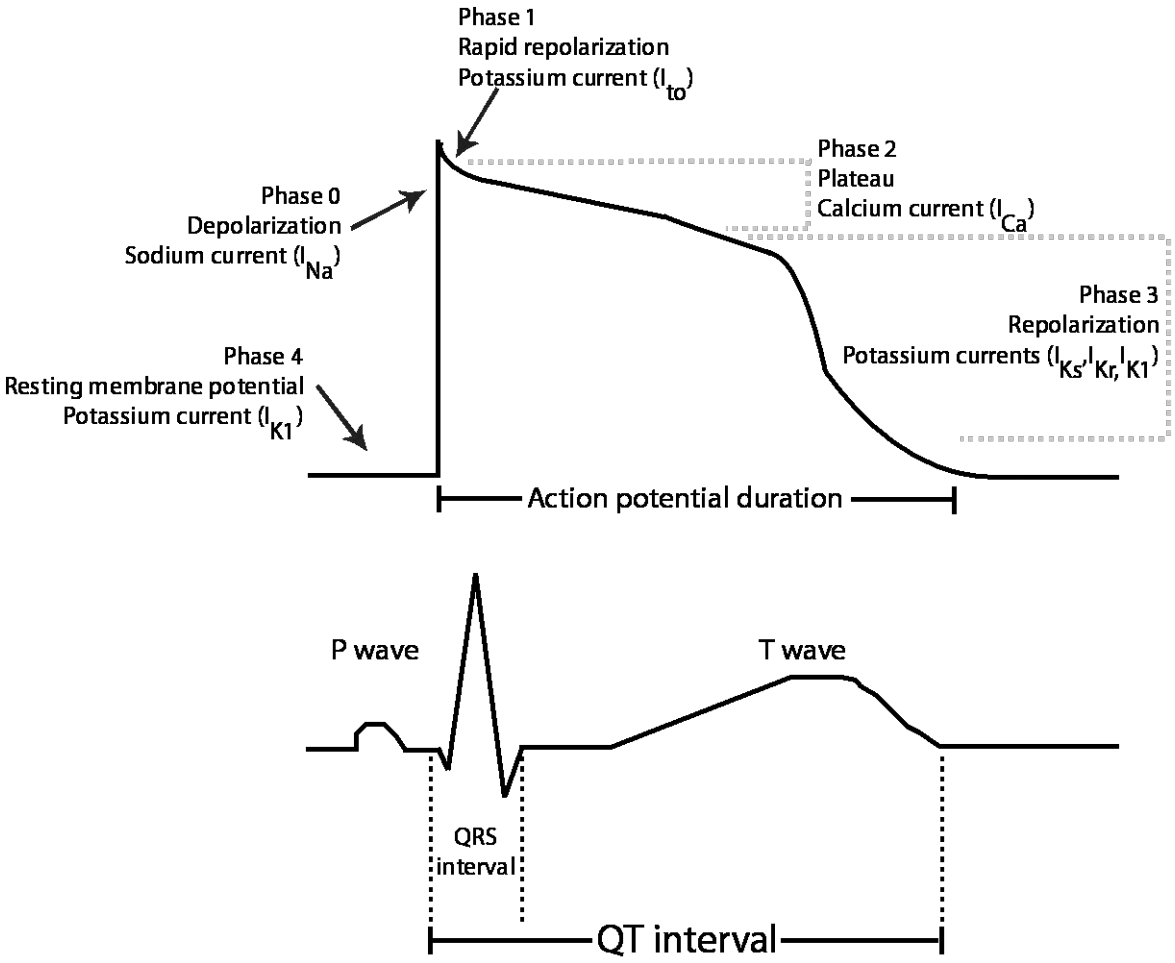

Figure 1.3 Cardiac action potential. Above, depiction of a cardiac action potential and the ion channel currents associated with each phase. **Below**, schematic representation of surface electrocardiogram (EKG) of the electrical events occurring within the heart. The P wave reflects atrial depolarization, the QRS complex reflects ventricular depolarization and the T wave is indicative of ventricular repolarization. Elongation of the QT interval is associated with Long QT syndrome.

Schematic generated by K. Chandrasekhar.

The autosomal dominant form is known as Romano-Ward syndrome (RWS) and results from nonfunctional mutant channels inhibiting their wild type subunit counterparts from normal alleles resulting in severe cardiac dysfunction (Romano et al. 1963; Ward 1964; Chouabe et al. 1997; Sanguinetti 1999; Hoppe et al. 2001). The autosomal recessive disease is Jervell and Lange-Nielsen syndrome (JLNS), which in its homozygous form displays both cardiac dysfunction and bilateral deafness (Jervell and Lange-Nielsen 1957; Neyroud et al. 1997; Schulze-Bahr et al. 1997; Splawski et al. 1997; Splawski et al. 2000).

Biophysical characterization of genetic mutations in either member of the Q1/E1 channel complex reveals mechanisms by which LQTS occurs. For example, S74L, D76N, V47F and W87R are mutations identified in E1 that cause RWS (Schulze-Bahr et al. 1997; Splawski et al. 1997; Duggal et al. 1998). S47L co-assembles with Q1 channels to form I_{Ks}-generating channels with altered biophysical properties. The S74L mutation results in a right shift of the midpoint of activation and increases the rate of channel deactivation. Co-expression of Q1 with D76N mutant E1 produces non-conducting channel complexes as the presence of one mutant peptide in the channel complex is sufficient to disrupt normal function (Splawski et al. 1997). V47F and W87R result in decreased current amplitude and an alteration of the gating kinetics of the Q1/E1 channel complex (Bianchi et al. 1999).

While biophysical data give us a handle on how LQTS-associated mutations affect channel function, biochemical characterization is also used to determine whether

current reduction is a result of improper biosynthetic processing of the Q1/E1 channel complex. For example, L51H is a JLNS-associated mutation in the transmembrane domain of E1 (Bianchi et al. 1999; Krumerman et al. 2004). In the *Xenopus* oocyte expression system, Q1/L51H E1 complexes did not produce Q1/E1-like currents (Bianchi et al. 1999). In human embryonic kidney (HEK) 293 cells, immunofluorescence staining of L51H in the absence or presence of Q1 channels revealed that L51H E1 peptides were largely retained in the endoplasmic reticulum (ER) and did not traffic to the cell surface (Krumerman et al. 2004). Additionally, currents produced by the co-expression of Q1 with L51H E1 were biophysically similar to Q1 channels expressed alone suggesting impaired assembly of the channel complex (Bianchi et al. 1999; Krumerman et al. 2004). Other RWS and JLNS-associated mutations have been identified by the genetic screening of LQTS-affected families but have yet to be characterized biochemically or functionally (Splawski et al. 2000; Ackerman et al. 2003; Lai et al. 2005; Napolitano et al. 2005; Shim et al. 2005).

K^+ ion homeostasis in the inner ear

The endolymph of the inner ear is an extracellular fluid where the predominant cationic species are K^+ ions involved in sensory transduction of the cochlea and the vestibular labyrinth (Fig. 1.4). Sensory transduction requires the flow of K^+ ions from the endolymph into the perilymph and back. This cyclical process maintains the high K^+ ion concentration in the endolymph. Q1 co-assembles with E1 in the stria vascularis to form

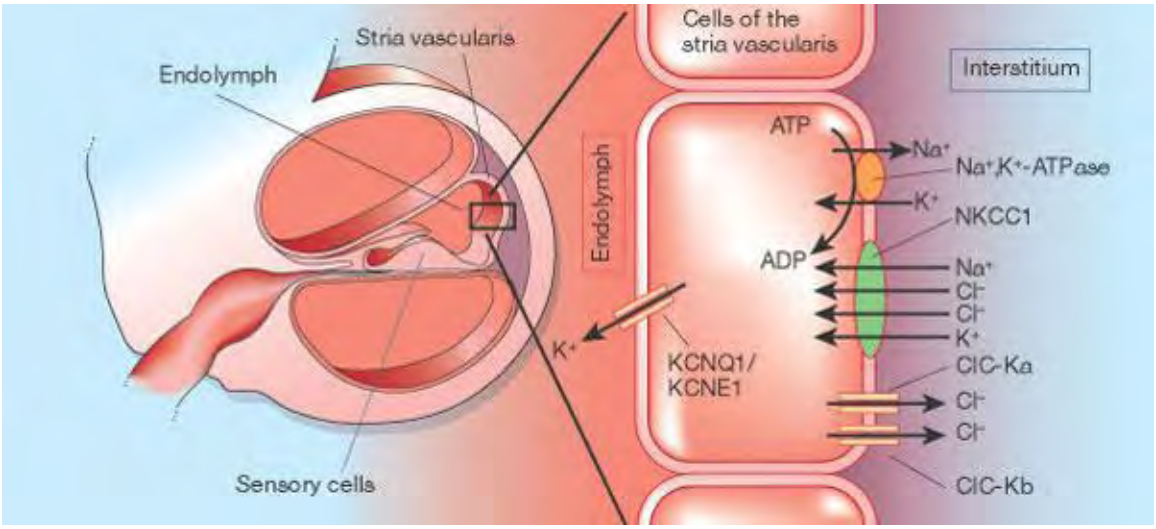

Figure 1.4 Ion transport in the inner ear. The balance of activities of various ion channels and ion transporters in the inner ear. The KCNQ1/KCNE1 K^+ channel complex located in the stria vascularis cells provides the sole pathway for the transport of K^+ ions to the endolymph fluid. K^+ ion homeostasis in the endolymph is necessary for sensory transduction.

Figure and figure legend adapted from Hunter, M., *Ion channels: Accessory to kidney disease.* Nature, 2001. **414** p. 502-503

K^+ channels responsible for the reabsorption of K^+ ions to the endolymph in the inner ear (Neyroud et al. 1997; Nicolas et al. 2001; Wangemann 2002).

The importance of the Q1/E1 channel complex in inner ear K^+ ion homeostasis was demonstrated in genetically altered mice that were lacking either Q1 or E1 protein, or carrying mutations in one or both proteins. In *kcne (-/-)* knockout mice, the endolymphatic space appears normal early in development. However, at postnatal day 3, gross morphological changes are apparent with an increase in size of the vestibular cells and collapse of the endolymphatic space because of an inability of the strial marginal cells to recycle K^+ ions to the endolymph (Nicolas et al. 2001). As a result, the *kcne (-/-)* knockout mice as well as mice expressing mutant Q1 or E1 showed severe symptoms of deafness (Vetter et al. 1996; Lee et al. 2000; Letts et al. 2000; Casimiro et al. 2001). Additionally, it was observed that in the vestibular dark cells of *kcne (-/-)* mice, Q1 protein was mislocalized to the cytoplasm rather than trafficking to the appropriate apical surface (Nicolas et al. 2001). Hence, the assembly of Q1 with E1 is necessary for the correct cellular trafficking and proper functioning of the channel complex in native cells.

Assembly of KCNQ1/KCNE channel complexes

Trafficking-deficient mutations associated with LQTS have been identified in both Q1 and the KCNEs (Bianchi et al. 1999; Yamashita et al. 2001; Gouas et al. 2004; Krumerman et al. 2004; Wilson et al. 2005; Harmer et al. 2010), highlighting the role of cellular quality control mechanisms in ensuring that correctly assembled channel complexes migrate to the plasma membrane. There are two cellular locations where Q1/KCNE co-assembly was proposed to be mediated – the plasma membrane and the ER. The plasma membrane-based assembly of Q1/KCNE channels was hypothesized by Grunnet et al. based on observations where injection of KCNE4 (E4) mRNA into oocytes expressing Q1 channels mediated a measureable change in recorded currents as a result of association of E4 peptides with Q1 channels already present at the plasma membrane (Grunnet et al. 2002). Additionally, the cellular distribution of Q1 channels in the presence and absence of KCNE peptides was determined by immunofluorescent labeling. Since the lifetimes of the cell surface expressed Q1/KCNE channel complexes were not measured in this study, it is also possible that channel complex turnover at the cell surface contributed to the observed current changes.

The ER-based assembly of Q1/E1 channel complexes was proposed by the observation that immature glycosylated E1 peptides associated with Q1 (Krumerman et al. 2004). In this study, the ER-retention and trafficking of E1 mutant peptides was biochemically characterized in HEK cells. HEK cells are a useful over-expression system for the biochemical characterization of various proteins. However, HEK cells have been

shown to contain endogenous K_v channels (Jiang et al. 2002) that can associate with E1 peptides (Lewis et al. 2004). Hence, HEK cells are not a good system in which to study E1 trafficking. Additionally, the detection of unglycosylated E1 on the cell surface in this study does not clearly show how Q1/E1 complex formation is regulated within cells. Nonetheless, the ER-based assembly hypothesis did signify the importance of regulation of Q1/E1 complex formation early in the biosynthetic pathway. Since unpartnered Q1 channels cannot generate the appropriate currents for I_{Ks} and K^+ ion recycling in the inner ear, correct Q1/E1 complex formation is necessary for their proper channel function in native cells.

The subunit stoichiometry between Q1 channels and E1 peptides has been subject to debate over the years. Q1 and E1 subunit mixing experiments suggested a two-fold or four-fold symmetry of subunit assembly with either 2 or 4 E1 peptides associating with 4 subunits of the Q1 channel (Wang and Goldstein 1995). In whole cell patch recordings, Q1 channel modulation was altered as a function of increasing concentrations of E1 suggesting that multiple stoichiometries for Q1/E1 assembly were possible (Wang et al. 1998). More recently, the charybdotoxin sensitivity of naturally assembled Q1/E1 channel complexes was compared to concatenated Q1/E1 counterparts of forced stoichiometries (Chen et al. 2003). This study determined that 2 E1 subunits assembled with a Q1 tetramer to form functional K^+ channel complexes. However, the possibility of multiple stoichiometries could not be ruled out. The use of a chemically modified charybdotoxin K^+ channel inhibitor confirmed that only 2 E1 subunits associated with 4 Q1 subunits to generate a functional Q1/E1 channel complex (Morin and Kobertz 2008).

The exact order of subunit association in the Q1/E1 channel complex and the cellular mechanisms that regulate the assembly process in native tissues are yet to be determined.

The process of Q1/E1 assembly in commonly used over-expression systems like *Xenopus* oocytes, HEK, Chinese hamster ovary (CHO) and African green monkey kidney (COS-7) cells is not tightly regulated for unpartnered Q1 channels. Homotetrameric Q1 channels can traffic efficiently and function at the cell surface in the absence of a KCNE partner (Pusch et al. 1998; Tinel et al. 2000; Melman et al. 2001). In *Xenopus* oocytes, Q1 mutants containing the R243C and W248R substitutions in the S4-S5 linker region form functional channels when expressed alone; however co-expression of these mutant Q1 channels with wild type E1 peptides suppressed current (Franqueza et al. 1999). Since E1 subunits are believed to associate closely with the S4-S5 linker region (Kang et al. 2008), it is possible that the loss of function observed on mutant Q1 assembly with E1 peptides was caused by the aberrant trafficking of improperly assembled channel complexes. However, in native cell types, Q1/KCNE complex assembly appears to be regulated. In *kcne1 (-/-)* mice, the apical localization of Q1 in the vestibular dark cells of the inner ear is disrupted in the absence of E1 protein (Nicolas et al. 2001).

The regulation of E1 trafficking is not well understood because the presence of endogenous K^+ channels in some heterologous systems muddles the interpretation of biochemical and electrophysiological studies of LQTS-associated E1 mutants (Bianchi et al. 1999; Krumerman et al. 2004). In Chapter II, we attempt to resolve this issue by

comparing the trafficking of solitary and channel-partnered E1 peptides in a panel of over-expression systems typically used in the field.

Glycosylation of KCNE peptides

The KCNE family of peptides exhibits a high degree of sequence homology, with one or more putative N-linked glycosylation consensus sites in the N-terminal region of the peptides (Fig. 1.5). The positioning of the N-linked glycosylation sites in the KCNE family are conserved in various species, in particular the site in close proximity to the N-terminus. Genetic analysis of a family exhibiting LQTS symptoms revealed a T7I mutation in E1 that is associated with JLNS (Schulze-Bahr et al. 1997). The T7I amino acid substitution prevents the addition of N-glycans to the N5 site in the consensus sequence (N-T-T). Similarly, a single nucleotide polymorphism in KCNE2 that results in the T8A mutation prevents N-glycosylation at N6 and is associated with drug-induced LQTS (Larsen et al. 2001; Lu et al. 2003). Functional effects of the removal of N-linked glycosylation sites on E1 peptides has been shown in *Xenopus* oocytes as an abolishment in channel activity (Takumi et al. 1991). In spite of these observations, the exact relationship between KCNE glycosylation and LQTS presentation is not currently well understood. In Chapter III, we determine the importance of N-linked glycosylation of E1 peptides and suggest a mechanism by which T7I is involved in LQTS presentation.

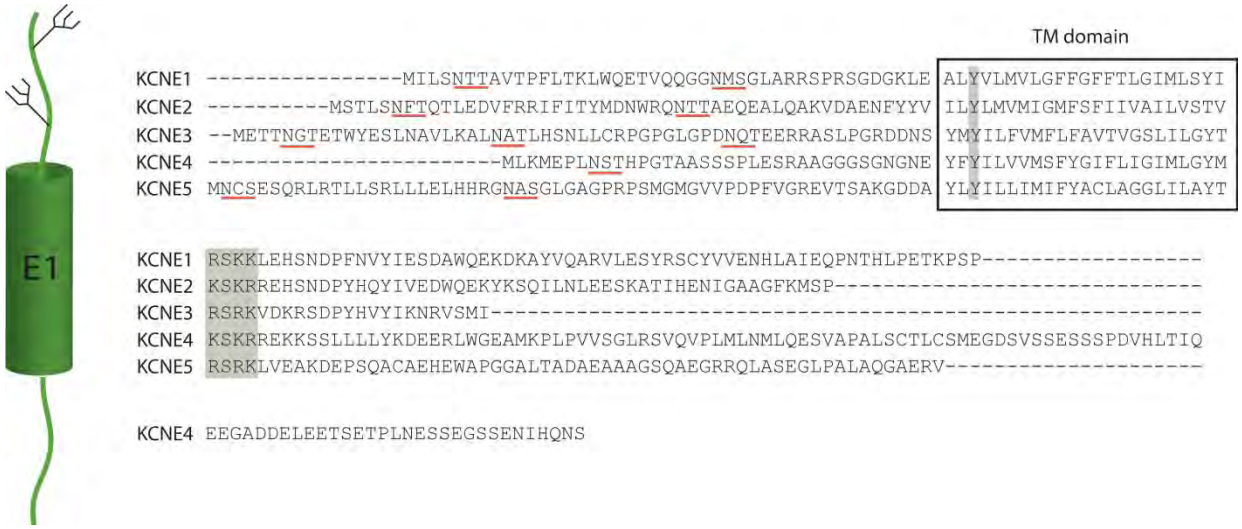

Figure 1.5 KCNE peptides. **Left**, schematic of the transmembrane topology of KCNE1 (E1) with extracellular N-glycan attachment sites denoted by branched structures. **Right**, amino acid alignment of members of the KCNE family. The N-glycosylation consensus sequences in each peptide are underlined in red; TM domain indicates the residues within the transmembrane region; conserved residues are colored in grey.

Schematic of KCNE1 peptide generated by K. Chandrasekhar. Amino acid alignment adapted from McCrossan, Z.A. and Abbott, G.W., *The MinK-related peptides*. Neuropharmacology, 2004. **47**(6):p. 787-821

Glycosylation is characterized by the enzyme-mediated addition of carbohydrate-rich glycans to proteins. The process of glycan addition to proteins is shared by the ER and Golgi compartments (Helenius and Aebi 2004). N-linked (or Asparagine-linked) glycosylation is a protein modification that is unique to the ER and often important for the primary ER quality control of glycoprotein assembly (Ellgaard and Helenius 2003). N-linked glycosylation is the process of coupling of a core N-glycan to nascent polypeptides. The core N-glycan is a 14-residue precursor oligosaccharide group composed of three glucoses, nine mannoses, and two N-acetyl glucosamine residues ($Glc_3Man_9GlcNAc_2$). The core N-glycan assembly is initiated in the cytosol by the addition of monosaccharides to a dolichol pyrophosphate carrier molecule by multiple monosaccharyltransferases (Fig. 1.6). Core N-glycan assembly is terminated in the ER when the dolichol pyrophosphate _flips' its orientation in the ER membrane and exposes its 7-residue intermediate N-glycan to monosaccharyltransferases in the ER lumen that load the remaining sugars onto the core N-glycan (Burda and Aebi 1999). In the ER, an oligosaccharyltransferase (OST) complex associated with the translocon scans the nascent polypeptide chain emerging into the ER lumen for the N-glycosylation consensus sequence Asn-X-Thr/Ser (NXT/S) where X is any amino acid except proline (Bause 1983; Silberstein and Gilmore 1996). When OST recognizes this sequence on the polypeptide chain, it immediately catalyzes the transfer of the core N-glycan from the lipid carrier to the nascent polypeptide through an N-glycosidic bond on the side chain of the asparagine residue in the consensus sequence. ER chaperones like calnexin and calreticulin, which oversee the folding and assembly of glycosylated channels use these

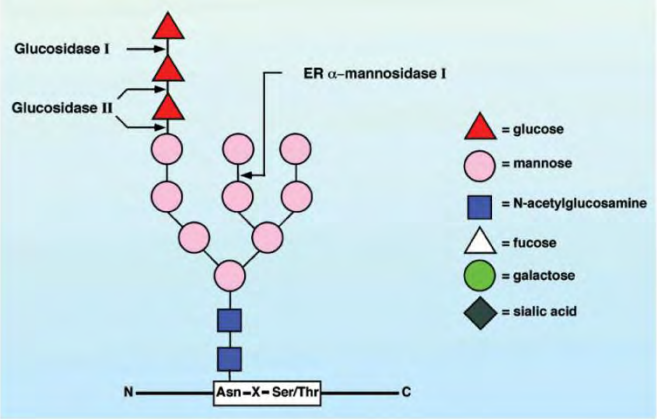
Glucosidase I
Glucosidase II
ER α–mannosidase I
= glucose
= mannose
= N-acetylglucosamine
= fucose
= galactose
= sialic acid
N
Asn–X–Ser/Thr
C

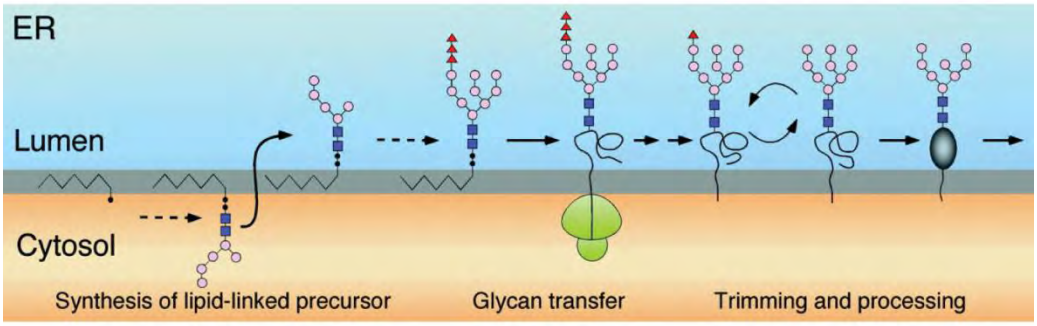
ER
Lumen
Cytosol
Synthesis of lipid-linked precursor
Glycan transfer
Trimming and processing

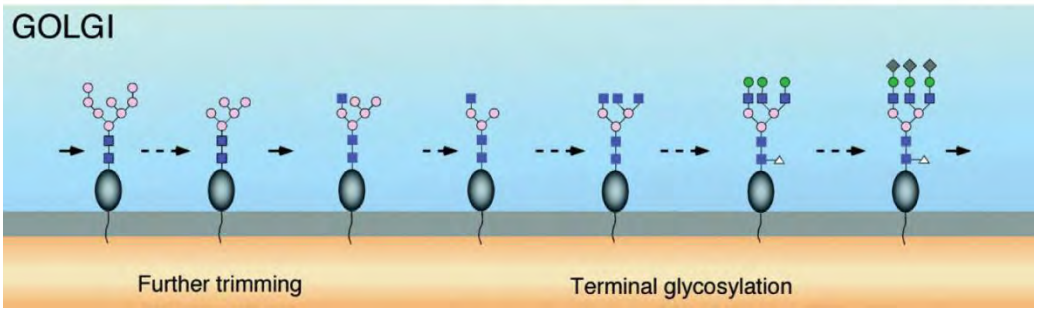
GOLGI
Further trimming
Terminal glycosylation

Figure 1.6 Cartoon of N-linked oligosaccharide and N-glycan modification through the biosynthetic pathway. **Above**, component sugars of the core N-linked glycan that is attached to a nascent polypeptide through an N-glycosidic bond at an Asn-X-Ser/Thr consensus site. Terminal glucose and mannose residues are removed in the ER by glucosidase and mannosidase enzymes. Symbols for the different sugars are shown in the legend. **Below**, biosynthesis of core N-glycan. Synthesis depicted from the initial addition of sugars to the dolichol pyrophosphate in the cytoplasm to the completed core N-glycan in the ER. Oligosaccharyltransferase complex catalyzes N-glycan transfer to the nascent polypeptide as it enters the ER lumen through the translocon. Three terminal glucose residues are removed by ER glucosidases I and II and the polypeptide is allowed to undergo folding/assembly till it reaches its native structure. Subsequent trimming of a mannose sugar allows protein migration from the ER to the Golgi compartment. Various glycan modification reactions are catalyzed in the Golgi; only one of many sugar trimming and addition pathways is shown. Terminal glycosylation results in the addition of GlcNAc, galactose, fucose, and sialic acid sugars to N-glycans. While glycoforms in the ER are homogenous, the Golgi-generated forms are usually diverse and varied owing to the multiple N-glycan modification pathways.

Figures and figure legends adapted from Helenius, A. and Aebi, M., *Intracellular Functions of N-linked Glycans*. Science, 2001. **291** p. 2364-2369

glycan _handles' on individual channel subunits to facilitate oligomeric assembly (Helenius and Aebi 2001; Helenius and Aebi 2004). Association with chaperones is important for the stability of channel subunits in the ER, as observed for the *Shaker* K^+ channel (Papazian 1999; Khanna et al. 2001; Khanna et al. 2004). Chaperone assembly with glycosylated polypeptides occurs after the cleavage of two terminal glucose residues from the core N-glycan by ER glucosidases I and II (Ellgaard and Helenius 2001; Ellgaard and Helenius 2003). A cycle of de-and re-glucosylation of N-glycans occurs until the polypeptide assumes its native assembled state. The core N-glycans can be further modified in the Golgi compartments where trimming and addition of sugar residues results in the maturation of the N-glycan attached to the nascent protein.

Endoglycosidases are glycan-specific enzymes used to cleave specific sugar residues from glycoproteins facilitating their identification. Differential sensitivity of N-glycans to various glycosidases can be used as markers to determine the cellular location of glycoproteins in the biosynthetic pathway. Two endoglycosidases, Endo H and PNGase F, have been used in the biochemical characterization of glycans on ion channels (Khanna et al. 2004; Krumerman et al. 2004). Endo H is an endoglycosidase that cleaves high mannose and some hybrid types of N-glycans such as those predominantly found in the ER while PNGase F cleaves almost all forms of N-glycans found throughout the secretory pathway. In Chapter II, we accurately define the glycosylation states of E1 peptides in the presence and absence of K^+ channel partners using the Endo H and PNGase F sensitivities of glycans on E1 as a means to examine the trafficking competency of E1 peptides.

Historically, N-glycosylation has been considered a co-translational process catalyzed by OST as the nascent polypeptide is threaded through the translocon. However, recent evidence using two different glycoprotein substrates suggests that post-translational N-glycosylation can also normally occur on glycoproteins containing multiple N-glycosylation consensus sites (Bolt et al. 2005; Lambert and Prange 2007). Ruiz-Canada et al. determined that there are two hetero-oligomeric forms of OST that can individually catalyze the co- and post-translational addition of N-glycans when glycoproteins contain multiple consensus sequences (Ruiz-Canada et al. 2009). In Chapter III, we investigate the process of N-glycan addition to nascent E1 peptides to determine the relative importance of each of the two N-glycosylation sites on E1 on overall protein stability and trafficking efficiency. Our findings suggest a mechanism by which glycosylation deficiency may be implicated in LQTS.

Unlike N-linked glycosylation which is initiated in the ER as a co-translational process, O-linked glycosylation is a post-translational protein modification. O-linked glycosylation has been thought to occur typically in the Golgi compartment although the enzymes catalyzing O-glycan transfer have been detected as early as the ER (Roth et al. 1986). While N-glycan attachment is characterized by the presence of consensus sequences on target proteins, O-glycan attachment is not dependent on the presence of specific consensus sites on proteins. In theory, all extracellularly exposed serine and threonine residues are potential O-glycan linkage sites; however, only certain residues are efficiently O-glycosylated based on the hydrophobicity and nature of residues surrounding the O-glycan attachment sites (Van den Steen et al. 1998). Predictive

algorithms can be used in determining potential O-linkage sites on a protein. The NetOGlyc3.1 server is an algorithm that uses structural and amino acid environmental information for O-glycan attachment from known O-glycosylated proteins to predict the likelihood of O-glycosylation at certain residues in an input amino acid sequence (Julenius et al. 2005). The process of O-glycan attachment on proteins is catalyzed by nucleotide sugar transporters which carry sugar groups to organelles where glycosyltransferases mediate the transfer of sugars to serine or threonine residues on proteins (Hirschberg et al. 1998). Structurally, O-glycans acquire diverse configurations of sugars owing to the multiple glycosyltransferases that catalyze the addition of different residues to growing O-glycan branches. In the trans-Golgi, O-glycans acquire terminal sialic acid residues that crown the carbohydrate chains (Roth et al. 1986).

Disruption of the cell surface glycosylation of cardiac ion channels has been implicated in ion channel dysfunction. Terminal sialic acid residues on N- and O-glycan modifications create a cloud of negative charge close to the membrane surface that impacts the positively charged voltage-sensing domains in ion channels. Voltage-sensing domain movement can trigger the opening and closing of channels in response to membrane depolarization. Ufret-Vincenty et al. show that the absence of glycosylation in voltage-gated Na^+ channels shifts the voltage dependence of activation and inactivation of the channels which recapitulates the phenotype observed in Na^+ channel arrhythmogenesis heart failure (Ufret-Vincenty et al. 2001). This study suggests that the negatively charged sialic acid residues can affect the voltage dependence of the channel based on a surface potential model where the presence of negative charge close to the

membrane affects its surface potential and thereby exerts an effect on the threshold of activation of the channel (Green and Andersen 1991).

The significance of glycosylation in channel function is not limited to Na^+ channels. Similar work on the $K_v4.3$ channel showed that channel glycosylation plays a significant role in the generation of the transiently-outward cardiac current (I_{to}) and that improper channel glycosylation leads to arrhythmogenic changes to this current (Ufret-Vincenty et al. 2001). Glycosylation of ancillary subunits has also been shown to be important in the modulation of Na^+ and K^+ channel function. Similar to E1, the β1 subunit of the Na_v channel complex is a single transmembrane-spanning protein with N-glycan attachment sites in its extracellular N-terminus. When its N-glycans are fully sialylated, the β1 subunit modulates channel gating by left shifting the midpoint of activation ($V_{1/2}$) to hyperpolarizing potentials (Johnson et al. 2004). In Chapter IV, we determine whether E1 peptides acquire sialylated O-glycans as a post-translational modification and discuss their potential role in Q1/E1 channel function.

The KCNE peptides are one class of β-subunits that associate with and modulate K^+ channels in a variety of tissues. The work presented in this thesis introduces the cellular mechanisms underlying assembly and trafficking of a specific Q1/KCNE K^+ channels – the Q1/E1 complex. The study of E1 trafficking can be applied to investigate the cellular trafficking of other K^+ channel/KCNE β-subunits. Additionally, the role of β-subunit glycosylation in the stability and functional modulation of K^+ channels enhances our understanding of how glycosylation can be implicated in ion channel dysfunction. N-

linked glycosylation is conserved throughout the KCNE family and mutations that disrupt the addition of N-glycans to KCNE peptides are associated with disease (Larsen et al. 2001; Lu et al. 2003; Park et al. 2003). Investigating the process of N-glycan addition to KCNE peptides could reveal novel mechanisms by which N-glycosylation defects are linked to LQTS. Lastly, the discovery of O-linked glycosylation on E1 peptides suggests additional roles for post-translational modifications on KCNE peptides in the stability and function of K^+ channel/KCNE complexes.

CHAPTER II

KCNE1 PEPTIDES REQUIRE CO-ASSEMBLY WITH SPECIFIC K^+ CHANNELS FOR EFFICIENT TRAFFICKING AND CELL SURFACE EXPRESSION

ABSTRACT

KCNE peptides are a class of type I transmembrane β-subunits that assemble with and modulate the gating and ion conducting properties of a variety of voltage-gated K^+ channels. Accordingly, mutations that disrupt the assembly and trafficking of KCNE-K^+ channel complexes give rise to disease. The cellular mechanisms responsible for ensuring that KCNE peptides assemble with voltage-gated K^+ channels have yet to be elucidated. Using enzymatic deglycosylation, immunofluorescence, and quantitative cell surface labeling experiments, we show that KCNE1 (E1) peptides are retained in the early stages of the secretory pathway until they co-assemble with specific K^+ channel subunits; co-assembly mediates E1 progression through the secretory pathway and results in cell surface expression. We also address an apparent discrepancy between our results and a previous study in human embryonic kidney cells, which showed wild type E1 peptides can reach the plasma membrane without exogenously expressed K^+ channel subunits. By comparing E1 trafficking in three cell lines, our data suggest that the errant E1 trafficking observed in human embryonic kidney cells may be due, in part, to the presence of endogenous voltage-gated K^+ channels in these cells.

INTRODUCTION

Voltage-gated K^+ channels have diverse physiological roles ranging from repolarization of excitable tissues to salt and water homeostasis in epithelial cells. To achieve such functional diversity, many K^+ channels function as membrane-embedded complexes made up of pore-forming α-subunits and tissue specific regulatory β-subunits. The KCNE type I transmembrane peptides are a class of small β-subunits that assemble with and modulate the function of several types of voltage-gated K^+ channels (McCrossan and Abbott 2004). E1 is the founding member of the family and has been shown to form complexes with $K_v3.1$, $K_v3.2$, $K_v4.2$, $K_v4.3$, HERG and KCNQ1 (Q1) K^+ channels (Barhanin et al. 1996; Sanguinetti et al. 1996; McDonald et al. 1997; Zhang et al. 2001; Deschenes and Tomaselli 2002; Lewis et al. 2004). When E1 assembles with Q1, the complex produces the slowly activating cardiac I_{Ks} current and is the exclusive pathway for endolymphatic K^+ recycling in apical membranes of strial marginal and vestibular dark cells (Marban 2002; Wangemann 2002). Conversely, unpartnered Q1 channels are ill-equipped to perform either function because they open and close too quickly to maintain the rhythmicity of the heartbeat and are significantly inactivated and non-conducting at the resting membrane potential of inner ear cells (Pusch et al. 1998). The biological importance of proper Q1/E1 complex formation is further underscored by the inherited mutations in either Q1 or E1 that disrupt the assembly and/or trafficking of the complex and give rise to cardiac arrhythmias, most notably long QT syndrome (Splawski et al. 2000). An autosomal recessive form of long QT syndrome also causes neural deafness (Tyson et al. 2000).

Although proper K^+ channel function requires completely assembled complexes at the plasma membrane, the cellular mechanisms that ensure K^+ channel α-subunits combine with membrane-embedded β-subunits are starting to be elucidated. For the ATP-sensitive K^+ channels (Kir6.1 and 6.2), which assemble with sulfonylurea receptors (sulfonylurea receptors 1/2A/2B) in a 4:4 stoichiometry, unpartnered channel and receptor subunits are stringently held in the endoplasmic reticulum (ER) via a RXR retention signal (Zerangue et al. 1999). Once an octomeric complex is formed, the K_{ATP}-sulfonylurea receptor complex is permitted to exit the ER and traffic to the cell surface.

In contrast, E1 subunits in complexes with voltage-gated K^+ channels may traffic differently than their K_{ATP} counterparts. Two different studies suggest that Q1/E1 complex formation occurs at the plasma membrane, which would require both proteins to traffic through the secretory pathway independently (Romey et al. 1997; Grunnet et al. 2002). More recently, it was proposed that Q1/E1 assembly occurs in the ER because mutant E1 proteins could retain Q1 channels there (Krumerman et al. 2004). However, unpartnered wild type E1 proteins freely exited the ER and migrated to the cell surface, an observation inconsistent with an ER-based assembly. A significant caveat with all of the above studies was that KCNE trafficking was studied in either *Xenopus* oocytes or human embryonic kidney (HEK) 293B cells, both of which possess endogenous transcripts of voltage-gated K^+ channels that have been shown to assemble with KCNE subunits (Sanguinetti et al. 1996; Jiang et al. 2002).

Here we examine the assembly and trafficking of wild type E1 subunits in the presence and absence of Q1 channels in Chinese hamster ovary (CHO) and African green monkey kidney (COS-7) cells, both of which are revered for their _electrical tightness' or lack of measurable endogenous K^+ currents. Using these cells, we find that the majority of E1 protein is localized to the ER when expressed alone. Co-expression with Q1 subunits promotes E1 protein trafficking through the secretory pathway, resulting in robust cell surface expression. Moreover, these results demonstrate that Q1/E1 complex formation occurs early in the secretory pathway and that unpartnered E1 subunits do not efficiently progress past the ER and *cis*-Golgi compartments until they assemble with Q1 channel subunits.

RESULTS

Active retention of unassembled membrane protein subunits is one mechanism by which a cell ensures that membrane-embedded K^+ channel complexes are properly assembled before the proteins arrive at their final cellular destination (Ellgaard and Helenius 2003). Distinguishing cellular markers for ER-resident proteins are immature N-linked glycans. The ER utilizes these high mannose oligosaccharide handles to promote protein folding, oligomerization, quality control, retention, and trafficking (Helenius and Aebi 2001). Once N-linked glycoproteins reach the Golgi, however, they are no longer subject to the rigorous quality control systems of the ER and migrate through medial and *trans*-Golgi compartments relatively unabated while acquiring

complex modifications to their N-linked glycans (Helenius and Aebi 2001). Because KCNE peptides have two well conserved N-linked glycosylation consensus sites, we utilized this hallmark of ER residency to determine the cellular locales of E1 peptides expressed alone, with Q1, and with KCNQ4 (Q4), a K^+ channel previously shown not to assemble with E1 (Fig. 2.1) (Melman et al. 2004). Transient expression of E1 alone in CHO cells gave rise to two strong bands at 16 and 22 kDa (though faint, higher molecular mass bands can be seen on this intentionally well developed, but not overexposed Western blot). When expressed with Q4, a similar banding pattern was observed with an additional band at 19 kDa. In contrast, expression with Q1 affords an additional, higher molecular mass band at ~40 kDa. The presence of this 40-kDa band was independent of the detergent lysis mixture used but only occurred in abundance when E1 was co-expressed with Q1. The abundance of the higher molecular mass form of E1 was dependent on the ratio of Q1/E1 DNA used for transient transfection. Limiting amounts of Q1 DNA yielded all three forms of E1 protein as shown in Fig. 2.1; optimizing the Q1/E1 DNA ratio (Experimental Procedures) afforded primarily the higher molecular mass species (Fig. 2.2; see also Fig. 2.6). We also observed the same gel banding patterns for E1 in COS-7 cells (Fig. 2.1).

The multiple bands and differences in gel shift mobility suggested that E1 peptides were differentially glycosylated depending on the presence of specific K^+

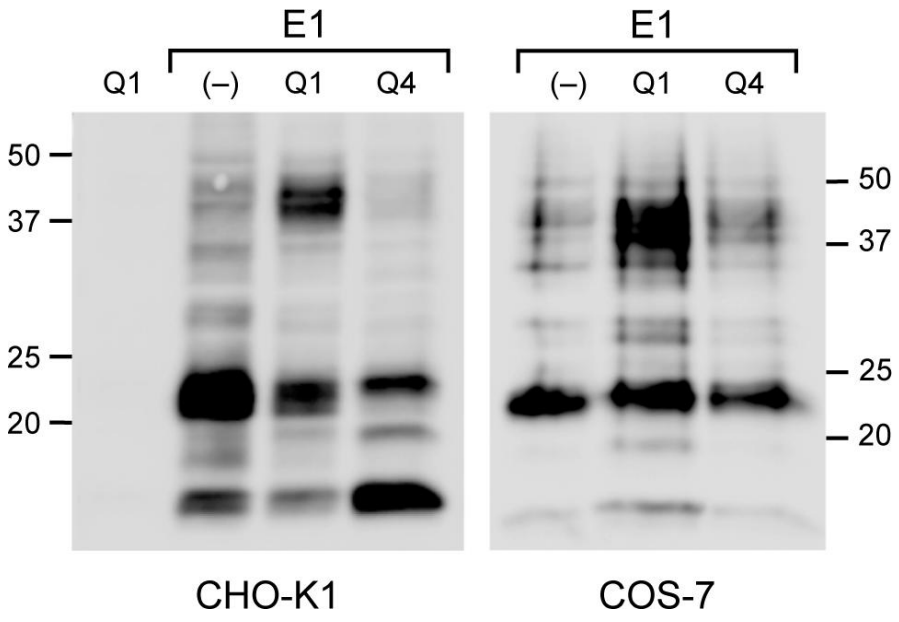

Figure 2.1 KCNE1 peptides migrate differently on denaturing gels when expressed with specific K^+ channel subunits. Immunoblots of HA-tagged E1 peptides from solubilized CHO cells or COS-7 cells transfected with Q1, E1, Q1/E1, or Q4/E1 DNA. Expression of E1 alone or with Q4 yields two intense bands at 16 and 22 kDa in CHO cells and one band at 22 kDa in COS-7 cells. Q1/E1 co-expression results in the appearance of an equally strong band at ~40 kDa. Q1 was transfected alone to serve as a negative control.

channel subunits. We therefore determined whether the gel shift mobility difference that was observed with Q1/E1 co-expression was due to maturation of the glycans on E1. The maturity of N-linked glycoproteins can be readily determined using two different glycosidases. EndoH is a glycosidase that removes the high mannose (immature) glycans found on ER and *cis*-Golgi proteins but is unable to process the complex (mature) glycoforms once the protein reaches the medial Golgi in the biosynthetic pathway. In contrast, PNGase F is an endoglycosidase that removes all N-linked oligosaccharides. Treatment of the E1 samples with either Endo H or PNGase F reduced the 22 kDa band to 16 kDa, consistent with the loss of two immature glycans (Fig. 2.2). Thus, when E1 is expressed alone, the majority of the N-linked glycan is immature; indicating that unpartnered E1 is localized to the ER and/or *cis*-Golgi. Enzymatic deglycosylation of the Q1/E1sample afforded a different result. Treatment with Endo H had no effect on the higher molecular mass band. However, the two faint bands centered at ~20 kDa collapsed to the unglycosylated form (16 kDa), identifying these two bands as E1 glycoproteins with one and two immature glycans. Heating the samples (95°C for 5 min) did not affect any of the bands, suggesting that the higher molecular mass band was not due to protein aggregation. All of the glycosylated forms of E1, however, were susceptible to PNGase F treatment, indicating that the higher molecular mass form of E1 possessed mature N-linked oligosaccharides. Because maturation of N-linked glycoproteins occurs in the medial and *trans*-Golgi, the presence of mature glycans in only the Q1/E1 sample shows that co-assembly with Q1 facilitates E1 peptide progression through the secretory pathway. Although the PNGase F-treated E1 protein was deglycosylated, several residual

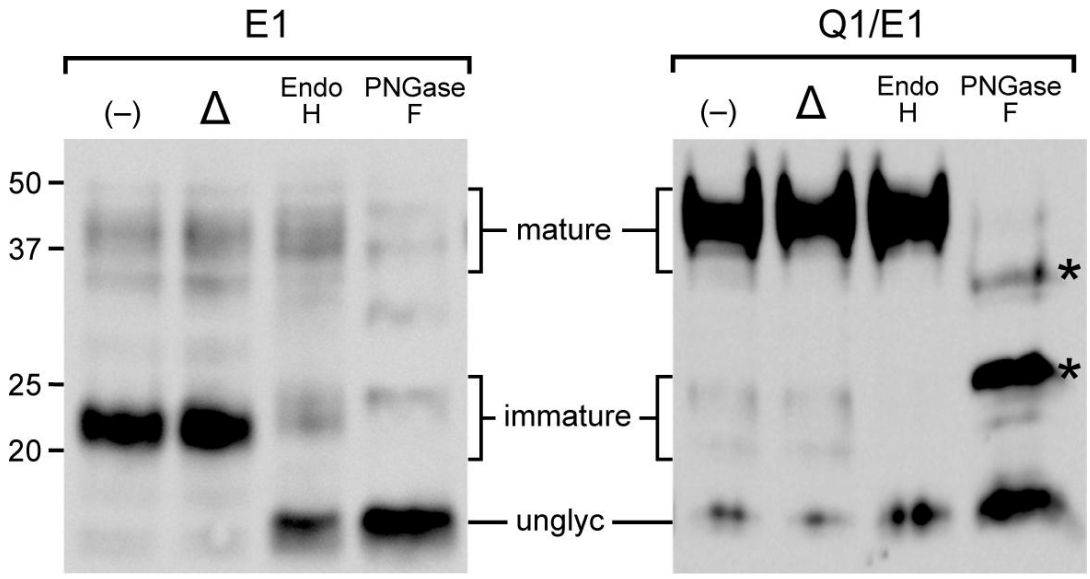

Figure 2.2 KCNE1 glycopeptides are predominately immature until they assemble with KCNQ1 subunits. Immunoblot of enzymatic deglycosylation of E1 *N*-linked glycopeptides in the presence and absence of expressed Q1. The samples were left untreated (–), heat-treated (Δ) to 95°C for 5 min, digested with Endo H, or PNGase F and separated by SDS-PAGE (15%). Mature, immature, and unglycosylated (*unglyc*) samples are indicated as determined by enzymatic deglycosylation. Asterisks (*) denote PNGase F digestion products that consistently migrated slower than immature and unglycosylated protein, which may be due to an additional post-translational modification.

bands were observed (indicated by the *asterisks*). Prolonged treatment with PNGase F, the addition of more enzyme, varying the concentration of SDS in the gel loading buffer, or heat denaturation did not change the intensity or mobility of these bands (data not shown). The residual banding is not partial digestion of the individual N-linked glycans because PNGase F directly cleaves the oligosaccharide from the peptide backbone (Lemp et al. 1990). It is possible that one of the two mature N-linked glycans on E1 is totally inaccessible to the enzyme; however, we have observed these similar bands with PNGase F-treated E1 mutants that possess only one N-linked glycosylation site (data not shown). These bands do not correspond to immature E1, because they have a slightly slower mobility that can be readily observed in either the E1 or the Q1/E1 PNGase F-treated samples. Moreover, PNGase F treatment of the E1 sample demonstrates that this enzyme cleaves both immature N-linked glycans efficiently. These additional bands were also resistant to a subsequent phosphatase treatment (Fig. 2.3). We also confirmed that ubiquitin modifications were absent on mature E1 peptides (Fig. 2.4) so these additional bands may be due to the presence of another type of post-translational modification.

Because maturation of *N*-linked glycans on E1 requires co-expression with Q1, we determined whether cell surface expression of E1 was also dependent on expression with specific K^+ channel subunits. Cell surface expression of E1 protein was visualized by immunofluorescence with permeabilized and non-permeabilized cells using an extracellularly HA-tagged version of E1 where the HA-tag was placed between the two N-glycosylation consensus sites (Wang and Goldstein 1995). In non-permeabilized cells,

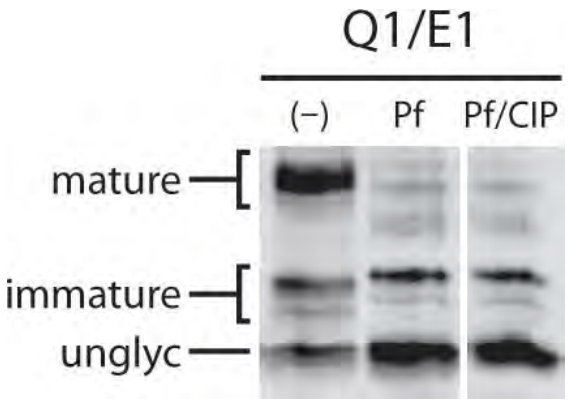

Figure 2.3 Mature KCNE1 peptides do not undergo phosphorylation. Immunoblot of enzymatic deglycosylation of E1 *N*-linked glycopeptides in the presence of expressed Q1. The samples were left untreated (–), digested with PNGase F alone (Pf), or PNGase F and Calf Intestinal Phosphatase (Pf/CIP) and separated by SDS-PAGE (15%). Mature, immature, and unglycosylated (*unglyc*) samples are indicated as determined by enzymatic deglycosylation. Pf/CIP treatment did not result in any change in migration pattern of PNGase F digestion products that consistently migrated slower than immature and unglycosylated protein.

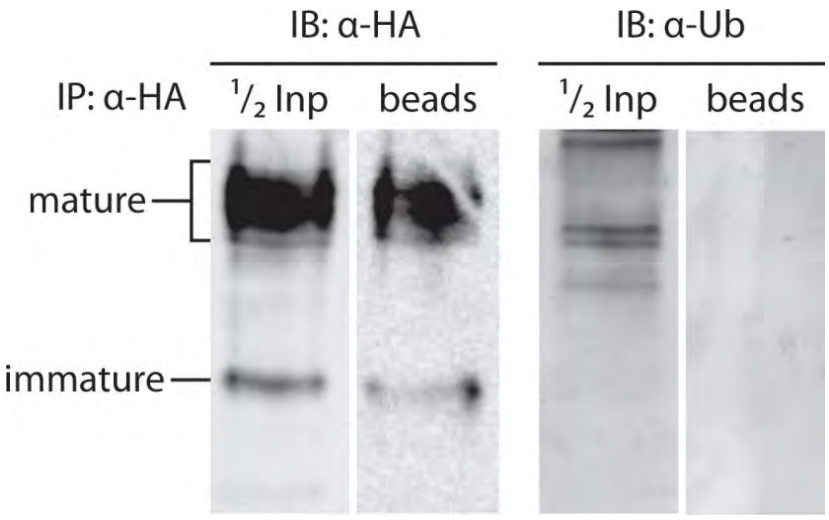

Figure 2.4 Ubiquitin modifications are absent on mature KCNE1 peptides. RIPKA-solubilized CHO cells expressing Q1/E1 were incubated with anti-HA antibody (IP: α-HA) to immunoprecipitate E1 protein. Samples run in duplicate and probed with anti-HA antibody (IB: α-HA) to visualize E1 protein or anti-ubiquitin (IB: α-Ub) to visualize ubiquitin attachment to E1. One-half of the total detergent solubilized lysate (*1/2 Input*) and the precipitates were analyzed by SDS-PAGE (15%).

no cell surface labeling of E1 was observed when E1 was expressed alone or with Q4 (Fig. 2.5, *E1* and *Q4/E1 panels*). Co-transfection with green fluorescent protein DNA verified that the absence of cell surface staining was not a result of untransfected cells. Permeabilization of the cells confirmed that the majority of the E1 protein was intracellular, as evidenced by the punctate staining pattern. In contrast, co-expression with Q1 resulted in striking cell surface staining of E1 in intact and permeabilized cells (Fig. 2.5, *Q1/E1panels*).

The plasma membrane protein levels of E1 were then quantitated by cell surface biotinylation. To minimize labeling of intracellular proteins and membrane recycling, cells expressing E1 with or without Q1 were labeled with a membrane-impermeant, amine-reactive biotin derivative at 4°C. When co-expressed with Q1, E1 shows robust cell surface expression (Fig. 2.6*A*). Moreover, no immature E1 was ever observed on the plasma membrane, which is consistent with the enzymatic deglycosylation assays (Fig. 2.2). Little to no protein was observed at the cell surface when E1 was expressed alone. To account for cell rupture during biotinylation, the ER-resident protein calnexin was used as an internal control in all experiments. The percentage of E1 protein at the cell surface was quantitated as a ratio of biotinylated proteins over the total protein input shown in Fig. 2.6*B*. For Q1/E1, ~35% of E1 protein was at the cell surface after background subtraction. For E1 alone, the percentage of protein detected on the cell surface by biotinylation was within error of background calnexin labeling (4 ± 1%).

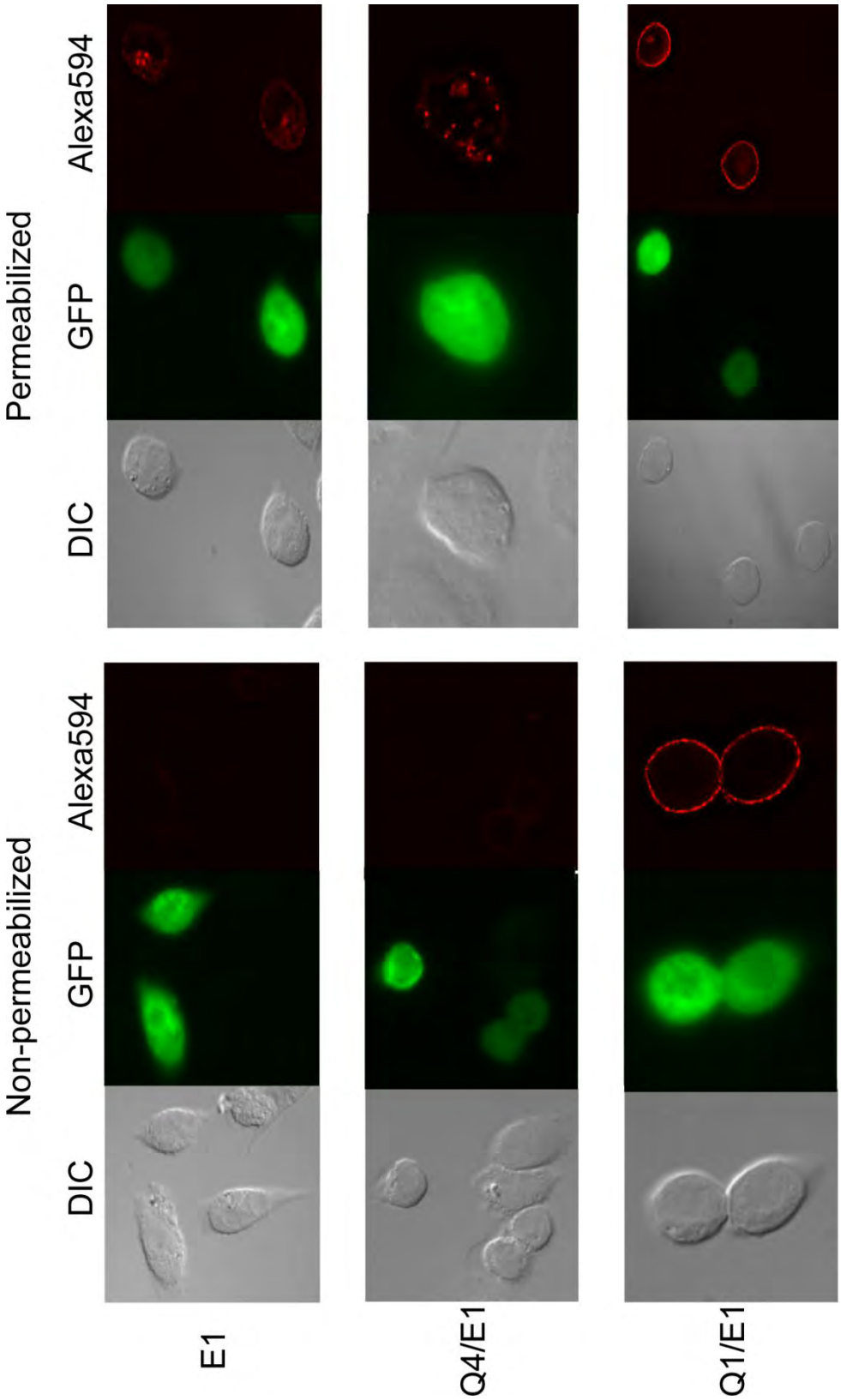
Non-permeabilized
Permeabilized
DIC
GFP
Alexa594
DIC
GFP
Alexa594
E1
Q4/E1
Q1/E1

Figure 2.5 Cell surface expression of KCNE1 requires co-expression with K^+ channel subunits that assemble with KCNE peptides. Cell surface immunostaining of E1 expressed alone or with Q4 or Q1 in CHO cells is shown. The cells were fixed and left intact to visualize cell surface staining or permeabilized to visualize total cellular staining. The images shown are single 0.4-μm planes through the center of each cell. Differential interference contrast (DIC) images show both untransfected and transfected cells. Green fluorescent protein (*GFP*) images identify transfected cells. Alexa 594 images show E1 protein staining with Alexa 594-conjugated antibodies. The fluorescent images were captured using the same exposure time and rendered identically to qualitatively compare the fluorescent intensities between panels. Note the strong cell surface staining for the Q1/E1 panels (non-permeabilized and permeabilized), whereas the E1 and Q4/E1 permeabilized panels show mostly punctate staining, indicative of intracellular distribution.

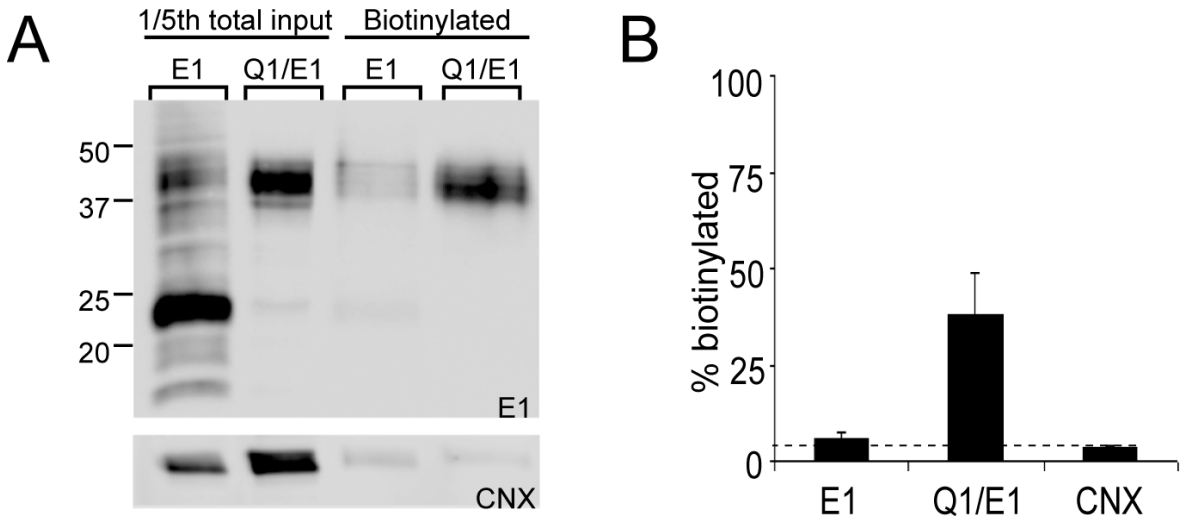

Figure 2.6 Quantification of the KCNE1 plasma membrane protein by cell surface biotinylation. *A*, a representative immunoblot of E1 expressed in CHO cells with and without Q1 channel subunits. Transfected cells were labeled with a membrane-impermeant biotin reagent and subsequently lysed, and the biotinylated proteins were isolated from 75 μg of total protein. Lanes identified as one-fifth of the total input are 15 μg of each sample lysate that was set aside to quantitate the total amount of biotinylated proteins. Biotinylated lanes are the streptavidin-bound proteins that were eluted from the beads and separated by SDS-PAGE (15%). The calnexin (*CNX*) immunoblot shows that the majority of the cells remained intact during the biotinylation procedure. *B*, quantification of the biotinylated E1 proteins. The percentage of biotinylated protein was calculated by dividing the band intensities in the biotinylated lane by the band intensities in the one-fifth total input lane, which were multiplied by five. There was no significant difference between background calnexin labeling and cell surface labeling of E1 when the peptide was expressed alone. Co-expression with Q1 results in 34 ± 11% E1 protein

on the cell surface after subtracting for background cell lysis (calnexin control).The *error bars* are standard error measurement (S.E.M.) from three immunoblots. The *dotted line* indicates background biotinylation, which was calculated from calnexin staining (4 ± 1%).

Because E1 does not reach the plasma membrane when it is expressed alone, we determined its intracellular localization. Results from enzymatic deglycosylation (Fig. 2.2) narrow the spectrum of intracellular locales to the ER and/or *cis*-Golgi because the glycans on E1 were predominately immature. Initial examination of the intracellularly localized E1 protein by immunofluorescence afforded weak overall staining. The strongest signals were punctate in nature and not reminiscent of ER staining, as can be seen in the E1 permeabilized cells in Fig. 2.5. Accordingly, E1 did not co-stain with ER markers (data not shown). These observations did not correlate with the strong protein expression seen in Western blots (Fig. 2.1). We wondered whether antibody accessibility to the E1 HA tag was being prevented by lumenal proteins binding to the E1 N terminus because this extracellular tag is positioned between the two N-linked glycosylation consensus sequences (Wang and Goldstein 1995). Thus, we repositioned the HA tag to the intracellular C-terminus of E1. This C-terminal construct behaved similarly to the extracellularly tagged construct in all aspects; it assembled with Q1 channel subunits to afford the cardiac I_{Ks} current and required co-expression with Q1 to reach the cell surface with mature N-linked glycans (data not shown). In contrast to the extracellularly tagged E1 construct, visualization of the C-terminally HA-tagged E1 protein by immunofluorescence gave strong perinuclear staining (Fig. 2.7*A*). Counterstaining with calnexin and overlaying the images showed that the majority of E1 protein co-stains with this ER marker, although some E1 protein did not. E1 also co-stained with the *cis*-Golgi marker, β‘-COP (Palmer et al. 1993); however, the majority of the E1 protein stained in a pattern similar to

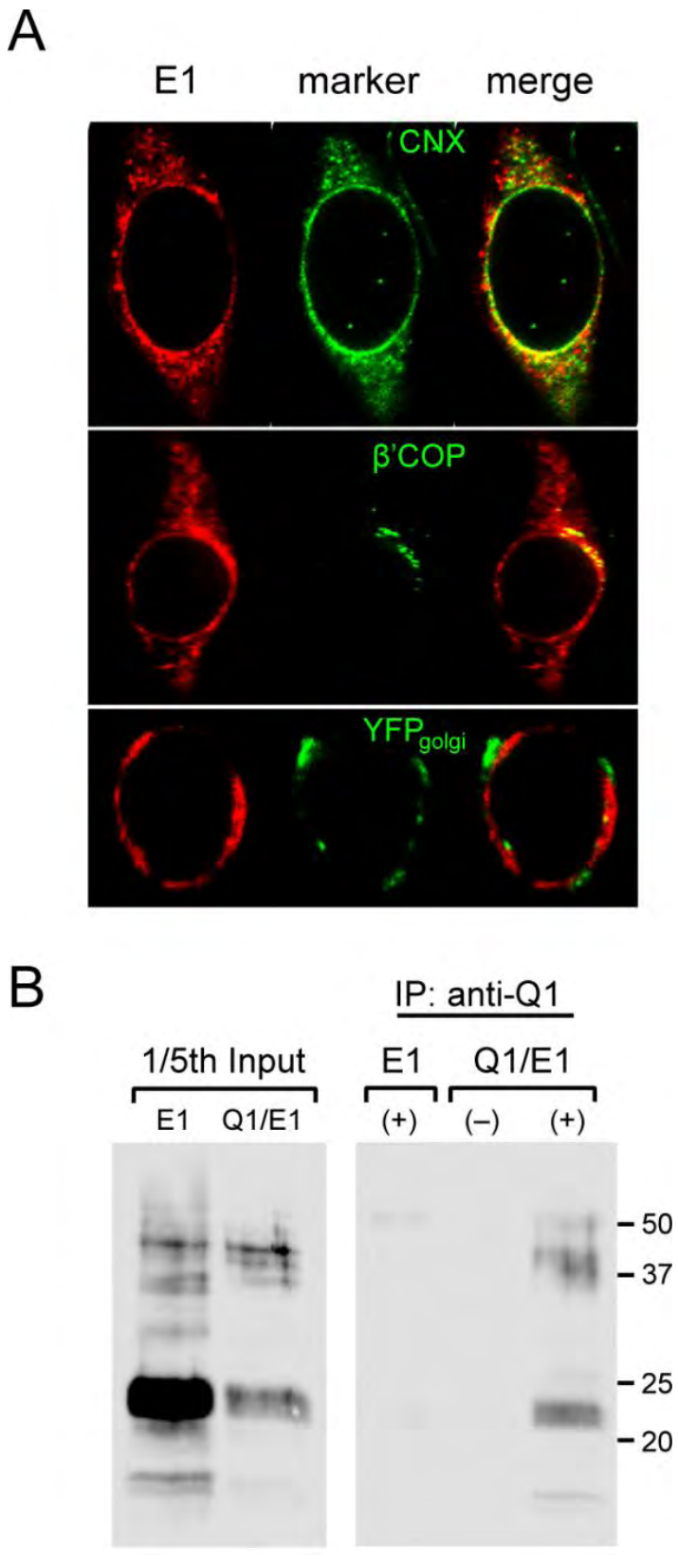
A
E1
marker
merge
CNX
β'COP
YFP golgi
B
IP: anti-Q1
1/5th Input
E1
Q1/E1
E1
Q1/E1
(+)
(–)
(+)
50
37
25
20

Figure 2.7 Intracellular distribution of KCNE1 peptides in CHO cells. *A*, co-localization of E1 with intracellular markers. CHO cells expressing E1 alone were labeled for E1 along with an ER marker, calnexin (*CNX*), a *cis*-Golgi network marker (β'-COP), or a *trans*-Golgi network marker, EYFP-Golgi (YFP-Golgi). *B*, co-immunoprecipitation (*IP*) of E1 with anti-Q1 antibody. Digitonin-solubilized CHO cells expressing E1 alone (E1) or co-expressed with Q1 (Q1/E1) were incubated with (+) or without (–) anti-Q1 antibody. One-fifth of the total detergent solubilized lysate (*1/5th Input*) and the precipitates were analyzed by SDS-PAGE (15%).

calnexin. Little to no co-staining was observed when E1 was expressed with EYFP-Golgi, which localizes to the *trans*-Golgi network. The intracellular staining of E1 showed that the majority of the protein resides in the ER when it is expressed alone. We determined whether Q1 subunits could co-assemble with the immature glycoforms of E1 found in the ER. Fig. 2.7*B* shows that all glycoforms, mature, immature, and unglycosylated, co-immunoprecipitate with Q1. Immunoprecipitation of E1 required co-expression with Q1 because no bands were observed when E1 was expressed alone.

To verify that there are inherent differences in cellular trafficking of E1 in HEK cells *versus* CHO and COS-7 cells and not variability in experimental design, reagents, or constructs, we also examined E1 protein expression and trafficking in HEK cells. Unlike in CHO and COS-7 cells, expression of E1 in HEK cells primarily afforded the higher molecular mass species when it was expressed alone or with Q1 (Fig. 2.8). Treatment with Endo H and PNGase F confirmed that this species contained mature N-linked glycosylation. As we observed with CHO and COS-7 cells, PNGase F digestion of E1 peptides from HEK cell lysates resulted in bands (indicated by the *asterisks*) that migrated slower than both immature and unglycosylated protein. Nonetheless, these results show that the N-linked glycans on E1 peptides in HEK cells mature without transiently expressed K^+ channel subunits.

Given that E1 peptides in HEK cells exit the ER and traffic through the Golgi without co-expressed K^+ channel subunits, we determined whether these peptides were reaching the plasma membrane. Using immunofluorescence, some cell surface staining

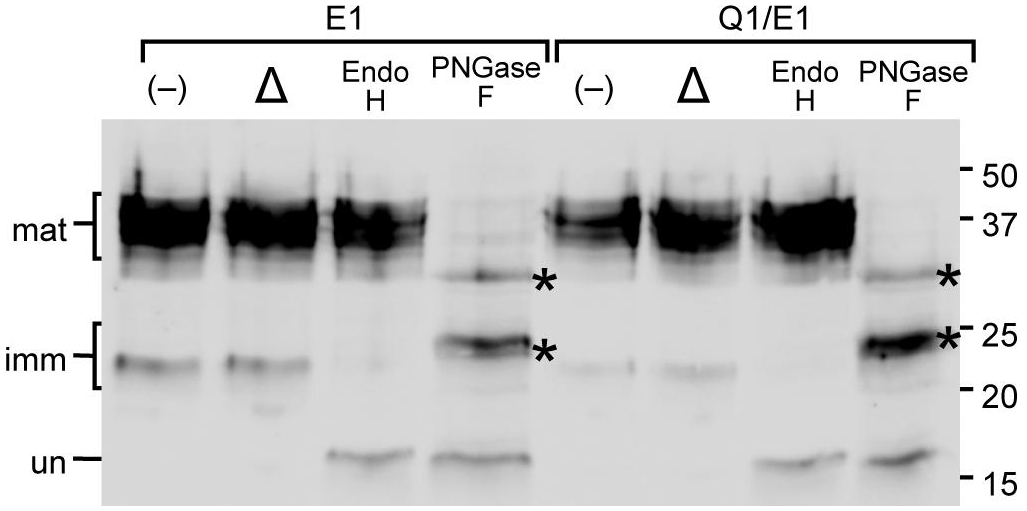

Figure 2.8 KCNE1 glycopeptides in HEK cells mature when expressed with or without K^+ channel subunits. Shown is an immunoblot of enzymatic deglycosylation of E1 peptides from SDS-solubilized HEK cells transfected with E1 or Q1/E1 DNA. Expression of E1 with or without Q1 channel subunits results in robust expression of a 37 kDa band that was identified as the mature *N*-linked glycan after enzymatic deglycosylation. The samples were left untreated (–), heat-treated (Δ) to 95°C for 5 min, digested with Endo H or PNGase F, and separated by SDS-PAGE (15%). Mature (*mat*), immature (*imm*), and unglycosylated (*un*) samples are indicated as determined by enzymatic deglycosylation. The asterisks (*) denote PNGase F digestion products that consistently migrated slower than unglycosylated or immature, which was also observed in CHO (Fig. 2.2) and COS-7 (data not shown).

was observed for E1 when expressed alone (Fig. 2.9*A*). However, the number of fluorescent cells and the intensity of cell surface staining were noticeably less than what was observed for Q1/E1. Quantitation of the cell surface proteins in HEK cells using biotinylation confirmed this qualitative observation (Fig. 2.10*A*). When E1 was expressed alone, 4 ± 2% of the protein was at the cell surface after calnexin subtraction; co-expression with Q1 increased the E1 cell surface protein to 22 ± 3% (Fig. 2.10*B*).

The combination of weak cell surface expression and the overwhelming maturation of the N-linked glycans on E1 when it is expressed in HEK cells prompted us to examine its intracellular distribution. The C-terminally HA-tagged version of E1 was expressed in HEK cells and overlaid with a panel of intracellular markers (Fig. 2.9*B*). Negligible co-staining was observed with the ER marker, calnexin. Modest co-staining was observed with β'-COP, but a substantial amount of E1 co-localized with EYFP-Golgi in the *trans*-Golgi network. However, in all merged images, there was some E1protein that did not co-stain with any of the markers used. In total, these results in HEK cells demonstrate that the E1 protein traffics through the ER and to the Golgi apparatus without an exogenously expressed K^+ channel.

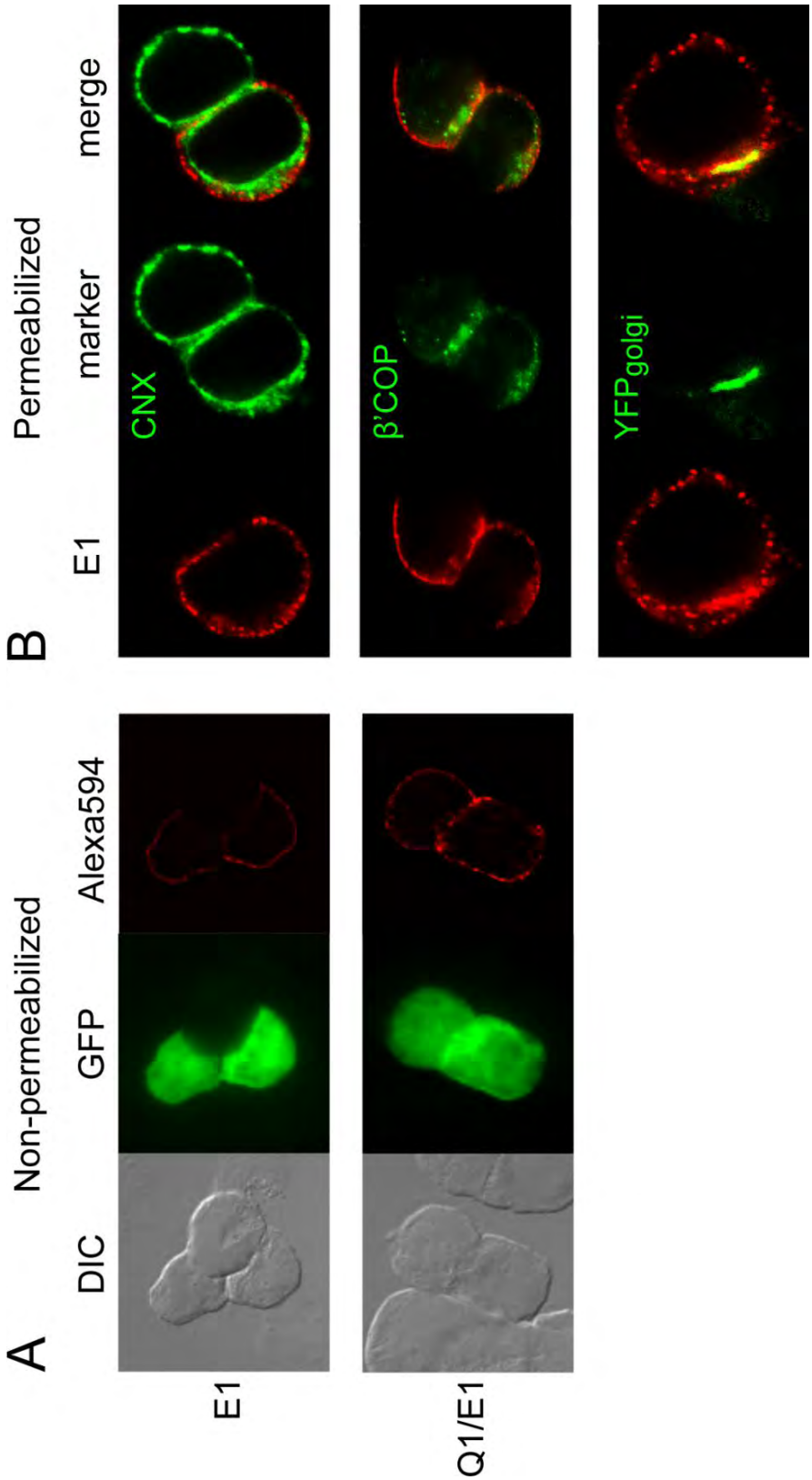
A
Non-permeabilized
DIC
GFP
Alexa594
E1
Q1/E1
B
Permeabilized
E1
marker
merge
CNX
β'COP
YFPgolgi

Figure 2.9 Solitary KCNE1 peptides traffic to the *trans*-Golgi in HEK cells and depend on KCNQ1 K^+ channel subunits for cell surface expression. *A*, cell surface immunostaining of E1 in HEK cells. Intact cells transfected with E1 or Q1/E1 DNA were fixed, labeled with Alexa 594-conjugated antibodies, and visualized by wide field microscopy. The images shown are single 0.4-μm planes through the center of each cell. Differential interference contrast (*DIC*) panels show both transfected and nontransfected cells. Green fluorescent protein (*GFP*) panels identify transfected cells. Alexa 594 panels show cell surface staining of E1. *B*, co-localization of E1 with intracellular markers. HEK cells expressing E1 alone were labeled for E1 along with an ER marker, calnexin (*CNX*), a *cis*-Golgi network marker (β'-COP), or a *trans*-Golgi network marker, EYFP-Golgi (YFP_{Golgi}). Note that the calnexin/E1 panels have two cells, but only the bottom cell expresses E1.

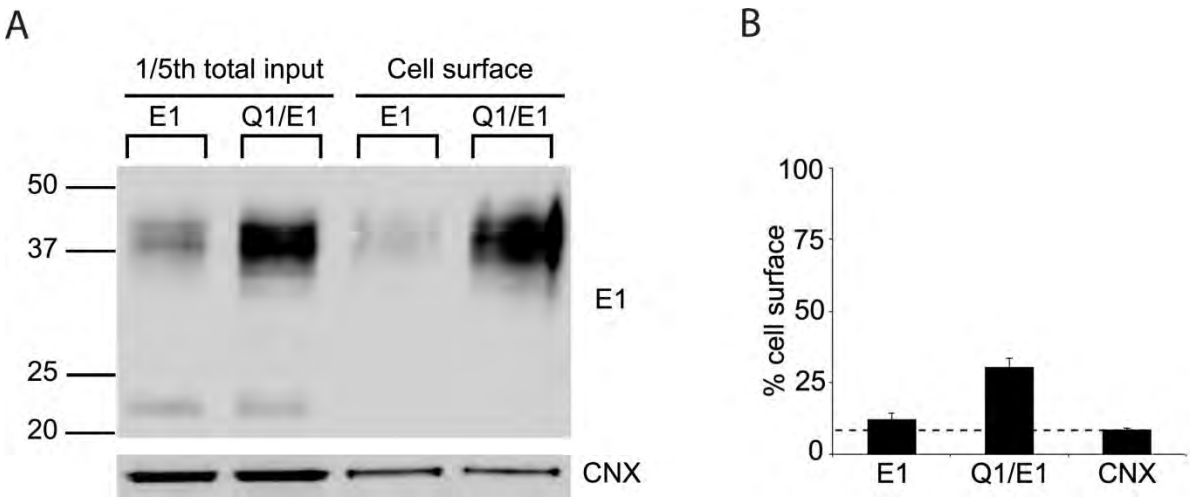

Figure 2.10 Mature KCNE1 peptides depend on KCNQ1 K^+ channel subunits for cell surface expression in HEK cells. *A*, a representative immunoblot of E1 expressed in HEK cells with and without Q1 channel subunits. Transfected cells were labeled as described for CHO cells. The calnexin (*CNX*) immunoblot shows that the majority of the cells remained intact during the biotinylation procedure. *B*, quantification of the biotinylated E1 proteins. The percentage of biotinylated protein was calculated by dividing the band intensities in the biotinylated lane by the band intensities in the one-fifth total input lane, which were multiplied by five. When expressed alone, 4 ± 2% of E1 peptides were present on the cell surface while co-expression with Q1 results in 22 ± 11% E1 protein on the cell surface after subtracting for background cell lysis (calnexin control).The *error bars* are standard error measurement (S.E.M.) from three immunoblots. The *dotted line* indicates background biotinylation, which was calculated from calnexin staining (8 ± 1%).

DISCUSSION

We studied the trafficking of E1 peptides through the biosynthetic pathway by following the maturation of the oligosaccharides on E1 because N-linked glycan processing is intimately tied to cellular compartmentalization (Helenius and Aebi 2004). By expressing E1 alone, with Q1, or with Q4 (a K^+ channel that does not assemble with E1), we determined that E1 glycoproteins do not mature unless they are co-expressed with K^+ channel subunits that assemble with KCNE peptides. In addition, cell surface expression of E1 was also co-dependent on Q1 subunit expression, which was demonstrated in both qualitative and quantitative cell surface labeling experiments. Moreover, only the mature form of E1 was ever observed at the cell surface, indicating that the immature E1 protein bands observed at ~20 kDa do not correspond to E1 protein in functioning Q1/E1 complexes at the plasma membrane. Our results in CHO and COS-7 cells recapitulate what has been observed in *Caenorhabditis elegans* where a KCNE homolog requires its corresponding K^+ channel subunits to reach the cell surface (Bianchi et al. 2003).

The presence of immature N-linked glycans on E1 indicates that these proteins have yet to traffic beyond the *cis*-Golgi in the biosynthetic pathway and strongly suggests that unpartnered E1 peptides are actively prevented from trafficking past these early compartments in the secretory pathway. Co-localization experiments using a panel of intracellular markers place the majority of the E1 protein in the ER and a small fraction in the *cis*-Golgi. Although these results cannot rule out Q1/E1 complex assembly in the *cis*-Golgi, the sheer abundance of unpartnered E1 peptides in the ER and co-

immunoprecipitation of the immature and unglycosylated E1 with Q1 strongly suggest that Q1/E1 complex assembly occurs in the ER. An ER-based assembly for Q1/E1 complexes directly contradicts two previous functional studies where it was proposed that complex assembly occurs at the plasma membrane (Romey et al. 1997; Grunnet et al. 2002). The basis for this proposal was that *Xenopus* oocytes expressing unpartnered Q1 K^+ currents could be converted to KCNE-modulated currents within 24 h by a subsequent injection of KCNE mRNA. However, this functional change was the only evidence in support of this hypothesis. The cell surface and ER lifetimes of Q1 protein were not measured, nor was it directly shown that previously unpartnered plasma membrane Q1 channels acquired newly synthesized KCNE peptides. The fact that the majority of the unassembled E1 peptides reside in the ER, possess immature N-linked glycans, and do not reach the cell surface in the absence of Q1 channel subunits eliminates a plasma membrane-based assembly mechanism for Q1/E1 complexes.

Enzymatic deglycosylation assays also revealed that E1 peptides potentially possess another post-translational modification, because we routinely observed digestion products that migrated slower than unglycosylated E1 (Figs. 2.2 and 2.8) in all three cell lines: CHO, COS-7, and HEK. These bands appeared whether the E1 peptide possessed one or both N-linked glycosylation sites. In addition, changing the detergent composition used for cell lysis or the concentration of SDS in the loading buffer did not change the migration or intensity of these bands. The modification may be specific to E1 because PNGase F treatment of KCNE3 (E3) peptides co-expressed with Q1 channels in *Xenopus* oocytes (Gage and Kobertz 2004), and CHO cells (Gage and Kobertz, unpublished

results) resulted in complete digestion of E3 to unglycosylated peptides. The retarded migration is not due to phosphorylation because treatment with phosphatase had no effect on the mobility of these bands (Fig. 2.3). These residual bands were also resistant to a subsequent neuraminidase treatment, suggesting that the removal of the sialic acids does not change the mobility of the E1 protein on a denaturing gel. Neuraminidase treatment of the N-linked glycans on Q1/E1, however, did show a subtle redistribution of the heterogeneous E1mature bands consistent with the removal of terminal sialic acid residues from N-glycans (data not shown).

Previous studies of E1 trafficking in HEK cells observed that wild type E1 peptides could readily exit the ER with or without a co-expressed K^+ channel (Krumerman et al. 2004). In light of our contrasting results using CHO and COS-7 cells, we re-examined the cellular processing of E1 protein in HEK cells. As was previously reported, E1 peptides exited the ER without the exogenous expression of K^+ channels subunits. Using immunofluorescence, E1 protein could be detected at the plasma membrane in some cells; however, quantitative analysis of the cell surface population by biotin labeling revealed that the expression of E1 alone was barely detectable after background subtraction (4 ± 2%) and was considerably lower when compared with co-expression with Q1 (22 ± 3%). Visualization of the intracellular distribution of E1 in HEK cells by immunofluorescence showed that the majority of the protein has trafficked past both the ER and *cis*-Golgi. Some E1 protein is localized to the *trans*-Golgi network; however, a fair amount of E1 does not co-stain with any of the secretory pathway markers used. The presence of E1 protein in the ER and *cis*- and *trans*-Golgi leaves open

the possibility that Q1/E1 complex assembly in HEK cells may not be confined to the early compartments of the secretory pathway. This series of experiments suggests that the majority of the E1 protein in HEK cells exits the ER but is trapped in the *trans*-Golgi or is trafficked to another compartment in the cell. Redistribution of E1 peptides to intracellular vesicles may be an ancillary mechanism that occurs in HEK cells to redirect unassembled, mature E1 peptides to recycling and degradation compartments.

These contrasting results suggest that there are inherent differences in KCNE trafficking in HEK *versus* CHO or COS-7 cells. Traditionally, the biochemical investigation of K^+ channel α- and β-subunits has been performed in HEK cells because copious amounts of protein can be generated; however, these cells have been avoided for electrophysiological studies because endogenous voltage-gated K^+ currents can be measured (Jiang et al. 2002). It is now known that some of these K^+ channels can assemble with KCNE peptides, including E1 (Lewis et al. 2004). The presence of native K^+ channels in HEK cells could explain the enigmatic trafficking of E1. In HEK cells, E1 peptides do not reach the plasma membrane unaccompanied but assemble with endogenous K^+ channel subunits in the secretory pathway. This inference harkens back to the initial discovery of E1 by expression cloning in *Xenopus* oocytes, where exogenously introduced E1 peptides assembled with endogenous Q1 channel subunits and trafficked to the plasma membrane producing the cardiac I_{Ks} current (Takumi et al. 1988; Folander et al. 1990). The low cell surface expression of E1 supports the idea that it forms complexes with limiting amounts of endogenous K^+ channel subunits. However, the lack of immature E1 observed in our immunoblots suggests that protein overexpression may also

contribute to the artificial ER exit of E1 in HEK cells. Whether cell surface expression of E1 is mediated by endogenous K^+ channels or by overwhelming the retention/retrieval machineries of the cell, studying the assembly and trafficking of KCNE peptides in HEK cells should be avoided.

The ER has two well known mechanisms for retaining misfolded and unassembled protein subunits: recognition of ER retention/retrieval signal sequences and chaperone-mediated retention of N-linked glycoproteins. The best studied ER retention signal to date is the RXR motif, which has been shown to regulate the ER exit of K_{ATP} channel subunits and sulfonylurea receptors (Zerangue et al. 1999). ER retention through this motif is a stringently controlled mechanism because neither protein can escape the ER with this signal sequence exposed. E1 peptides do not possess such a motif nor are they exquisitely retained in the ER when overexpressed in CHO or COS-7 cells, because faint bands that corresponded to mature glycoprotein were always observed with solitary expression of E1 (Figs. 2.1 and 2.2). Because we also observe some E1 protein in the *cis*-Golgi, it is possible that E1 is subject to ER retrieval. E1 does possess a KK*XX* sequence, which is a known ER retrieval signal sequence (Ellgaard and Helenius 2003); however, the juxtaposition of this motif to the transmembrane domain suggests that it may function only as a membrane stop transfer signal (Shikano and Li 2003). It is likely that E1 peptides are, in part, retained in the ER via their N-linked glycans through the calnexin/calreticulin quality control pathway, which has been shown to aid in the stability and ER exit of K^+ channel α-subunits (Khanna et al. 2004). A calnexin/calreticulin association with the E1 N-terminus would also explain the lack of ER staining that we

observed with the extracellularly HA-tagged E1 construct, which necessitated repositioning of the tag. If E1 peptides are retained in the ER by calnexin or calreticulin, this mechanism would be applicable to all KCNE peptides because the N-linked consensus site closest to the N-terminus is conserved throughout the family. It is also feasible that multiple retention/retrieval machineries are acting on unassembled E1 peptides or that Q1/E1 co-assembly promotes active export of the complex from the ER.

The goal in preventing unassembled K^+ channel α- and β-subunits from leaving the ER is to ensure the formation of fully assembled K^+ channel complexes because unpartnered K^+ channels would have inappropriate gating and ion conducting properties. Although our results show that unpartnered E1 peptides reside primarily in the ER, homotetrameric Q1 channels have been shown to exit the ER and function at the plasma membrane in several different ion channel expression systems, including CHO and COS-7 cells (Pusch et al. 1998; Tinel et al. 2000; Melman et al. 2001). In E1 knock-out mice, however, Q1 channels do not traffic to the apical membranes of vestibular dark cells, where they would normally be found with E1 in wild type cells (Nicolas et al. 2001). In addition, RNA interference experiments in *C. elegans* suggest that the stability of the K^+ channel complex is dependent on the presence of both pore-forming and KCNE-like subunits (Bianchi et al. 2003). The discordant observation of unpartnered Q1 channels at the cell surface in expression systems may be due to Q1 channels leaking from the ER as a result of overexpression. Consistent with swamping the ER with overexpressed protein is the fact that the majority of the Q1 protein in expression systems is intracellular (Schroeder et al. 2000). Moreover, Q1 expressed in *Xenopus* oocytes or CHO cells is not

N-linked glycosylated (Gage and Kobertz, unpublished data) and thus not subject to glycosylation dependent ER retention. An alternative explanation for the ER exit of unpartnered Q1 channels is that E1 protein synthesis always precedes Q1 subunit expression in native tissues. With this temporal control, the ER is always chock full of E1 peptides that can readily assemble with newly synthesized K^+ channel subunits. This mechanism alleviates the need to retain unpartnered Q1 channels as long as the rate of co-assembly with E1 is faster than ER exit of the homotetrameric channel. There is some *in vivo* evidence in the developing ear to support this notion, because E1 protein is expressed in embryonic mouse vestibular dark cells 24 h before the Q1 protein (Nicolas et al. 2001).

Many studies have shown that modulation of voltage-gated K^+ channels by KCNE peptides provides the functional diversity required for these complexes to work in the nervous system, muscle, colon, ear, and heart; however, for proper biological function these complexes must reach the plasma membrane fully assembled. Our results show that E1 peptides cannot advance past the *cis*-Golgi until they associate with Q1 channel subunits, which is the first step in the assembly and trafficking of KCNE-K^+ channel complexes. Given that mutations in KCNE peptides affect the assembly and trafficking of the entire K^+ channel complex and cause long QT syndrome, identifying the cellular machineries that directly ensure the proper assembly and trafficking of healthy K^+ channel/KCNE complexes will be critical for following and interpreting the aberrant assembly and trafficking of diseased complexes.

EXPERIMENTAL PROCEDURES

Plasmids and cDNAs—Human Q1 and E1 were subcloned into pcDNA3.1 (–) (Invitrogen). Two hemagglutinin A (HA)-tagged versions of E1 were used. For cell surface immunofluorescence experiments, an extracellular HA tag (YPYDVPDYA) was incorporated in the E1Nterminus between residues 22 and 23 based on the work of Wang and Goldstein (Wang and Goldstein 1995). For intracellular immunolocalization experiments, an HA tag was appended to the E1 C-terminus via a SGSG linker.

Cell Culture and Transfections—Chinese Hamster Ovary-K1 (CHO) cells were cultured in F-12K nutrient mixture (Invitrogen). HEK cells and African green monkey kidney (COS-7) cells were cultured in Dulbecco‘s modified Eagle‘s medium (Sigma). All of the media were supplemented with 10% fetal bovine serum (Hyclone) and 100 units/ml penicillin/streptomycin (Invitrogen). For biochemical analysis, the cells were plated at 60–75% confluency in 35-mm dishes. After 24 h, the cells were transiently transfected at room temperature with E1 alone, Q1/E1, or Q4/E1 at a ratio of 0.5 μg/1.5 μg with 8 μl of Lipofectamine (Invitrogen) for CHO cells or at a ratio of 0.25 μg/0.25 μg (COS-7 cells), 1.25 μg/2.5 μg (HEK cells) with 10 μl of Lipofectamine 2000 (Invitrogen). Empty pcDNA3.1 (–) plasmid DNA (0.5 μg for CHO, 0.25 μg for COS-7, and 1.25 μg for HEK) was co-transfected in samples containing only E1 DNA to keep the total transfected DNA constant in all wells. To increase the amount of E1 protein with complex glycans in CHO cells, 0.75 μg of Q1 DNA was used in the co-transfection. For immunofluorescence studies, the cells were plated at 50% confluency onto sterile 12-mm glass coverslips (untreated for CHO cells, poly-D-lysine treated for HEK cells) in 24-well plates. For cell

surface immunofluorescence, the cells were transiently transfected with E1 alone, Q1/E1, or Q4/E1 by scaling down the DNA (optimized ratio for CHO cells) and lipid levels by one-fifth; 0.2 μg of a vector containing green fluorescent protein was co-transfected to serve as a transfection control. For co-localization with ER and *cis*-Golgi markers, 0.3 μg of E1 was transfected; to visualize *trans*-Golgi, 0.3 μg of $EYFP_{Golgi}$ (Clontech) was also transfected. Co-localization studies were performed 24 h post-transfection. For all other experiments, the cells were used 48 h post-transfection.

Cell Lysis and Western Blot Analysis—The cells were washed in ice-cold PBS (3 x 2 ml) and lysed at 4°C in three different detergent buffers: 1% SDS lysis buffer (10 mM Tris·HCl, pH 7.5, 150 mM NaCl, 1 mM EDTA, 1% SDS (w/v)), 1.5% digitonin lysis buffer (20 mM Tris·HCl, pH 7.4, 140 mM NaCl, 10 mM KCl, 1 mM $MgCl_2$, 1.5% digitonin), and RIPKA lysis buffer (10 mM Tris·HCl, pH 7.4, 140 mM NaCl, 10 mM KCl, 1 mM EDTA, 1% Triton X-100, 0.1% SDS, 1% sodium deoxycholate). All of the detergent buffers were supplemented with protease inhibitors, 1 mM phenylmethylsulfonyl fluoride, and 1 μg/ml each of leupeptin, pepstatin, and aprotinin. For expression gels, CHO cells were lysed in 300 μl of 1% SDS buffer, and COS-7 cells were lysed in 250 μl of RIPKA buffer. Cell debris was pelleted in a microcentrifuge (16,100 x *g* for 10 min at room temperature). The supernatants were diluted with SDS-PAGE loading buffer containing 100 mM dithiothreitol, separated on a 15% SDS polyacrylamide gel, and transferred to nitrocellulose (0.2 μ; Schleicher & Schuell). The membranes were blocked in Western blocking buffer (5% nonfat dry milk in Tris-buffered saline containing 0.2% Tween 20 (TBS-T)) for 30 min at room temperature and

then incubated with rat anti-HA (Roche Applied Science) (1:750) in Western blocking buffer overnight at 4°C. The membranes were washed in TBS-T (four times for 5 min) and incubated with goat anti-rat horseradish peroxidase-conjugated antibody (Santa Cruz Biotechnology, Inc.) (1:2000) in Western blocking buffer for 45 min at room temperature. The membranes were subsequently washed with TBS-T (four times for 5 min). Horseradish peroxidase-bound proteins were detected by chemiluminescence using SuperSignal West Dura Extended Duration Substrate (Pierce) and a Fujifilm LAS-3000 CCD camera.

Endo H and PNGase F Deglycosylation Analysis—The cell lysates (30 µl) were diluted to 0.5% SDS with water and raised to 1% Nonidet P-40 (for PNGase F analysis only), 1% β-mercaptoethanol, 50 mM sodium citrate, pH 5.5 (for EndoH analysis) or 50 mM sodium phosphate, pH 7.5 (for PNGase F analysis) and then digested with Endo Hf (1 µl) or PNGase F (2 µl) (New England BioLabs, Inc.) for 30 min at 37°C. The samples were then raised to 100 mM dithiothreitol and 3.5% SDS before resolving by SDS-PAGE (15% gel) and analyzed by Western blot.

KCNE1 Co-immunoprecipitation—Cells were washed in ice-cold PBS (3 x 2 ml) and lysed at 4 °C in 250 µl of 1.5% digitonin buffer. The cell debris was pelleted in a microcentrifuge (16,100 x *g* for 15 min at room temperature). 30 µl of cell lysate was incubated with 5 µl of anti-Q1 antibody (Santa Cruz Biotechnology, Inc.) for 2 h at room temperature. The samples were bound to protein G beads (Pierce) for 2 h at room temperature to separate out antibody-bound protein complexes from the cell lysate. The

beads were washed (three times with 500 µl) in digitonin-free wash buffer (20 mM Tris·HCl, pH 7.4, 140 mM NaCl, 10 mM KCl, 1 mM $MgCl_2$. Co-immunoprecipitated proteins were eluted from the beads using 1x SDS-PAGE loading buffer with 200 mM dithiothreitol for 15 min at room temperature. One-fifth of the total input used for the co-immunoprecipitation assay and eluted proteins were resolved by SDS-PAGE (15% gel) and analyzed by Western blot.

Immunofluorescence—For visualization of intact cells, the cells were first labeled with rat anti-HA antibody (1:200) in culture medium for 30 min at 37°C. The cells were rinsed quickly in warm PBS (3 x 2 ml) before fixing in 4% paraformaldehyde (10 min at room temperature). The cells were then blocked in blocking solution (PBS containing 5% normal goat serum (Vector Laboratory, Inc.), 1% IgG-free bovine serum albumin (Sigma)) for 30 min at room temperature. For permeabilized samples, the cells were first washed in PBS (3 x 2 ml) and then fixed in 4% paraformaldehyde (10 min at room temperature). The cells were blocked in Triton blocking buffer (blocking solution containing 0.2% Triton X-100) and then incubated with rat anti-HA antibody (1:500) in Triton blocking buffer for 1 h at room temperature. Non-permeabilized and permeabilized samples were then washed with PBS (3x5 min) and incubated with goat anti-rat Alexa Fluor 594-conjugated antibody (Molecular Probes) (1:2000) in blocking solution or Triton blocking solution, respectively, for 45 min at room temperature. The cells were then washed with PBS (two times for 5 min; then for 1 h). The coverslips were dried at 37°C for 45 min before mounting on slides with ProLong® Gold Antifade mounting solution (Molecular Probes). For co-staining with intracellular markers, the

cells were fixed in 100% methanol at –20°C for 8 min, rehydrated in PBS for 5 min, and blocked overnight in SeaBlock Blocking buffer (Pierce). The cells were first incubated with rabbit anti-calnexin (Stressgen) (1:500) or concentrated mouse serum from monoclonal antibody CM1A10 for β‘- coatomer protein (anti-β‘COP) (Palmer et al. 1993; Gomez et al. 2000) (1:10) in SeaBlock Blocking buffer at room temperature for 90 min. The cells were then washed with PBS (3 x 10 min) and incubated with donkey anti-rabbit Alexa Fluor 488-conjugated antibody (1:500) or donkey anti-mouse Alexa Fluor 488-conjugated antibody (1:250) (Molecular Probes) in SeaBlock blocking buffer at room temperature for 90 min. The cells were washed in PBS (three times for 10 min) and labeled for E1 as described above with rat anti-HA (1:100) followed by goat anti-rat Alexa Fluor 594-conjugated antibody (1:500) in SeaBlock blocking buffer. After a final set of PBS washes (three times for 10 min), the coverslips were mounted on slides with Vectashield® mounting medium (Vector Laboratories). All of the cells were visualized using a Zeiss Axiovert 200M microscope with a 63x 1.4 N.A. oil immersion objective. *z* stacks were generated by obtaining optical sections through the samples 0.4 μm apart along the *z* axis. Deconvolution of *z* stack images was performed with a constrained iterative algorithm on Slidebook 4.0 software (Intelligent Imaging Innovations) using a measured point spread function. The images are displayed as single 0.4-μm planes through the center of each cell.

Cell Surface Biotinylation—Cells were rinsed with ice cold PBS^{2+} buffer (four times with 2 ml; PBS containing 1 mM $MgCl_2$, 0.1 mM $CaCl_2$) at 4°C to arrest membrane internalization. The cells were then incubated with 1 mg/ml sulfo-NHS-SS-biotin (Pierce)

in PBS^{2+} buffer twice for 15 min at 4°C. To quench the excess biotinylation reagent, the cells were washed quickly (three times with 2 ml) with quench solution (PBS^{2+} containing 100 mM glycine) and then incubated with quench solution twice for 15 min at 4°C. The cells were lysed in RIPKA buffer for 30 min at 4°C. Cell debris was removed by centrifugation (16,100 x *g* for 10 min at 4°C). Total protein in each sample was quantitated by BCA analysis. Of these samples, 75 µg of total protein was separated by affinity chromatography on 25 µl of Immunopure® immobilized streptavidin beads (Pierce) overnight at 4°C, whereas 15 µg was saved as an input control to determine the percentage of biotinylated proteins. The beads were washed (three times with 500 µl) in 0.1% SDS wash buffer (10 mM Tris·HCl, pH 7.4, 150 mM NaCl, 1 mM EDTA, 0.1% SDS). Biotinylated proteins were eluted from the beads using 2xSDS-PAGE loading buffer with 200 mM dithiothreitol for 15 min at 55°C. The inputs and eluted proteins were resolved by SDS-PAGE (15% gel) and analyzed by Western blot. The images of nonsaturated bands were captured on a Fujifilm LAS-3000 CCD camera, and the band intensities were quantitated using MultiGauge V2.1 software (FujiFilm). An ER-resident protein, calnexin, was used as a control to determine the percentage of cell rupture that occurred during the labeling process. Background cell lysis was quantitated as a ratio of biotinylated calnexin protein to total input calnexin. The percentage of E1 protein on the cell surface was calculated from the ratio of avidin-bound protein to total input protein after background lysis subtraction.

CHAPTER III

POST-TRANSLATIONAL N-GLYCOSYLATION OF KCNE1 PEPTIDES: IMPLICATIONS FOR MEMBRANE PROTEIN ASSEMBLY IN THE ENDOPLASMIC RETICULUM

ABSTRACT

N-linked glycosylation of membrane proteins is critical for their proper folding, co-assembly and subsequent migration through the secretory pathway. Here we examine the kinetics and efficiency of N-linked glycan addition to type I transmembrane KCNE1 K^+ channel β-subunits, where mutations that prevent N-glycosylation give rise to disorders of the cardiac rhythm and congenital deafness. We show that KCNE1 has two distinct N-linked glycosylation sites: a traditional co-translational site and a consensus site ~20 residues away that unexpectedly acquires N-linked glycans after protein synthesis (post-translationally). Mutations that prevent N-glycosylation at the co-translational site concomitantly reduce post-translational glycosylation, resulting in a large population of unglycosylated KCNE1 peptides that do not reach the cell surface with their cognate K^+ channel. This long range disruption of post-translational N-glycan addition directly explains how a single point mutation can prevent N-glycosylation at multiple consensus sites, providing a new biogenic mechanism for human disease. These results demonstrate that post-translational N-glycosylation in the endoplasmic reticulum

is a cellular mechanism that ensures type I transmembrane proteins acquire the maximal number of glycans needed for proper complex assembly and trafficking.

INTRODUCTION

Asparagine-linked (N-linked) glycosylation is a highly conserved protein modification that eukaryotic cells utilize for the proper folding, assembly and trafficking of membrane and secreted proteins. The initial attachment of N-linked glycans to polypeptides occurs in the endoplasmic reticulum (ER), where the oligosaccharyltransferase (OST) complex efficiently transfers a high mannose oligosaccharide onto asparagine residues within the primary consensus sequence N-X-T/S-Y (sequon, where X and Y can be any natural amino acid other than proline) (Marshall 1972; Silberstein and Gilmore 1996). Although commonly referred to as a post-translational protein modification, N-linked glycosylation in mammalian cells typically occurs during translation as the nascent polypeptide is threaded through the translocation tunnel into the ER lumen (Weerapana and Imperiali 2006). Recently, however, one of the mammalian isoforms (STT3B) of the active site subunit of the ER resident OST complex has been shown to mediate post-translational N-glycosylation of a secreted protein, human blood coagulation factor VII (Ruiz-Canada et al. 2009). To date, factor VII is the only reported full-length protein that is post-translationally N-glycosylated in mammalian cells with intact N-glycosylation machinery (Bolt et al. 2005). Factor VII curiously contains two distinct sequons: one sequon is modified co-

translationally whereas the second sequon is modified post-translationally, yet the biological significance of a protein harboring both a co- and post-translational sequon is unclear.

Besides the structurally-distorting proline residue, three other factors can reduce or eliminate N-glycosylation of sequons: (1) Residues at the X-position – NXS sequons with negatively-charged (Asp and Glu) and hydrophobic (Trp and Leu) at the X-position are poorer substrates for the OST complex (Shakin-Eshleman et al. 1996; Kasturi et al. 1997); (2) Proximity to the C-terminus – sequons within ~60 residues of the C-terminus often elude the OST complex, as the chain-terminated protein is believed to more rapidly enter the ER lumen through the translocation tunnel (Nilsson and von Heijne 2000); (3) Proximity to a transmembrane domain – sequons that are less than 12 residues away from a transmembrane segment are inaccessible to the OST active site (Nilsson and von Heijne 1993; Cheung and Reithmeier 2007). Bioinformatic interrogation of the residues flanking sequons (up to 20 residues) has not identified any other sequence motifs that have long range effects on N-glycosylation efficiency (Gavel and von Heijne 1990; Ben-Dor et al. 2004).

KCNE1 (E1) is the founding member of a family of type I transmembrane K^+ channel β-subunits that have multiple sequons in their extracellular N-termini. E1 peptides have two sequons at N5 and N26, both of which are obligatorily glycosylated in native tissues as well as in standard electrophysiological expression systems (Finley et al. 2002; Chandrasekhar et al. 2006; Teixeira et al. 2006). E1 co-assembles with KCNQ1

(Q1) K^+ channels to produce the slowly activating cardiac I_{Ks} current (Barhanin et al. 1996; Sanguinetti et al. 1996) and to recycle potassium in apical membranes of strial marginal and vestibular dark cells in the inner ear (Wangemann 2002). A mutation that disrupts the sequon at N5 (T7I), gives rise to an inherited autosomal recessive form of Long QT Syndrome (LQTS), a disorder of the cardiac rhythm that is accompanied with neural deafness, Jervell and Lange-Nielsen Syndrome (JLNS) (Schulze-Bahr et al. 1997). A single nucleotide polymorphism in the equivalent threonine in KCNE2 (T8A) provokes drug-induced LQTS with the commonly prescribed antibiotic, sulfamethoxazole (Sesti et al. 2000; Park et al. 2003). However, the biogenic mechanism that underlies the importance for glycosylation at this absolutely conserved sequon remains to be elucidated.

Given the genetic linkage between N-glycosylation and KCNE biology, we determined the efficiency and kinetics of N-glycosylation of the two closely-spaced sequons in E1 and the effects of N-glycan occupancy on co-assembly with K^+ channel subunits and cell surface expression. By comparing wild type to a panel of E1 glycosylation mutants in metabolic labeling experiments, we found that the N-terminal sequon (N5) acquires its N-linked glycan during translation whereas the second glycan is primarily added to the internal sequon (N26) post-translationally. In contrast to wild type E1 peptides, mutants lacking the co-translational site are poorer substrates for post-translational glycosylation. Moreover, E1 subunits harboring the LQTS-associated mutation, T7I, exit the translocation tunnel unglycosylated where co-assembly with Q1 inhibits post-translational glycosylation. These results provide a new biogenic mechanism

for channelopathies and demonstrate a need for post-translational glycosylation of membrane proteins in the endoplasmic reticulum.

RESULTS

N-glycan Occupancy of KCNE1 Sequons

The addition of N-linked glycans via the OST complex to nascent polypeptides in the ER translocation tunnel is conserved from yeast to humans. Accordingly, the initial attachment of N-linked glycans to the two N-terminal sequons in E1 is identical in a wide range of cells from native (cardiomyocytes and inner ear cells) to traditional expression systems (*Xenopus* oocytes, HEK-293, CHO-K1 and COS-7 mammalian cells) (Gage and Kobertz 2004; Chandrasekhar et al. 2006; Teixeira et al. 2006; Wu et al. 2006). To examine the two N-linked glycoforms of E1 individually (Fig. 3.1A), we made an initial panel of single glycosylation mutants that would result in glycan addition to either the N-terminal sequon (N26Q) or the internal sequon (N5Q, T7I) and compared them to wild type E1 (WT). We first examined these E1 mutants without a cognate K^+ channel in order to follow N-glycosylation without interference from co-assembly with K^+ channel subunits. To do this, we expressed these E1 constructs in CHO-K1 cells since these cells lack endogenous voltage-gated K^+ channel subunits that assemble with E1 peptides (Chandrasekhar et al. 2006). Transient expression of a C-terminal, HA-tagged WT E1 peptide yielded two strong bands at 17 and 23 kDa on a Western blot (Fig. 3.1B, left), which we confirmed with enzymatic deglycosylation (Fig. 3.2) were the unglycosylated

A

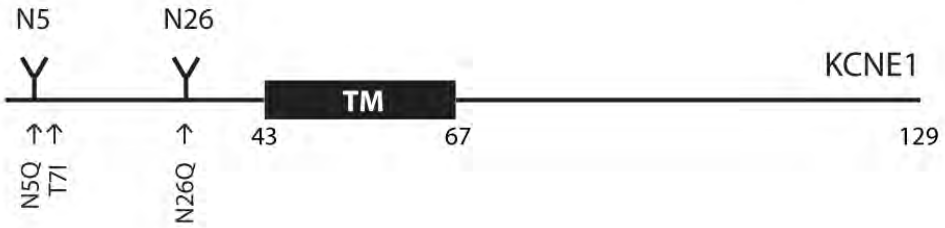
N5
N26
KCNE1
TM
43
67
129
N5Q
T7I
N26Q

B

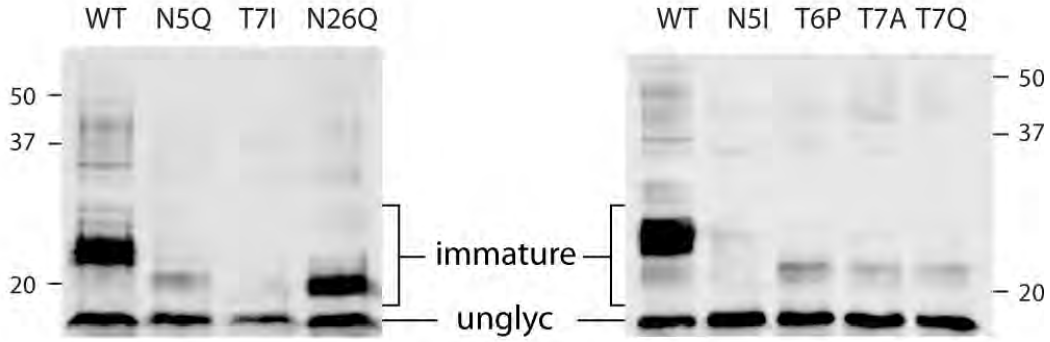
WT
N5Q
T7I
N26Q
WT
N5I
T6P
T7A
T7Q
50
37
20
immature
unglyc

C

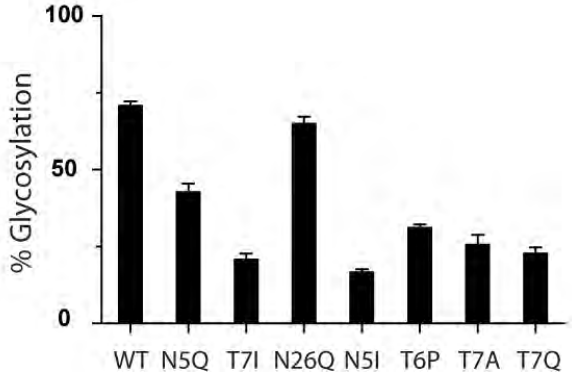
% Glycosylation
100
50
0
WT
N5Q
T7I
N26Q
N5I
T6P
T7A
T7Q

Figure 3.1 Differential N-linked glycosylation of WT and mutant KCNE1 peptides. (**A**) Schematic representation of KCNE1. The glycosylation mutants N5Q, T7I and N26Q are indicated by arrows. TM, transmembrane domain. (**B**) Immunoblots of WT and glycosylation mutant E1 peptides from solubilized CHO cells. 30 μg of total protein was loaded per lane. Immature and unglycosylated (unglyc) are denoted. (**C**) Bar graph of the percentage of glycosylated WT and mutant E1 peptides. Error bars are SEM from n = 3 – 6 immunoblots.

and immaturely N-linked glycosylated peptides, respectively (Chandrasekhar et al. 2006). Ablation of the N-terminal sequon (N5Q, T7I) unexpectedly prevented glycosylation of the internal sequon, resulting in mostly unglycosylated protein. In contrast, disruption of the internal sequon (N26) had no significant effect on glycosylation of the N-terminal sequon, though as expected, the mono-glycosylated protein migrated faster than doubly-glycosylated WT.

Since there was a difference in hypoglycosylation between the hydrophilic N5Q and hydrophobic T7I mutants (Fig. 3.1C), we disrupted the N-terminal sequon with various residues to determine how mutations at the N-terminal sequon affect glycosylation at the internal site 20 residues away. Substitution of asparagine for isoleucine (N5I) reduced glycosylation at the internal site similarly to T7I (Fig. 3.1B, right). Mutation to residues less hydrophobic than isoleucine (T7A or T7Q) afforded slightly more glycosylated E1 peptide than the isoleucine mutants; however, the differences were not statistically significant (Table 3.1). Distorting the N-terminal sequon with proline (T6P) had an intermediate reduction in glycosylation, falling significantly between the isoleucine mutants and N5Q. This trend (T7I, N5I > T6P > N5Q > WT) suggests that a hydrophobic disruption of the N-terminal sequon has a long range affect on glycosylation of the internal site, resulting in an accumulation of unglycosylated E1 peptides.

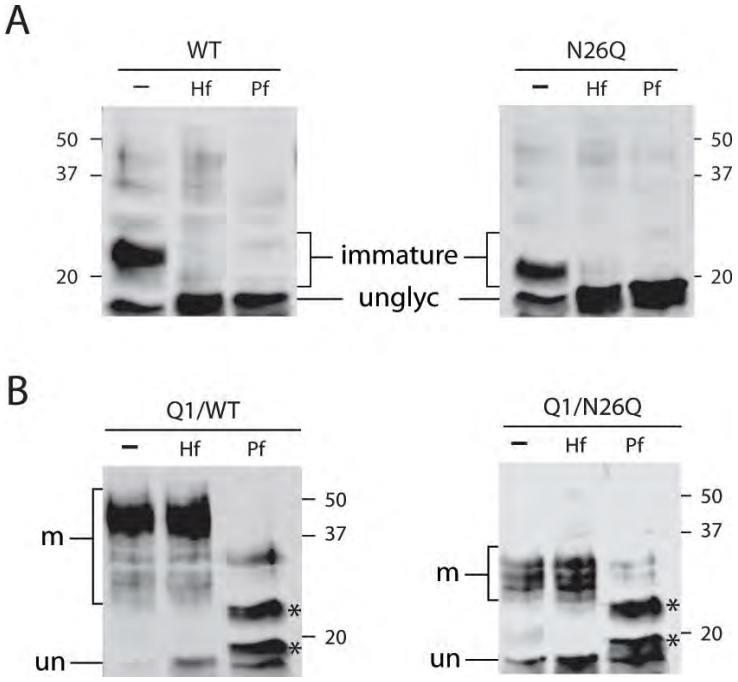

Figure 3.2 Identification of the mature, immature and unglycosylated WT and N26Q KCNE1 peptides. Immunoblots are from enzymatic deglycosylation of WT and N26Q KCNE1 peptides. The samples were left untreated (–), digested with Endo H (H_f) or PNGase F (P_f). (**A**) E1 peptides expressed alone. Endo H susceptibility of the 23 kDa band (WT) and the 20 kDa band (N26Q) identified these bands as immaturely glycosylated E1 protein, which collapsed to the ~17 kDa unglycosylated form (unglyc; un). (**B**) Q1/E1 co-expression resulted in the appearance of higher molecular weight bands: WT: ~40 kDa; N26Q: 25-30 kDa. Resistance to Endo H, but susceptibility to PNGase F identified these higher molecular weight bands as peptides with mature N-linked glycans (m). As was previously reported (Chandrasekhar et al., 2006), exhaustive digestion with PNGase F results in a series of bands (denoted by asterisks) that are the result of an additional unidentified post-translational modification.

Table 3.1 Statistical Analysis of Glycosylation Mutants[1]

	WT	N26Q	N5Q	T6P	T7A	T7Q	N5I	T7I
WT		ns	***	***	***	***	***	***
N26Q	ns		***	***	***	***	***	***
N5Q	***	***		*	***	***	***	***
T6P	***	***	*		ns	ns	**	*
T7A	***	***	***	ns		ns	ns	ns
T7Q	***	***	***	ns	ns		ns	ns
N5I	***	***	***	**	ns	ns		ns
T7I	***	***	***	*	ns	ns	ns	

[1]Data are from 3 – 6 individual experiments. Tukey's multiple comparison test was used to determine the significantly differently glycosylated mutants as ***, $p < 0.0001$; **, $p < 0.01$; *, $p < 0.05$ (one-way ANOVA with Tukey post-hoc analysis). ns indicates the values were not significantly different from each other ($p > 0.05$).

Cellular Stabilities of WT and Mutant KCNE1 Peptides

To identify the cellular mechanism responsible for the large population of unglycosylated protein observed with the N-terminal sequon mutants (N5Q, T7I), we first determined whether the singly-glycosylated mutants had different protein stabilities. Cells expressing WT and mutant peptides were metabolically-labeled with ^{35}S for 10 min, chased with cold media, and the E1 peptides were isolated by immunoprecipitation at various time points (Fig. 3.3A). Since the zero time point is diluted with partially synthesized peptides (Hershey 1991), the 5 min chase point was defined as maximally-labeled protein for the glycosylation mutants; for WT, the 10 min time point was used due to the delay in protein decay (Fig. 3.3B). The total protein (unglycosylated and glycosylated) for each time point was normalized, plotted and fitted to a single exponential decay (Fig. 3.3B). Surprisingly, the WT and the single site glycosylation mutants had experimentally similar protein stabilities (Table 3.2). Moreover, this similarity in protein stability did not change when we measured the decay of just the singly-glycosylated form of N26Q. These results show that protein stability does not significantly contribute to the glycosylation ratios observed with the single site glycosylation mutants.

Co- and Post-translational N-Glycosylation of KCNE1 Peptides

We next determined whether the N-glycosylation rates of WT and the mutant E1 peptides were different. To follow the rapid kinetics of N-linked glycosylation, we

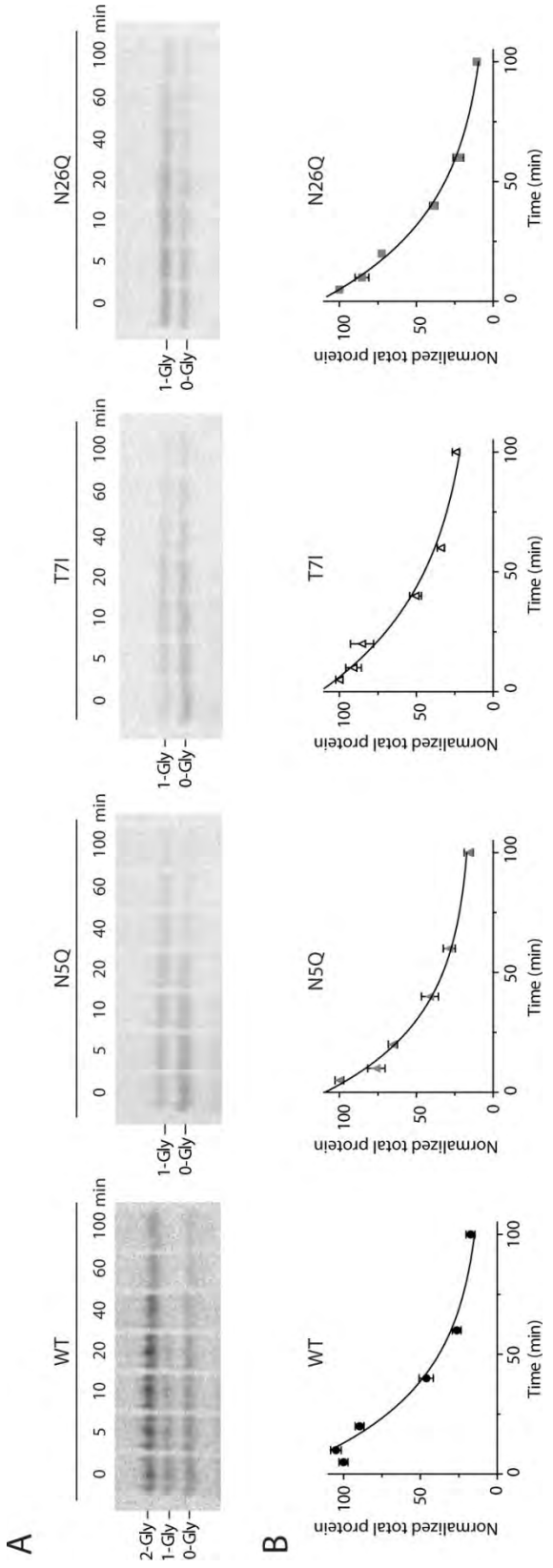
A
WT
N5Q
T7I
N26Q
0 5 10 20 40 60 100 min
2-Gly
1-Gly
0-Gly
B
Normalized total protein
Time (min)
0
50
100

Figure 3.3 Protein stability of WT and KCNE1 glycosylation mutants are similar. (**A**) Representative fluorographs for WT and glycosylation mutants. S^{35}-labeled CHO cells were chased for the indicated times and the E1 peptides were immunoprecipitated, separated by electrophoresis, and detected by autoradiography. 2-Gly: doubly glycosylated; 1-Gly: singly glycosylated; 0-Gly: unglycosylated. (**B**) Graphs of densitometric analysis. The total protein at each time point was quantified by densitometry, normalized to the total protein at 5 min (except WT: 10 min) and plotted versus chase time. WT: closed circles; N5Q: gray triangles; T7I: open triangles; N26Q: gray squares are mean ± SEM (n = 3 – 4) for each chase point for WT, N5Q, T7I and N26Q respectively. Data were fitted to a single exponential and rate of decay values are tabulated in Table 3.2.

Table 3.2 Protein decay and post-translational glycosylation rates of KCNE1 peptides[1]

KCNE1 peptide	Rate of decay (min)	Post-translational glycosylation (min)
WT	33 ± 4^{ns}	8.5 ± 2.0^{ns}
N5Q	33 ± 5^{ns}	15 ± 5
T7I	46 ± 3^{ns}	20 ± 4
N26Q	38 ± 2^{ns}	ND
N26Q (1-gly)	37 ± 3^{ns}	NA

[1]Data are from 3 – 5 individual experiments. Data were fitted to a single exponential. Values are mean ± SEM. ^{ns} indicates that the rates were not significantly different from each other (one-way ANOVA with Tukey post-hoc analysis ($p > 0.05$)) ND, not detectable; NA, not applicable.

metabolically-labeled cells using 2 min pulses. This shorter pulse allowed us to differentiate between co- and post-translational N-linked glycosylation since the translation of all of the E1 polypeptides initiated during the pulse will be completed by the 5 min chase (Hershey 1991). Figure 3.4A shows a time course for WT and mutant E1 peptides. At each chase time point, the different glycosylation states were plotted as a percentage of the total protein (Fig. 3.4B). For WT, the doubly-glycosylated form of the protein steadily increased whereas the singly- and unglycosylated forms decreased over the duration of the 20 min time course. The increase in doubly-glycosylated E1 after the 5 min chase indicates that N-linked glycans were attached after protein translation. Therefore, we used the E1 mutants to determine which N-linked glycosylation site(s) were responsible for the slower, post-translational glycosylation of WT. For N26Q, the singly glycosylated form of the protein was abundant within the first 5 minutes, consistent with N-linked glycan addition to the N-terminal sequon during translation. Conversely, N5Q and T7I were poorly glycosylated during the protein translation time window, resulting in predominantly unglycosylated protein. However for both N5Q and T7I, the singly glycosylated form exponentially increased over 5 – 20 min whereas the glycosylation state of N26Q remained constant after 5 min (Fig. 3.4B, Table 3.2). This kinetic difference in N-linked glycan addition identified the internal glycosylation site as a source of the post-translational glycosylation observed with WT. These results demonstrate that the glycosylation timing and efficiency at the two sequons on E1 are different: N-linked glycans are readily added to the N-terminal sequon during translation whereas glycosylation of the internal site is delayed and less efficient.

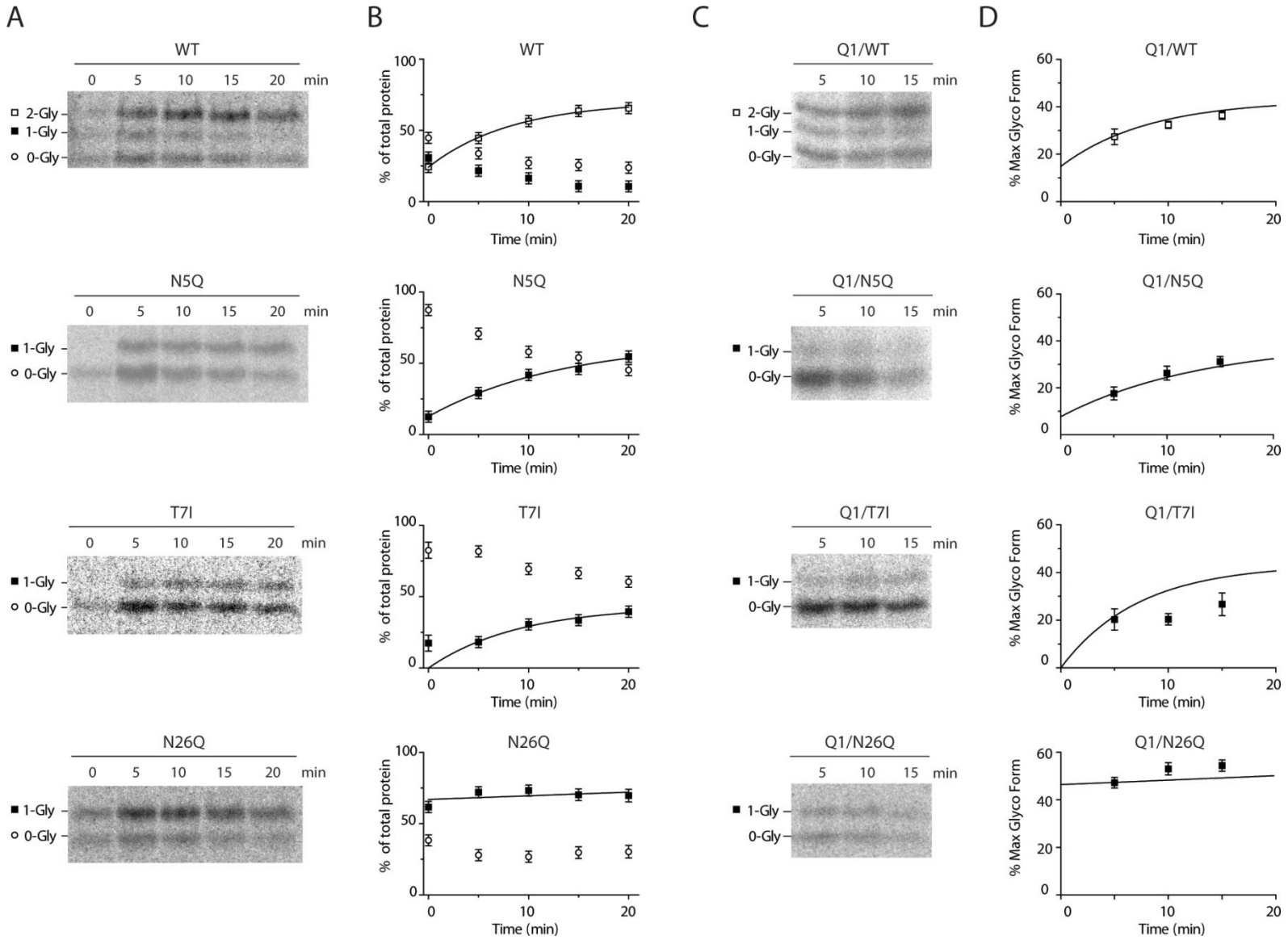
A
WT
0 5 10 15 20 min
2-Gly
1-Gly
0-Gly
N5Q
0 5 10 15 20 min
1-Gly
0-Gly
T7I
0 5 10 15 20 min
1-Gly
0-Gly
N26Q
0 5 10 15 20 min
1-Gly
0-Gly
B
WT
% of total protein
Time (min)
N5Q
% of total protein
Time (min)
T7I
% of total protein
Time (min)
N26Q
% of total protein
Time (min)
C
Q1/WT
5 10 15 min
2-Gly
1-Gly
0-Gly
Q1/N5Q
5 10 15 min
1-Gly
0-Gly
Q1/T7I
5 10 15 min
1-Gly
0-Gly
Q1/N26Q
5 10 15 min
1-Gly
0-Gly
D
Q1/WT
% Max Glyco Form
Time (min)
Q1/N5Q
% Max Glyco Form
Time (min)
Q1/T7I
% Max Glyco Form
Time (min)
Q1/N26Q
% Max Glyco Form
Time (min)

Figure 3.4 KCNE1 peptides are co- and post-translationally N-glycosylated. (**A, C**) CHO cells were pulsed for 2 min, chased for the indicated times and the E1 peptides were immunoprecipitated, separated by electrophoresis, and detected by autoradiography. Representative fluorographs for WT and E1 mutants expressed alone (**A**) and with Q1 channel subunits (**C**). (**B**) Graphs of densitometric analysis for Fig. 3.4A. The percentage of the different glycoforms with respect to total protein is plotted for each time point. After 5 min, the fully glycosylated forms of WT, N5Q and T7I increased whereas N26Q remained constant. The increase in glycosylation was fitted to a single exponential and tabulated in Table 3.2. N26Q is a linear fit for comparison purposes. Data (n = 3 – 5) are mean ± SEM for each chase point. (**D**) Graphs of densitometric analysis for Fig. 3.4C. The percentage of the maximally glycosylated form of WT (two) and the E1 mutants (one) with respect to total protein is plotted for each time point. The fits from Fig. 3.4B were scaled to compare the post-translational glycosylation rates in the presence of Q1 channel subunits (solid lines). Data (n = 3 – 5) are mean ± SEM for each chase point. Glycosylation states in all panels are labeled: 2-Gly: open square; 1-Gly: closed square; 0-Gly: open circle.

Since KCNE peptides are regulatory subunits that co-assemble with K^+ channel subunits in the ER (Krumerman et al. 2004; Chandrasekhar et al. 2006), we next determined whether the presence of K^+ conducting subunits affected the post-translational glycosylation of E1 peptides. Cells co-expressing Q1 channel subunits with WT and mutant E1 peptides were pulsed for 2 min and chased at different times to observe post-translational glycosylation (Fig. 3.4C). Although co-expression with Q1 channel subunits eventually leads to N-glycan maturation in the Golgi complex (*vide infra*), the chase time points needed to detect post-translational glycosylation are too short to observe mature glycosylated E1. Thus, in these experiments, the immature form of E1 is predicted to be the end glycoform as shown in Figure 3.4C. The maximally-glycosylated form of the E1 peptides in the presence of Q1 was calculated from the pulse chase data in Figure 3.4C, plotted in Figure 3.4D, and compared to post-translational glycosylation of solitary E1 peptides by re-plotting the curves from Figure 3.4B (solid lines). Co-expression with Q1 reduced the overall glycosylation efficiency of the E1 peptides; however, the rate of post-translational glycosylation of WT and N5Q was unaffected. As expected, the glycosylation of N26Q was also relatively unaffected by Q1 co-expression since this mutant primarily acquires its N-glycans during translation. In striking contrast, post-translational glycosylation of T7I was strongly inhibited, suggesting that co-assembly with Q1 channel subunits prevents the OST complex from attaching an N-linked glycan to the T7I internal sequon.

Consequences of KCNE1 Hypoglycosylation

We subsequently determined whether the compounded hypoglycosylation of the E1 mutants altered their ability to traffic to the cell surface with Q1 subunits. Given the contrasting differences in the current profiles between unpartnered Q1 channels and Q1/E1 complexes (Fig. 3.5A), we initially used electrophysiology to measure the function of WT and mutant Q1/E1 complexes. Unpartnered Q1 channels give rise to small currents that rapidly activate as well as inactivate with depolarization. In contrast, Q1/E1 complexes have larger currents that slowly activate over many seconds and show no measurable signs of inactivation. Thus, co-assembly with E1 bestows the Q1 channel with the appropriate properties to maintain the rhythmicity of the heartbeat and provide salt and water transport in the inner ear. Co-expression of Q1 with the glycosylation mutants afforded currents that were an amalgam of unpartnered Q1 channels (Fig. 3.5B, arrowheads) and Q1/E1 complexes. Since the amount of unpartnered Q1 currents varied from cell to cell for each individual mutant, we measured the currents from several cells and normalized current activity relationships for the E1 mutants to WT (Fig. 3.5C). The systematic decrease in maximal current of the glycosylation mutants followed the hypoglycosylation trend (Fig. 3.1C), consistent with fewer Q1/E1 complexes functioning at the cell surface.

To directly measure the plasma membrane expression of the mutant E1 peptides co-expressed with Q1 channel subunits, we used cell surface biotinylation. This biochemical approach also allowed for the identification of the E1 glycoforms present on

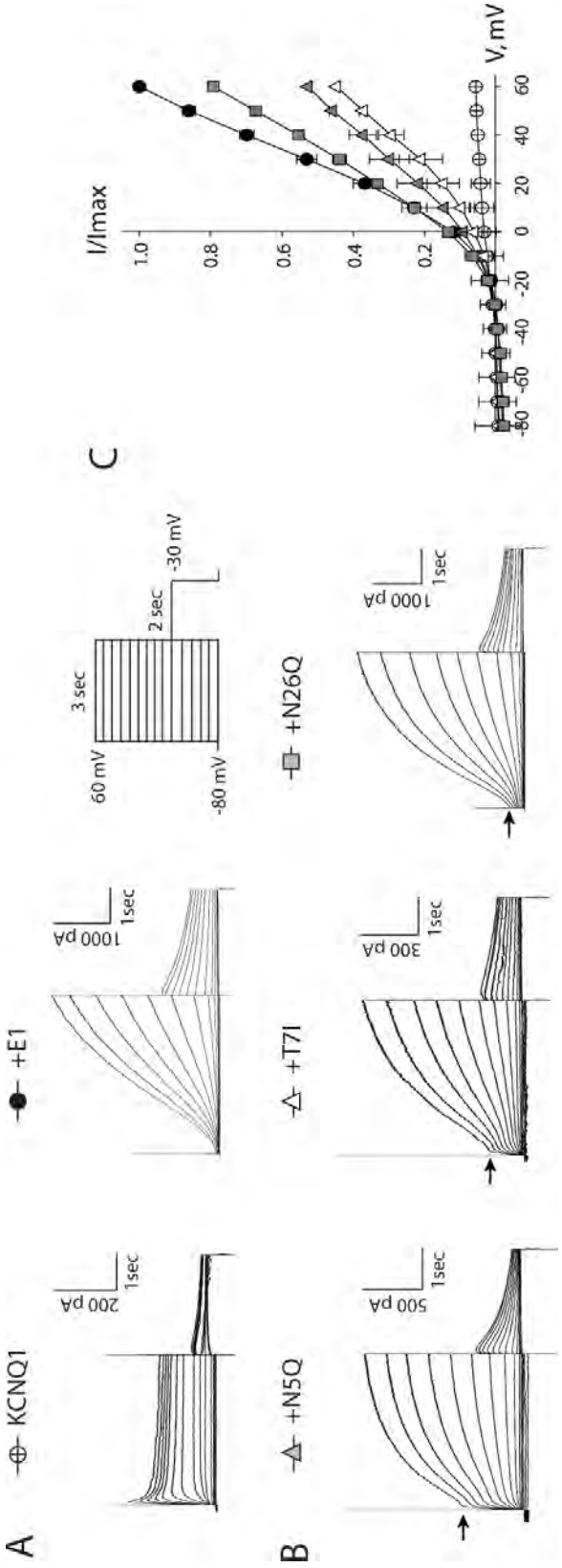
A
KCNQ1
200 pA
1sec
+E1
1000 pA
1sec
B
+N5Q
500 pA
1sec
+T7I
300 pA
1sec
+N26Q
1000 pA
1sec
C
60 mV
3 sec
2 sec
-30 mV
-80 mV
I/Imax
1.0
0.8
0.6
0.4
0.2
-80
-60
-40
-20
0
20
40
60
V, mV

Figure 3.5 Current properties of KCNQ1 channels co-expressed with KCNE1 glycosylation mutants. (**A**) Representative families of I_{Q1} and I_{Ks} currents recorded by perforated patch clamp from CHO cells using the following voltage protocol: the currents were evoked by 3-s depolarization pulses from a holding potential of -80 mV to test voltages –70 to +60 mV in 10-mV increments at an interpulse interval of 30 s. The depolarization pulses were followed by repolarization to –30 mV for 2 s to monitor tail currents. Cells were transfected with a KCNQ1 plasmid only (KCNQ1) or cotransfected with WT KCNE1 (+E1). (**B**) Representative families of currents recorded from cells expressing KCNQ1 and the KCNE1 mutants (+N5Q, +T7I or +N26Q). Arrowheads indicate current from unpartnered Q1 channels. (**C**) Relative mean peak currents (I/I_{max}) were normalized to the maximal WT I_{ks} (+E1) and plotted as a function of the pulse voltage (V). Data (n = 3 – 5) are mean ± SEM.

the plasma membrane. Cells expressing WT and mutant Q1/E1 complexes were labeled with a membrane impermeant, amine-reactive biotin reagent at 4˚C to prevent membrane recycling and minimize labeling of intracellular proteins. The biotinylated proteins were isolated with streptavidin beads (Beads) and normalized to their respective endogenous calnexin (CNX) signal (½ Input) to compare the cell surface expression of WT to the E1 mutants (Fig. 3.6). To verify that the cells remained intact during biotinylation, we also monitored the labeling of an ER-resident protein, calnexin – CNX (Beads), and subtracted out this background intracellular labeling to calculate the normalized cell surface expression in Figure 3.6B. E1 peptides with a single glycan attached to the N-terminal sequon (N26Q) had cell surface expression that was similar to WT (Fig. 3.6) and was dependent on co-expression with Q1 (Fig 3.7). In contrast, E1 mutants lacking the N-terminal sequon (N5Q, T7I) were challenging to detect at the plasma membrane even when they were co-expressed with Q1.

We next used enzymatic deglycosylation to determine which glycoforms of the mutants were present at the plasma membrane. As we have previously shown with WT Q1/E1 complexes, E1 peptides are post-translationally modified in the Golgi, resulting in a strong, but diffuse band centered between 37 and 50 kDa, which is due in part to the maturation of the N-linked glycans (Chandrasekhar et al. 2006). Using deglycosylation enzymes (Fig. 3.2B), we identified the unglycosylated, immaturely and maturely N-glycosylated forms of WT and mutant E1 peptides, which are denoted in Figure 3.6A. Although all three glycoforms of WT and the E1 mutants were present in the cells (Fig. 3.6A, ½ Inputs), only maturely N-glycosylated protein was detected at the cell surface

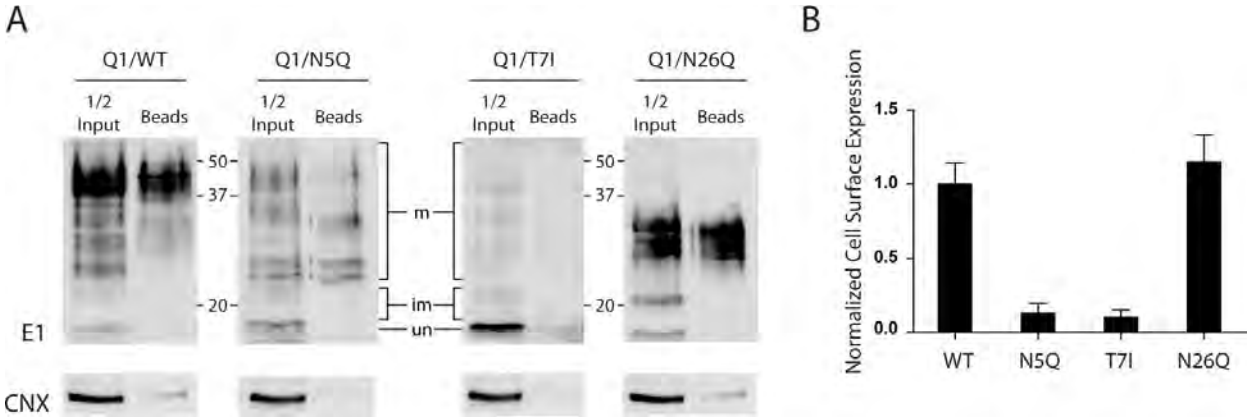
A
Q1/WT
Q1/N5Q
Q1/T7I
Q1/N26Q
1/2 Input
Beads
50
37
20
m
im
un
E1
CNX
B
Normalized Cell Surface Expression
1.5
1.0
0.5
0.0
WT
N5Q
T7I
N26Q

Figure 3.6 Mature KCNE1 glycopeptides reach the plasma membrane. (**A**) Representative immunoblots of WT and the glycosylation mutants co-expressed with KCNQ1. Transfected CHO cells were labeled with a membrane impermeable biotin reagent, lysed, and the biotinylated proteins were isolated with streptavidin beads. Lanes denoted as (½ input) are half the sample lysate that was set aside to quantitate the total amount of biotinylated proteins. (Beads) lanes represent the streptavidin-bound proteins that were isolated and separated by SDS-PAGE. The calnexin (CNX) immunoblots were used both to determine the amount of background lysis and to compare the cell surface expression of the mutants to WT. The mature (m), immature (im) and unglycosylated (un) forms of the E1 glycopeptides were identified by enzymatic deglycosylation (Fig. 3.2). (**B**) Quantification of the biotinylated E1 proteins on the cell surface. Band intensities for biotinylated E1 proteins were calculated as described in the Experimental Procedures and normalized to input calnexin for the corresponding data set. The error bars are SEM from n = 3 – 4 immunoblots.

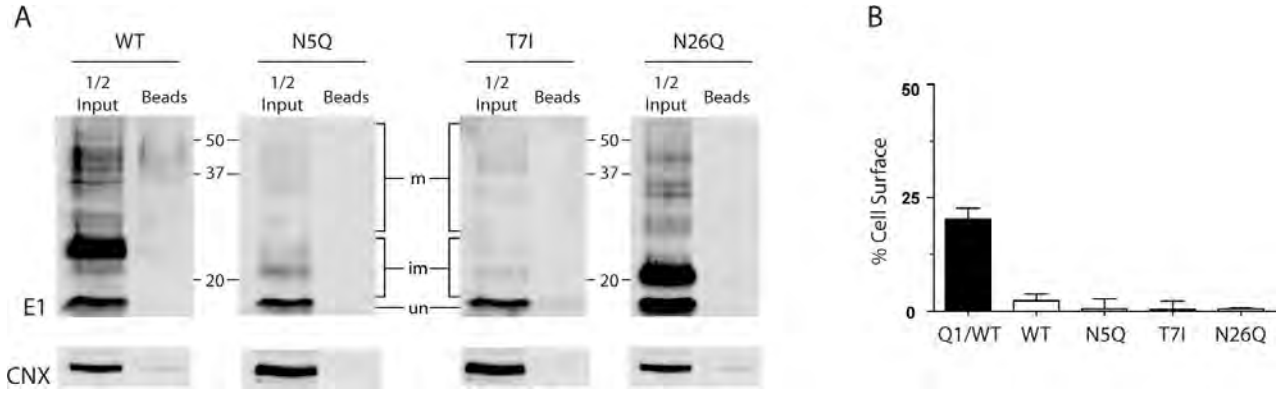

Figure 3.7 Cell surface expression of WT and mutant KCNE1 peptides requires KCNQ1 channels. (**A**) Representative immunoblots of WT and the glycosylation mutants. Transfected CHO cells were labeled with a membrane impermeable biotin reagent, lysed, and the biotinylated proteins were isolated with streptavidin beads. Lanes denoted as (½ input) are half of the sample lysate that was set aside to quantitate the total amount of biotinylated proteins. (Beads) lanes represent the streptavidin-bound proteins that were isolated and separated by SDS-PAGE. The calnexin (CNX) immunoblots were used to determine the amount of background lysis. The mature (m), immature (im) and unglycosylated (un) forms of the E1 glycopeptides were identified by enzymatic deglycosylation (Fig 3.2). (**B**) Quantification of the biotinylated E1 proteins on the cell surface. To obtain the percentage of E1 protein on the cell surface, the percentage of CNX labeling was subtracted from the percentage of biotinylated E1 protein, which was determined by dividing the band intensities in the beads lane by twice the band intensity in the corresponding half input lanes. Statistically, there was no cell surface expression of E1 peptides when expressed alone: WT: 2.3 ± 3%; N5Q: 0.5 ± 2.2; T7I: 0.3 ± 1.9; N26Q 0.5 ± 0.2 (open bars). Cell surface expression of WT E1 protein co-expressed with Q1 is

shown for comparison (Q1/E1: filled bar) where 20 ± 3% of the E1 protein is on the cell surface. The error bars are SEM from n = 3-4 immunoblots.

over background calnexin labeling. Moreover, the abundance of intracellular, unglycosylated T7I peptides in the presence of Q1 channel subunits is consistent with the inhibition of post-translational glycosylation of T7I in Figure 3.4D. In total, these results demonstrate that cell surface expression of E1 peptides requires the acquisition of at least one N-linked glycan to reach the plasma membrane. Thus, mutations that directly prevent co- and reduce post-translational N-glycosylation result in a large population of unglycosylated E1 peptides, which severely reduces the number of functional Q1/E1 channel complexes at the cell surface.

DISCUSSION

Motivated by the genetic evidence that the N-terminal sequon in KCNE peptides plays an important role in cardiac biology (Schulze-Bahr et al. 1997; Sesti et al. 2000; Park et al. 2003), we individually examined the kinetics and extent of N-linked glycosylation of the two E1 sequons. The results from our investigation provide four mechanistic insights into the biogenesis and N-glycosylation of these type I transmembrane peptides: (1) The two N-linked consensus sites on E1 are handled differently in the ER: glycans are added to the N-terminal sequon during translation whereas the glycans are predominately attached to the internal site after translation has been completed. (2) Post-translational glycosylation of E1 peptides lacking a co-translational site is less efficient, compounding hypoglycosylation and resulting in a majority of unglycosylated peptides. (3) Co-assembly with Q1 channel subunits

additionally inhibits post-translational glycosylation of some mutant E1 peptides. (4) Unglycosylated E1 peptides do not reach the cell surface with or without Q1 K^+ channels. Thus, mutations that inhibit co-translational N-glycosylation reduce the population of functioning Q1/E1 complexes at the cell surface, providing a biogenic mechanism for Long QT and Jervell and Lange-Nielsen Syndromes.

Post-translational Glycosylation of Properly Folded KCNE subunits

Post-translational glycosylation has been historically associated with cells with compromised N-glycosylation machinery (Duvet et al. 2002) or that express truncated glycoproteins (Kolhekar et al. 1998). All E1 constructs used here are full-length. Moreover, post-translational glycosylation affords the predominant glycoform of E1 – the doubly glycosylated form – which assembles with Q1 subunits to afford K^+ channel complexes that generate the hallmark cardiac I_{Ks} current (Fig. 3.5). Similarly, post-translational glycosylation of E1 is neither a cell-specific artifact nor a result of depleting the key components of the N-glycosylation pathway. Post-translational glycosylation of E1 was observed in several standard mammalian cell lines (Fig. 3.8A), consistent with the conservation of the STT3B subunit, which has been recently shown to attach N-glycans to secreted proteins after translation (Ruiz-Canada et al. 2009). Although exogenous expression of E1 was needed to generate a detectable protein signal, it did not saturate the co-translational machineries or deplete the dolichol-linked oligosaccharides since co-translational glycosylation of endogenous cathepsin C was unaffected (Fig.

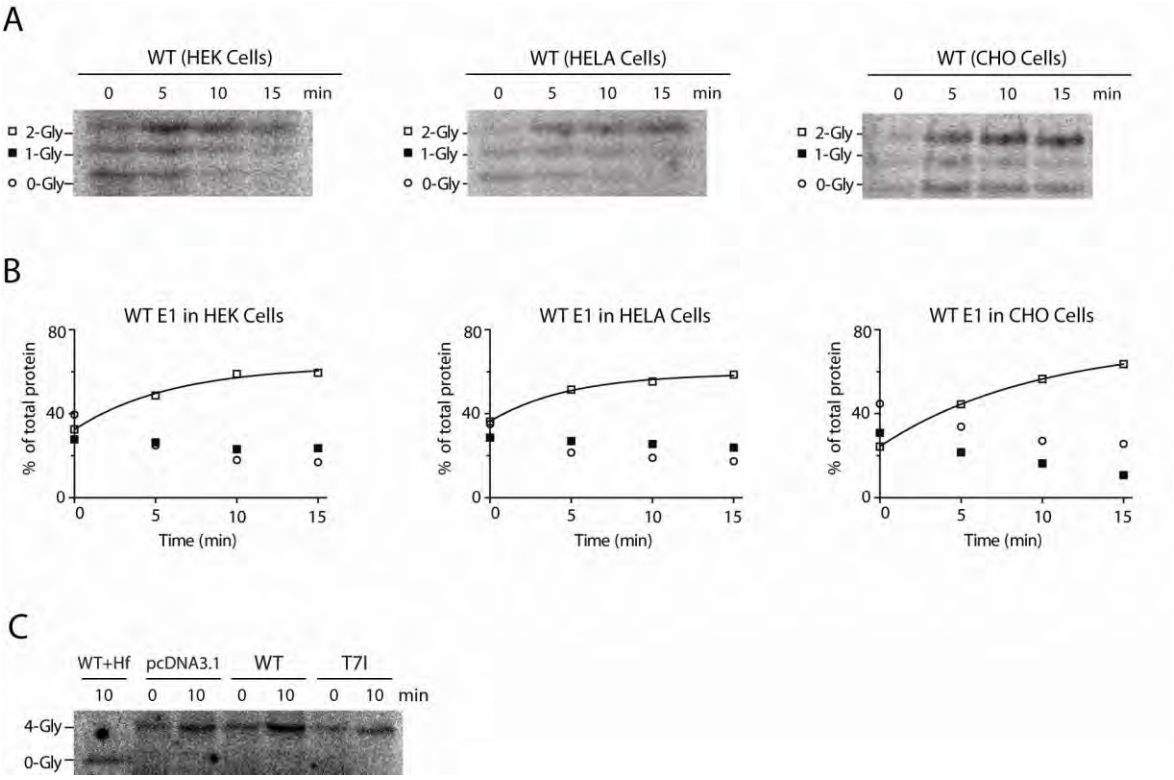

Figure 3.8 Post-translational N-glycosylation of exogenously expressed KCNE1 peptides occurs in various cell types with fully functional co-translational machinery. (**A**) Cells were pulsed for 2 min, chased for the indicated times and the E1 peptides were immunoprecipitated, separated by electrophoresis, and detected by autoradiography. Representative fluorograph for WT E1 expressed in CHO cells is shown for comparison. (**B**) Graphs of densitometric analysis for Figure 3.8A. The percentage of the different glycoforms with respect to total protein is plotted for each time point. After 5 min, the fully glycosylated forms of WT protein increased in all mammalian cell lines. Glycosylation states in all panels are labeled: 2-Gly: open square; 1-Gly: closed square; 0-Gly: open circle. (**C**) Representative fluorograph for human cathepsin C. HeLa cells transfected with empty vector (pcDNA3.1), WT or T7I were pulsed for 2 min and chased

for the indicated times. Endogenous cathepsin C was immunoprecipitated, separated by electrophoresis and detected by autoradiography. Only the fully glycosylated protein (4-Gly) was observed at 0 and 10 min chase points, demonstrating that plasmid-based expression of E1 peptides does not compromise the co-translational N-glycosylation machinery. Endo H (Hf) was used to identify unglycosylated cathepsin C (0-Gly).

3.8C). Taken together, these results suggest that post-translational glycosylation of E1 is a native mechanism that affords assembly-competent regulatory subunits essential for proper electrical excitability.

Proteins with Distinct Co- and Post-translational Sites

For a type I transmembrane peptide with closely-spaced N-linked consensus sites, the cellular mechanisms that define its co- and post-translational glycosylation sequons are likely to be different. One possible explanation for distinct co- and post-translational sequons is that the E1 N-terminus is oriented in the ER translocation tunnel such that the OST complex has access to only the N-terminal sequon. Similarly, the internal sequon could simply be occluded by the translocation tunnel. Previous investigations have utilized the ―rule of 14" for membrane proteins: N-linked consensus sequences need to be at least 12-14 residues away from a transmembrane domain to be a substrate for the OST complex (Nilsson and von Heijne 1993; Cheung and Reithmeier 2007). However, the E1 internal sequon satisfies this rule, as it is 18 residues away from the predicted start of the transmembrane segment. Moreover, the E1 internal sequon is glycosylated, it just occurs after translation. Our results suggest the ER proteins responsible for post-translational glycosylation have a different set of structural requirements that define which consensus sites are acceptable substrates.

Post-Translational versus Post-Translocational N-glycosylation

We have shown that the internal sequon of E1 acquires N-linked glycans after translation, but do these modifications occur outside of the protein translocation tunnel? Although we cannot rule out the possibility that some glycans are post-translationally added when the fully-synthesized peptide resides in the translocation tunnel, two experimental observations support a mechanism where post-translational glycosylation occurs after the transmembrane segment slides into the hydrophobic confines of the membrane. Currently, there are two models for the timing of the lateral entry of a transmembrane segment into the ER membrane based on photo-crosslinking studies. The first model requires the completion of translation before exiting the translocation pore (Do et al. 1996) whereas the second model suggests that certain transmembrane segments can enter the lipid environment before translation is terminated (Heinrich et al. 2000; McCormick et al. 2003). Thus, the observation of N-glycosylation events 10 – 15 minutes after translation of a ~150 residue type I transmembrane peptide (Fig. 3.4B) is consistent with post-translocational glycosylation. Moreover, post-translational glycosylation of the T7I mutant was inhibited by co-expressing Q1 channel subunits (Fig. 3.4D) that co-assemble with E1 peptides in the ER (Krumerman et al. 2004; Chandrasekhar et al. 2006). Since the protein translocation tunnel cannot simultaneously house a six-transmembrane spanning Q1 subunit and an E1 peptide, these data support the conclusion that post-translational glycosylation of type I transmembrane peptides occurs outside of the protein translocation tunnel.

Efficiency of Post-Translational N-glycosylation of Type I Transmembrane Peptides

The panel of E1 mutants that we examined revealed some basic structural requirements for post-translational glycosylation of type I transmembrane peptides. First, unlike co-translational glycosylation, long range point mutations (~20 residues away) affect post-translational glycosylation, as ablation of the N-terminal sequon with more hydrophobic residues led to less post-translational glycosylation (Fig. 3.1C). This trend is consistent with the best substrate for post-translational glycosylation, wild type E1, which is decorated with hydrophilic carbohydrates at its N-terminal sequon. Interestingly, we could not detect any post-translational glycosylation of the N26Q mutant, which suggests that the N-terminal sequon is a poor substrate for post-translational glycosylation. This phenomenon has been previously observed with water soluble proteins where rapid protein folding sequesters the sequon from the OST complex (Ruiz-Canada et al. 2009). However, the N-terminus of E1 is not predicted to have a globular fold nor does it possess any lumenal cysteines for disulfide bond formation. While we could not directly measure post-translational glycosylation of N26Q (Fig. 3.4B), the steady state populations (0 and 2 glycans) of WT peptides suggest that the N-terminal sequon acquires N-linked glycans post-translationally when the internal sequon is glycosylated. Differences in the degradation rates of the differently glycosylated WT peptides could also explain the lack of the singly glycosylated species; however, the degradation rates of WT and mutant E1 peptides were comparable in the absence of Q1 channel subunits (Fig. 3.3). Nonetheless, these data hint that glycan occupancy directly affects post-translational glycosylation efficiency of type I transmembrane peptides.

Cellular Advantages of Doubly-Glycosylated Type I Transmembrane Peptides

The spacing of the N-linked glycosylation consensus sites in E1 is absolutely conserved among vertebrates. Moreover, 4 out of the 5 human KCNE peptides have at least two N-linked sites and the spacing between the sequons is relatively consistent (16 – 23 aa). A potential benefit of having two sequons is to increase the probability that KCNE peptides are at least singly glycosylated in the ER. KCNE peptides with only an N-terminal sequon would likely mimic the N26Q mutant, which is not a substrate for post-translational glycosylation (Fig. 3.4B). Another potential advantage of a doubly-glycosylated KCNE peptide is that it would improve the interactions (via multivalency) with the lectin family of chaperones in the ER (Helenius and Aebi 2001), which have been hypothesized to interact with E1 (Chandrasekhar et al. 2006). The initial delay in the decay of WT peptides that we observed is consistent with the notion that there is an increase in the probability of lectin chaperone association with newly synthesized E1 peptides harboring two glycans (Fig. 3.3B).

Biogenic Model for Long QT Syndrome

From our results, we propose a model for E1 peptide biogenesis, co-assembly with Q1 channel subunits, and the implications for Long QT and Jervell-Lange Nielsen Syndromes (Fig. 3.9). In this model, WT peptides co-translationally acquire an N-terminal glycan before exiting the translocon. Once free from the proteinaceous environment of the translocon, post-translational glycosylation of E1 peptides occurs

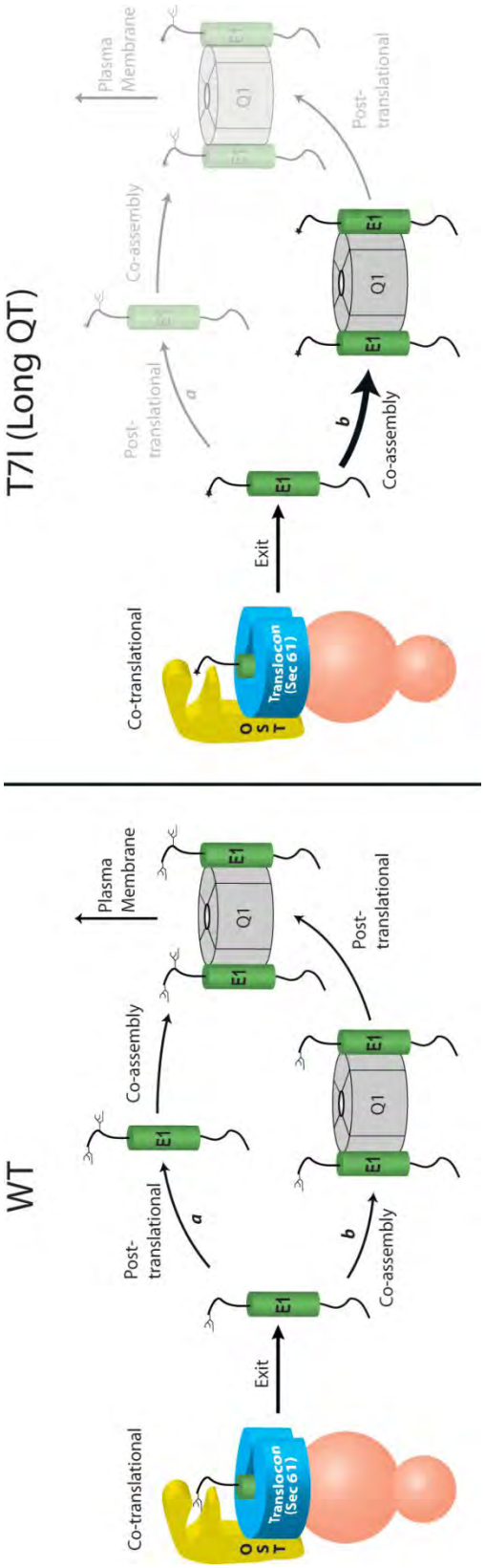
T7I (Long QT)
Co-translational
OST
Translocon (Sec 61)
Exit
E1
Post-translational
a
Co-assembly
Q1
Plasma Membrane
b
WT

Figure 3.9 Model of KCNE1 biogenesis, N-glycosylation and co-assembly with KCNQ1 channels. N-linked glycans are added to the N-terminal sequon (N5) of E1 peptides during translation (Co-translational) and laterally exit the translocon into the membrane. Post-translational glycosylation of WT peptides at N26 occurs either before (***a***) or after (***b***) co-assembly with Q1 channel subunits. Once fully glycosylated, the Q1/E1 complex exits the ER and traffics to the plasma membrane. For the Long QT mutation, T7I, post-translational glycosylation is inhibited by co-assembly with Q1 channel subunits resulting in Q1/E1 complexes that do not reside at the plasma membrane.

either before or after co-assembly with Q1 channel subunits (pathways ***a*** and ***b***, respectively). Once fully glycosylated, Q1/E1 complexes exit the ER and traffic to the plasma membrane. For WT peptides, we cannot rule out either pathway ***a*** or ***b*** since co-expression with Q1 channel subunits had no significant effect on post-translational glycosylation. In contrast, post-translational glycosylation of T7I was inhibited by Q1 co-expression, which shunts the unglycosylated peptides towards co-assembly, resulting in a pool of unglycosylated Q1/T7I complexes that do not reside at the plasma membrane (Fig. 3.9, T7I) as evidenced by the lack of cell surface expression of these channel complexes (Fig. 3.6). Therefore, the lack of N-linked glycosylated E1 peptides in the heart would decrease the number of Q1/E1 complexes at the cell surface, leading to a reduction in the cardiac I_{Ks} current and a prolongation of the QT interval. Alternatively, a smaller population of assembly-competent E1 peptides could result in either unpartnered Q1 channels trafficking to the cell surface (as we observed in Fig. 3.5B) or assembly with different KCNE peptides since the mRNA for all five KCNE peptides is expressed in heart tissues (Bendahhou et al. 2005; Lundquist et al. 2005). Either scenario would result in ill-equipped Q1 channels, which would increase the probability of an arrhythmic event. A similar reduction of Q1/E1 complexes in the developing ear would prevent the proper potassium flux into and thus the formation of the endolymphatic space. Given the absolute conservation of the N-terminal site in KCNE peptides, we predict that mutations that prevent N-linked glycosylation in other members of the KCNE family will also compromise K^+ channel complex assembly and give rise to channelopathies.

EXPERIMENTAL PROCEDURES

Plasmids and cDNAs—Human Q1 and E1 were subcloned into pcDNA3.1 (–) (Invitrogen). E1 constructs (wild type and mutants) possessed a C-terminal HA (YPYDVPDYA) epitope tag (Chandrasekhar et al. 2006). To produce the N5Q, N5I, T6P, T7I, T7A, T7Q and N26Q mutants, site-directed mutagenesis was performed using QuikChange® (Stratagene) and the mutations were confirmed by DNA sequencing of the entire gene.

Cell culture and transfections—Chinese Hamster Ovary (CHO-K1) cells were cultured in F-12K nutrient mixture (Gibco – Invitrogen). HeLa cells and HEK cells were cultured in Dulbecco's modified Eagle's medium (Sigma). All of the media were supplemented with 10% fetal bovine serum (Hyclone) and 10^2 U/mL penicillin/streptomycin (Gibco – Invitrogen). Cells were plated at 60 – 75% confluency in 35 mm dishes for all experiments except pulse-chase (60 mm). After 24 h, cells were transiently transfected at RT with Lipofectamine (Invitrogen) 8 µl per mL of Opti-MEMI (Gibco - Invitrogen) for CHO cells or with 10 µl of Lipofectamine 2000 (Invitrogen) per mL of Opti-MEM for HeLa cells and HEK cells and returned to fresh media after 6 hr (2 hr for electrophysiology). DNA ratios (in µg): E1/empty pcDNA 3.1 plasmid: 1.25/1.25; Q1/E1 (Western Blots): 1.25/1.25; Q1/E1 (Pulse-chase): 0.75/1.75; Q1/E1 + pEGFP-C3 (electrophysiology): 0.5/2 + 0.25. Cells were used 48 h post-transfection for Western Blots; 24 h for pulse-chase and electrophysiological experiments.

Cell lysis and Western Blot Analysis—Cells were washed in ice-cold PBS (3 × 2 mL) and lysed at 4°C in RIPKA buffer (in mM): 10 Tris·HCl, pH 7.4, 140 NaCl, 10 KCl, 1 EDTA, and 1% Triton-X, 0.1% SDS, 1% sodium deoxycholate and supplemented with protease-inhibitors: 1 mM phenylmethylsulfonyl fluoride (PMSF) and 1 μg/mL each of leupeptin, pepstatin and aprotinin (LPA). Lysates were diluted with SDS-PAGE loading buffer containing 100 mM DTT, loaded on a 15% SDS-polyacrylamide gel, transferred to a nitrocellulose membrane, and blocked in Western blocking buffer (5% nonfat dry milk in Tris-buffered saline containing 0.2% Tween-20 (TBS-T)) for 30 min at RT. Membranes were incubated overnight at 4°C with rat anti-HA (Roche) (1:750) in Western blocking buffer and washed in TBS-T next day and incubated with goat anti-rat horseradish peroxidase (HRP)-conjugated antibody (Jackson Immunoresearch Labs, Inc.) (1:2000) in Western blocking buffer for 45 min at RT. Membranes were washed with TBS-T and incubated with SuperSignal West Dura Extended Duration Substrate (Pierce) for 5min. HRP-bound proteins were detected by chemiluminescence using Fujifilm LAS-3000 CCD camera and quantified using the Image Gauge V2.1 software (Fujifilm).

Enzymatic deglycosylation assay—NP-40, BME, and reaction buffer (G5 for Endo H; G7 for PNGase F) were added to the cell lysates (20 μL), which were diluted with water such that the final concentrations were 1% for NP40 and BME. Endo H_f (2 μL) or PNGase F (1 μL) (New England BioLabs, Inc.) were added to the samples and incubated at 37°C for 30 min. The samples were brought to a final concentration of 100 mM DTT and 1.3% SDS and separated on an SDS-PAGE (15% gel) and analyzed by Western Blot as described above.

Cell surface biotinylation—Transfected cells were rinsed with ice-cold PBS^{2+} buffer (PBS containing 1 mM $MgCl_2$, 0.1 mM $CaCl_2$), incubated with 1 mg/mL sulfo-NHS-SS-biotin (Pierce) in PBS^{2+} buffer for 2 × 15 min at 4°C. The biotin reagent was quenched by washing with (3 × 2 mL) with quench solution (PBS^{2+} containing 100 mM glycine) and then incubated with quench solution for 2 × 15 min at 4°C. Cells were lysed in RIPKA buffer and cell debris was removed by centrifugation. For each sample, 75 µg of total protein was quantitated by BCA analysis and incubated with 25 µL of Immunopure® Immobilized streptavidin beads (Pierce) overnight at 4°C. One-half of the input (37.5 µg of total protein) was saved as a control for each sample. Beads were washed 3 times with 0.1% SDS buffer (500 µL) and biotinylated proteins were eluted first with 30 µl 2× SDS-PAGE and 200 µM DTT mix for 15 min at 55°C, then with 30 µl 200 µM DTT for 5 min at 55°C and the two elutions were combined to achieve 60 µl final volume. Half of the input and bead-eluted proteins were separated by SDS-PAGE, analyzed by Western Blot as described above, and quantified in the linear range. To compare the cell surface populations of WT to the mutant E1 peptides, the band intensities in the beads lanes were divided by twice the band intensity in the corresponding calnexin ½ input lanes and WT was normalized to 1. Since some cell lysis and intracellular labeling of proteins occurs during biotinylation, the amount of calnexin (CNX) labeling was first subtracted from each biotinylated E1 sample.

Pulse-chase experiments—Cells were washed in PBS (2 × 2 mL) and starved in Dulbecco‘s modified Eagle medium (DMEM) High Glucose (Gibco - Invitrogen) supplemented with 10% fetal bovine serum (Hyclone) and 10^2 U/mL

penicillin/streptomycin (Gibco – Invitrogen) and 2 mM glutamine (Invitrogen) for 1 h at 37°C. Then, 100 μCi/mL [^{35}S] methionine and [^{35}S] cysteine (MP Biomedicals, Inc.) was added to the starve media and the cells were pulsed 10 min for decay experiments and 2 min for post-translational glycosylation studies. After the radioactive pulse, cells were washed in PBS (2 × 2 mL) and chased in standard medium at various times. The cells were washed in PBS (2 × 2 mL) and lysed for 30 min at 4°C in 300 μL low salt lysis buffer consisting of (in mM): 50 Tris·HCl, pH 7.4, 150 NaCl, 20 NaF, 10 Na_3VO_4, and 1% NP-40, 1% CHAPS supplemented with protease-inhibitors (PMSF and LPA).

Radioimmunoprecipitation assay—Lysates were pelleted at 16,100 g for 10 min at RT and supernatant was precleared with a slurry of Immobilized Protein G Beads (Pierce) in lysis buffer rotating for 2 h at 4°C. The beads were pelleted and the precleared supernatants were rotated overnight at 4°C with 25 μl Protein G Beads/(1 μl) rat anti-HA (Roche) antibody mix or with 25 μl Protein G Beads/(1 μl) goat anti-human cathepsin C (R&D Systems) antibody mix. The beads were pelleted at 16,100 g for 10 min at RT and washed twice in low salt lysis buffer and then twice in high salt buffer consisting of (in mM): 50 Tris·HCl, pH 7.4, 500 NaCl, 20 NaF, 10 Na_3VO_4, and 1% NP-40, 1% CHAPS, followed by a final wash with low salt lysis buffer. For cathepsin C enzymatic deglycosylation assay, beads were resuspended in 400 μl low salt lysis buffer with Endo H_f (20 μL) (New England BioLabs, Inc.) and incubated at 37°C for 1 h followed by a final wash with low salt lysis buffer. The washed and pelleted beads were eluted in 50 μL of 2 X SDS and 100 mM DTT mix at 55^{o}C for 15 min. Supernatants were separated by SDS-PAGE (15%) and visualized by autoradiography. Signals were captured on a FLA-

3000 phosphorimager and quantified using the Image Gauge V2.1 software (Fujifilm). The rates of protein decay and post-translational glycosylation were fitted to a single exponential.

Perforated Patch Whole-Cell Recordings—I_{Q1} and I_{Ks} were recorded in the whole-cell perforated patch configuration. Briefly, on the day of the experiment, cells were seeded on the surface of cover glass and placed in a custom recording bath filled with a modified Tyrode‘s solution contained (in mM): 145 NaCl, 5.4 KCl, 10 HEPES, 5 $CaCl_2$ (pH 7.5 with NaOH). Transfected (eGFP-expressing) cells were selected using an Axiovert 40 CFL inverted light microscope (Zeiss). For the perforated patch configuration, a glass electrode (pipette resistance: 2.5-3.5 MΩ) filled with internal electrode solution containing (in mM): 126 KCl, 1 $MgSO_2$, 0.5 $CaCl_2$, 5 EGTA, 4 K_2-ATP, 0.4 GTP, 25 HEPES (pH 7.5 with CsOH), and 60 μg/ml Amphotericin B (Sigma; prepared in DMSO) was attached to the cell. Once a GΩ seal was achieved and access resistance was dropped to the level enough to record membrane potential (<15 MΩ), Tyrode‘s solution was replaced with the extracellular bath solution contained (in mM): 160 NaCl, 2.5 KCl, 2 $CaCl_2$, 1 $MgCl_2$, 8 glucose, and 10 HEPES (pH 7.5 with NaOH). Initially, the electrical access to the inside of the cell was monitored using 3-s depolarizing test pulse from the holding potential of –80 mV to +20 mV taken every 15 s. Cells with pronounced rundown were discarded, and only those expressing stable currents were used. The I_{Q1} and I_{Ks} currents were elicited using a family voltage protocol as described in Figure legend 3.4. All measurements were performed at RT (24 ± 2°C).

CHAPTER IV

KCNE1 PEPTIDES ACQUIRE O-LINKED GLYCANS AS A POST-TRANSLATIONAL MODIFICATION

ABSTRACT

Post-translational modifications such as N- and O-linked glycans are important sugar assemblies that define the biosynthetic trafficking and ultimate cellular destinations of their associated proteins. KCNE1 peptides have been shown to contain two putative N-linked glycosylation sites at N5 and N26. Mutations that disrupt glycosylation at the N terminal sequon disrupt the efficiency of trafficking of these peptides with their cognate K^+ channel partners. Here we report that KCNE1 peptides acquire O-linked glycosylation as a post-translational modification in over-expression systems and native cardiac tissues. We define specific threonine residues as sites of O-glycan attachment in the N-terminus of KCNE1. We also investigate the role of O-glycans in channel complex trafficking and function by comparing the cell surface expression and electrophysiological characteristics of wild type and O-glycan deficient mutant KCNQ1/KCNE1 channel complexes. Our observations suggest that the presence of O-glycans on KCNE1 peptides may likely only contribute to the anchoring of these channel complexes in the extracellular milieu and play no significant role in channel modulation.

INTRODUCTION

O-linked glycosylation is a complex protein modification that occurs on the side-chain hydroxyl groups of serine and threonine residues (Van den Steen et al. 1998). Unlike their N-glycan modification counterpart, the process of O-linked glycosylation does not involve a consensus sequence making the prediction of O-glycan sites of attachment a challenging process. Additionally, not every serine or threonine residue found in the amino acid sequence of a protein is a substrate for this modification. The preferential addition of O-glycans to specific residues is dependent on various factors such as the tissue-specific expression of different glycosyltransferases involved in O-glycosylation, the accessibility of side-chain hydroxyl groups and the amino acid environment around potential serine and threonine sites (Van den Steen et al. 1998). Therefore, a predictive algorithm like NetOGlyc3.1 can be used to determine whether specific residues on proteins are likely O-glycosylated (Julenius et al. 2005).

While O-linked glycosylation does not commonly occur on ion channel proteins, the terminal sialic acid sugars that cap O-glycan branches are also found on mature N-glycans. Sialylation of N-glycans on Na_v and $K_v4.3$ channels has been implicated in modulation of channel function (Ufret-Vincenty et al. 2001; Ufret-Vincenty et al. 2001). The negatively charged sialic acid sugars on N-glycans are thought to impact the voltage-dependence of activation of cardiac Na_v channels through charge effects on the voltage sensors as proposed by the surface potential model (Green and Andersen 1991). Additionally, removal of the sialic acid groups from Na_v channels has been shown to cause channel dysfunction as observed in arrhythmogenesis (Ufret-Vincenty et al. 2001).

Similarly, sialic acid modifications on accessory subunits can contribute to modulation of the biophysical properties of ion channels. The β1 accessory subunit of the Na_v/β1 channel complex possesses sialic acid modifications that have been attributed to Na_v channel function (Johnson et al. 2004). The Na_v/β1 channel complex normally possesses fast activation and deactivation kinetics with a hyperpolarized shift in voltage sensitivity compared to Na_v channels alone; the removal of sialic acid groups from β1 subunits results in a depolarizing shift in the voltage sensitivity of $Na_v1.2$, $Na_v1.5$, and $Na_v1.7$ α-subunits.

KCNE1 (E1) is the first discovered member of the KCNE family of type I transmembrane K^+ channel β-subunits. The KCNE peptides have been shown to contain multiple N-glycan sequons in the extracellular N-termini (Fig. 1.5). The primary N-glycosylation site proximal to the N-terminus is evolutionarily conserved among all members of the KCNE family and genetic mutations at this site have been implicated in disease and functional defects of channel conductance (Takumi et al. 1991; Schulze-Bahr et al. 1997; Larsen et al. 2001; Lu et al. 2003; Park et al. 2003). We have previously demonstrated that E1 protein stability and trafficking is altered in the absence of N-glycans at the primary sequon (Figs. 3.5 and 3.6). Previous studies in our lab have shown that E1 may contain an additional post-translational modification that is observed as an incompletely digested band upon PNGase F removal of all N-glycans from mature E1 (Chandrasekhar et al. 2006). We previously ruled out phosphorylation and ubiquitination of E1 as potential modifications of mature E1 (Figs. 2.3 and 2.4).

KCNE3 (E3), another member of the KCNE peptide family, does not appear to possess additional post-translational modifications as evidenced by the complete digestion of mature E3 with PNGase F to unglycosylated protein (Gage and Kobertz 2004). These results suggest the presence of a protein modification that may be unique to E1 peptides. Analysis of the N-terminal sequence of E1 with the NetOGlyc3.1 algorithm (Julenius et al. 2005), proposed multiple O-glycan attachment sites on E1. We subsequently tested the predictions by enzymatic deglycosylation of mature E1 with an O-glycosidase and determined that O-linked glycosylation of E1 contributed to the presence of the incomplete digestion products observed on PNGase F treatment. In order to define the sites of O-glycan attachment on E1, we generated chimeras of E1 with E3 by substituting specific N-terminal regions of E1 with the corresponding regions from E3 and by site-directed mutagenesis of potential residues on the E1 N-terminus. Finally, we determined whether the presence of O-glycans on E1 affected the trafficking and function of channel complexes containing KCNQ1 (Q1) and E1 peptides. Perforated patch clamp electrophysiological recordings from CHO-K1 cells co-expressing Q1 channels with mutant E1 peptides lacking O-glycans revealed no significant change in overall current compared to wild type channel complexes. Cell surface biotinylation studies indicated no difference in the steady state expression of mutant Q1/E1 channel complexes at the cell surface as compared to wild type complexes. Taken together, these observations suggest that, for E1 peptides, O-glycans may only play a structural role in the anchoring of Q1/E1 complexes in the extracellular milieu.

RESULTS

Glycosylation is an important post-translational modification that affects the stability and forward trafficking of proteins. We previously showed that the glycosylation state of E1 peptides can be used to visualize their migration through the biosynthetic pathway (Chandrasekhar et al. 2006). Enzymatic deglycosylation of N-glycans using Endo H and PNGase F is a useful tool in labeling the populations of E1 peptides as either the ER-associated (immature) or post-ER (mature) forms. Mature E1 peptides are resistant to Endo H treatment; however PNGase F digestion consistently results in residual banding after complete removal of all N-glycans on E1 as indicated by *asterisks* on the Western blot (Fig. 4.1). To test for the presence of O-glycans, lysates from CHO cells co-expressing Q1/E1 were digested with an O-glycosidase in combination with PNGase F and neuraminidase. PNGase F digestion of E1 completely removes N-glycans and allows for the visualization of the residual bands; neuraminidase removes sialic acid sugars from N- and O-glycans and promotes efficient cleavage of O-glycans by O-glycosidase. The PNGase F/neuraminidase/O-glycosidase (Tri) cocktail resulted in an almost complete loss of residual bands with an accumulation of unglycosylated E1 protein at 16 kD, showing that mature E1 peptides acquire O-linked glycosylation as an additional post-translational modification.

Enzyme deglycosylation of mature E1 in HEK and COS-7 cells revealed similar residual banding upon PNGase F digestion, suggesting that the additional O-linked

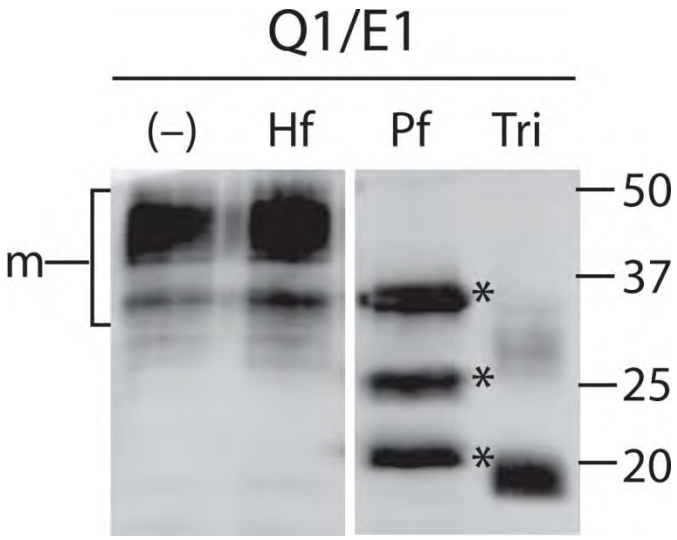

Figure 4.1 Mature KCNE1 protein acquires O-linked glycosylation. Immunoblot from enzymatic deglycosylation of wild type E1 co-expressed with Q1. The samples were left untreated (–), digested with Endo H (Hf), PNGase F (Pf) or an enzyme cocktail containing PNGase F, neuraminidase and O-glycosidase (Tri) and separated by SDS-PAGE (15%). Mature (m) samples are indicated as determined by enzymatic digestion. Upon treatment with Pf, incomplete cleavage products are observed and indicated by a*sterisks.* Almost complete loss of partial digestion products occurs upon Tri enzyme treatment.

modifications on E1 occur in multiple over-expression cell lines (Chandrasekhar et al. 2006). In order to establish that O-glycosylation of E1 in over-expression systems is a true representation of the modifications that E1 undergoes in native cells where the protein is localized, we obtained cardiac lysates from MK24 transgenic mice. These mice stably express a concatenated Q1/E1 construct denoted as MK24, by the cytoplasmic linkage of the C-terminus of E1 to the N-terminus of Q1. MK24 expresses a single copy of Q1 and E1 and was used in whole cell patch clamp experiments in transiently transfected CHO cells where its functional properties recapitulated those of wild type Q1/E1 channel complexes (Wang et al. 1998; Dilly et al. 2004). Additionally, biochemical analysis of the MK24 construct revealed robust expression of the fusion protein on a Western blot with anti-Q1 antibody (Marx et al. 2002; Dilly et al. 2004; Sampson et al. 2008). MK24 migrates slower than Q1 or E1 alone on 6% SDS-PAGE as multiple species from ~75 to 100 kD, accounting for the various glycosylated forms of E1 in the fusion construct (Fig. 4.2). Enzymatic deglycosylation with Endo H removed only immature glycans from E1, leaving the highest molecular weight species unaffected. PNGase F treatment results in collapse of all bands upon removal of N-glycans, with a faint residual product indicated by the *asterisk*. Tri treatment of MK24 results in an enhancement of the unglycosylated protein species with a decrease in intensity of the residual band, confirming that in native tissues, E1 peptides are post-translationally modified with O-glycans.

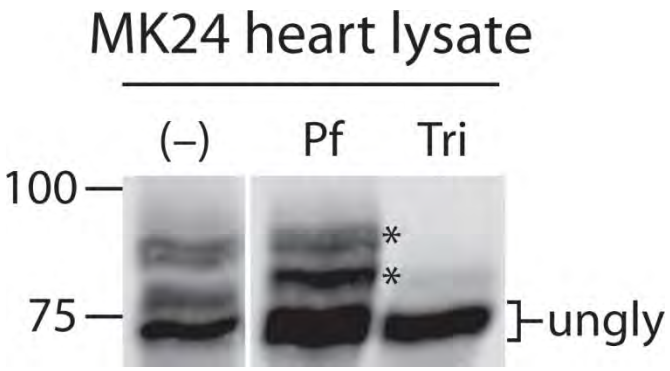

Figure 4.2 KCNE1 peptides in the MK24 fusion protein acquire O-glycans in mouse cardiac tissue. Immunoblot from enzymatic deglycosylation of MK24 Q1/E1 fusion protein. The samples were left untreated (–), digested with PNGase F (Pf), or an enzyme cocktail of PNGase F, neuraminidase and O-glycosidase (Tri) and separated by SDS-PAGE (6%). Unglycosylated (unglyc) products are indicated as determined by enzymatic deglycosylation. Pf treatment removes all N-glycans on mature E1 resulting in accumulation of unglycosylated protein and an intermediate species indicated by the *asterisks* as previously observed in CHO cells co-expressing Q1/E1 (Fig. 4.1). Tri treatment results in almost complete loss of the intermediate bands, with a corresponding increase in accumulation of unglycosylated protein.

Having confirmed the presence of O-glycans on E1 peptides in both CHO cells and native cardiac tissues, we next determined which amino acid residues acquired O-glycans on the E1 N-terminus. The N-terminal sequence of E1 contains numerous threonine and serine residues that could function as potential O-glycan linkage sites. To investigate specific regions of the N-terminus where O-glycan attachment could occur, we generated two chimeras of E1 and E3 by substituting each of the two N-glycan sites from E1 with complementary sites from E3. E3 is β-subunit protein from the KCNE family and is homologous to E1. It undergoes only N-linked glycosylation (Gage and Kobertz 2004) and provides a suitable O-glycan deficient background. The positioning and relative distances between two of the three N-glycosylation sites on E3 are similar to E1 (Fig. 1.5), allowing us to generate E1/E3 chimeras without altering the positions of the N-glycosylation sites in E1 which are important for protein expression and stability (Fig. 4.3A). Expression of the chimera proteins in the absence and presence of Q1 channels was determined to confirm their glycosylation competency and ability to assemble with Q1 channels (Fig. 4.3B). Unlike wild type E1, in the absence of Q1, chi1 migrates as both mature and immature protein. This observation is reminiscent of the unregulated ER exit of E3 peptides (Fig. 4.4). In the absence of Q1, chi2 migrates as immature and unglycosylated protein. Upon co-expression with Q1 channel, wild type E1 undergoes its characteristic shift in migration to the ~40 kD species which denotes mature glycosylated E1 (Chandrasekhar et al. 2006). Similarly, chi1 co-expression with Q1 results in a shift to a band at ~40 kD. In contrast, chi2 co-expressed with Q1 migrates

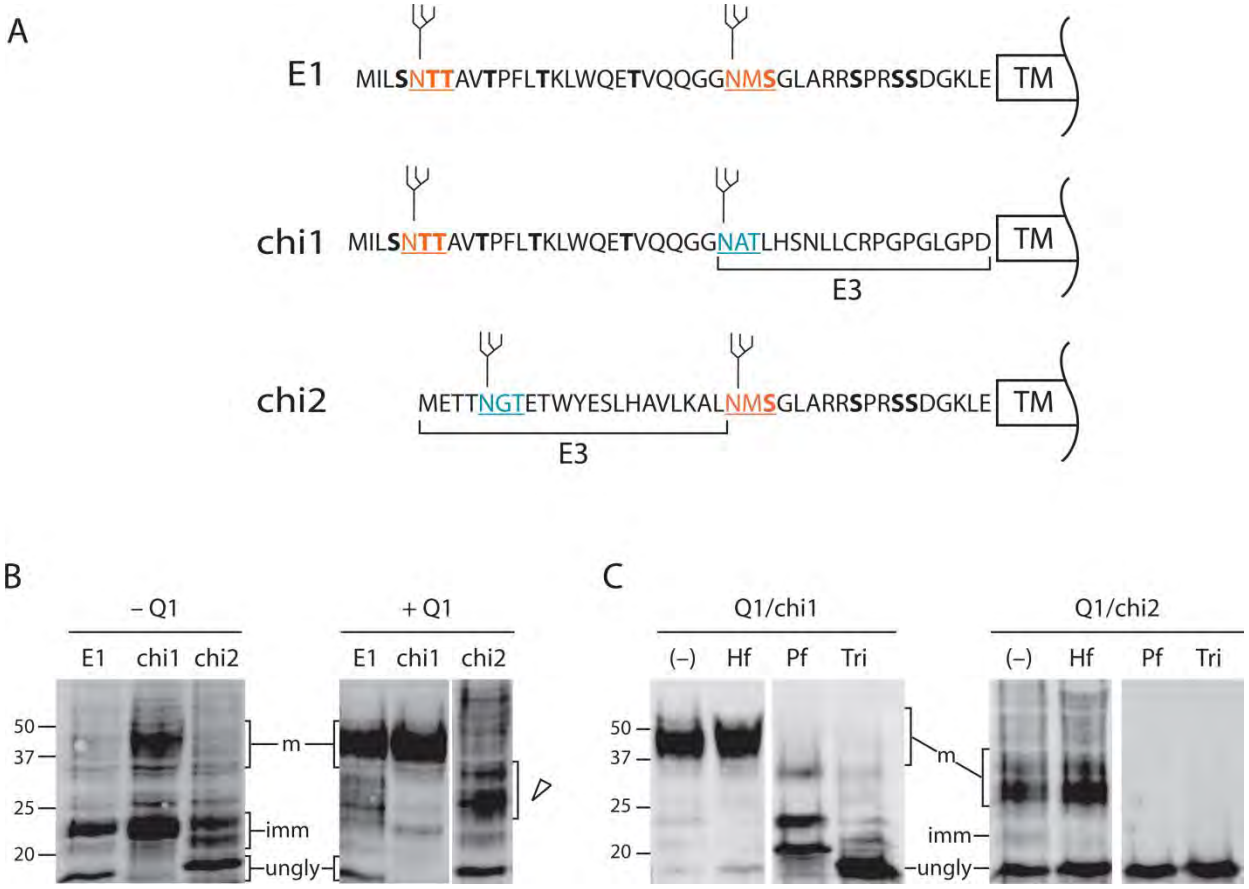

Figure 4.3 Generation of two KCNE1/KCNE3 chimera proteins to determine sites of O-glycan attachment on the KCNE1 N-terminus. (**A**) N-terminal amino acid sequence of E1 and chimeras (chi1 and chi2) depicting the N-terminal regions of E3 introduced into E1. N-glycosylation sites are color coded orange for E1 and blue for E3. N-glycosylation sites are underlined while putative O-glycan attachment sites are highlighted in bold face. (**B**) Immunoblot of wild type E1 (wt) and chimera peptides (chi1 and chi2) expressed in the absence or presence of Q1 K^+ channels. Samples are separated by SDS-PAGE (15%). Mature (m), immature (imm) and unglycosylated (ungly) samples are indicated based on mobility shifts compared to wt E1. Co-expression with Q1 results

in slower migration of chi2 as an intermediate cluster of bands indicated by an *open arrowhead*. (**C**) Immunoblots from enzymatic deglycosylation of chi1 and chi2 co-expressed with Q1. Samples were left untreated (–), digested with Endo H (Hf), PNGase F (Pf) or enzyme cocktail (Tri) and separated by SDS-PAGE (15%). Intermediate cluster of bands indicated by *open arrowhead* in panel B are identified as mature chi2 protein.

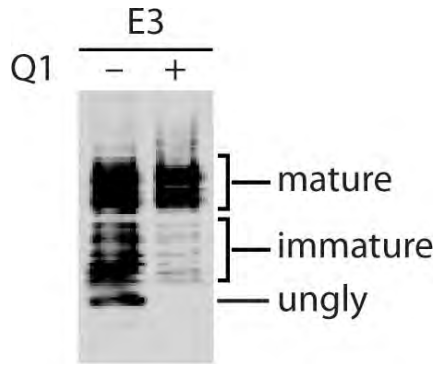

Figure 4.4 KCNE3 peptides acquire mature glycans in the presence and absence of KCNQ1 K^+ channel partners. Immunoblot of CHO cell lysates expressing E3 alone or co-expressed with Q1. In the absence of Q1, E3 peptides acquire mature glycans as indicated on the blot as a higher molecular weight species. This shift is more pronounced upon co-assembly with Q1 when the majority of the E3 peptides acquire mature glycans.

faster (~30 kD) than mature wild type E1, indicated by the *open arrowhead*. Enzymatic deglycosylation of the chimeras co-expressed with Q1 confirms the various glycosylation states of the protein (Fig. 4.3C). For Q1/chi1, Endo H digestion results in collapse of only faint immature chi1 bands to unglycosylated protein while PNGase F treatment results in collapse of mature chi1 to incompletely digested bands as observed for wild type E1. As with wild type E1, tri treatment of Q1/chi1 samples results in almost complete loss of residual banding. For Q1/chi2, the 30 kD species of chi2 is resistant to Endo H treatment but completely collapses to unglycosylated protein upon PNGase F digestion without the appearance of any residual bands. These observations show that chi2 acquires mature N-glycans and the O-linked glycosylation sites are located in the N-terminal region of E1 that has been replaced in chi2 (residues 1 – 25).

In the absence of defined consensus sites for the attachment of O-glycans on proteins, we refined the NetOGlyc3.1 sequence analysis of E1 residues 1 – 25 which returned a prediction for two potential O-linked glycosylation sites at threonine residues 6 and 7 (T6 and T7) (Fig. 4.5). T7 is necessary for the transfer of a core N-glycan to asparagine 5, and a genetic mutation at this residue (T7I) that prevents N-glycosylation at the first sequon is associated with Long QT Syndrome (LQTS) (Schulze-Bahr et al. 1997). Therefore, to prevent disruption of N-glycan attachment at N5, we mutated T6 to phenylalanine (T6F), a hydrophobic substitution severe enough to disrupt O-glycan attachment at both T6 and T7 (Hamby and Hirst 2008). Protein expression and enzyme deglycosylation of T6F in the presence of Q1 channels was visualized by Western blot (Fig. 4.6A). Co-expression of T6F with Q1 results in maturation of E1 although the

NetOGlyc 3.1 Server prediction results for E1 1-25 residues

Input sequence: Length: 25
MILSNTTAVTPFLTKLWQETVQQGG
.....TT...................

S/T	Pos	G-score	I-score	Y/N
S	4	0.420	0.053	.
T	6	0.523	0.030	T
T	7	0.504	0.037	T
T	10	0.457	0.075	.
T	14	0.454	0.078	.
T	20	0.533	0.021	T

G-score - best general predictor. Score >0.5 indicates glycosylated residue.
Higher score indicates more confident prediction
I-score - best isolated predictor in absence of neighboring glycosylated residues.

For threonine (T) residues, if G-score <0.5, but I-score is >0.5, residue is predicted to be glycosylated

Figure 4.5 Predictive analysis for O-glycan attachment sites on KCNE1 N-terminal residues. Summarized results from NetOGlyc 3.1 server reveals residues predicted to acquire O-glycan modifications in the first 25 amino acid sequence of E1. Based on G-score and I-score values, T6 and T7 are the best predicted residues to be modified.

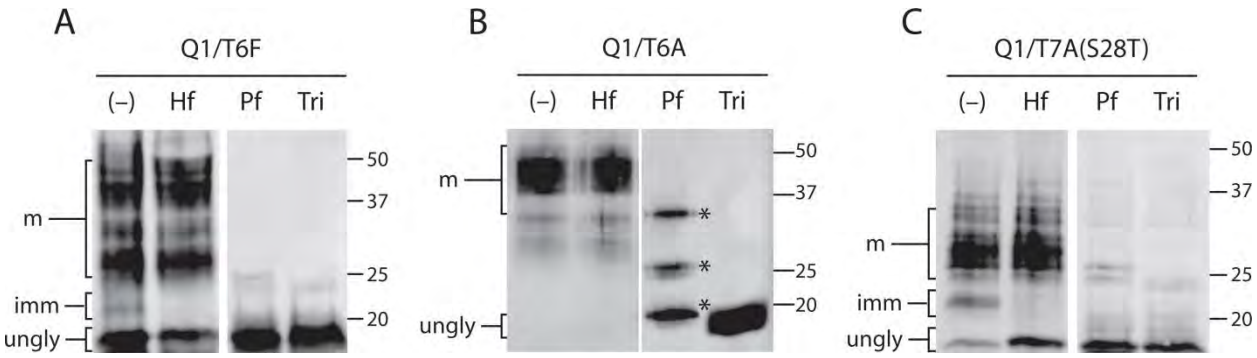

Figure 4.6 T6F mutation prevents O-linked glycosylation of KCNE1 peptides. (**A, B, C**) Immunoblots of enzymatic deglycosylation of threonine mutant E1 peptides co-expressed with Q1. The samples were left untreated (–), digested with Endo H (Hf), PNGase F (Pf) or enzyme cocktail (Tri) and separated by SDS-PAGE (15%). Mature (m), immature (imm) and unglycosylated (ungly) samples are indicated as determined by enzymatic deglycosylation. Pf digestion of mature T6F in panel A results in complete collapse to unglycosylated protein with no trace of residual bands. In panel B, enzymatic deglycosylation of T6A mutant reveals characteristic residual banding as observed with wild type E1 in Figure 4.1. In panel C, T7A abolishes almost all O-glycan attachment to E1 peptides as evidenced in Pf lane where mature E1 peptides collapse to the unglycosylated product.

efficiency of N-glycosylation is reduced. This observation is not unusual as hydrophobic amino acid substitutions around N5 have been shown to reduce the efficiency of N-glycosylation at that site (Fig 3.1). Endo H digestion results in the collapse of faint immature protein while the multiple mature glycan species are resistant to the enzyme. In contrast, PNGase F treatment of Q1/T6F samples results in the complete collapse of mature T6F to the unglycosylated form without any residual bands, indicating the absence of O-glycans on T6F peptides. Since the T6F mutation does not distinguish between the preferential addition of O-glycans to T6 or T7, we also generated single site mutations at T6 and T7 to the less severe hydrophobic residue alanine and evaluated their glycosylation pattern through the characteristic enzymatic deglycosylation previously used for T6F (Fig. 4.6B, C). We observed the loss of O-glycans from the T6A mutant only upon treatment with the enzyme cocktail. Interestingly, the T7A mutant afforded complete loss of glycosylated species upon PNGase F digestion. This result suggests that T7 functions as the major site that acquires O-linked glycans during the biosynthetic processing of E1 peptides.

We then determined whether the T6F mutation affected the trafficking and biophysical properties of Q1/E1 channel complexes. To directly measure the plasma membrane distribution of the T6F E1 peptides co-expressed with Q1 channel subunits, we used cell surface biotinylation. This approach allows us to measure whether the absence of O-glycans alters Q1/E1 complex trafficking to the cell surface. Cells expressing wild type and T6F mutant Q1/E1 complexes were labeled with a membrane-impermeant, amine-reactive biotin reagent at 4°C to prevent membrane recycling and

minimize labeling of intracellular proteins. The biotinylated proteins were isolated with streptavidin beads (Fig. 4.7A). To verify that the cells remained intact during biotinylation, we monitored the labeling of an ER-resident protein – calnexin and subtracted out the background intracellular labeling to calculation the cell surface expression of E1 peptides (Fig. 4.7B). We observed no significant difference in the cell surface labeling of wild type (28 ± 4%) *versus* T6F E1 (23 ± 2%) peptides in the presence of Q1 channels suggesting that the lack of O-glycans does not adversely affect the biosynthetic processing and trafficking of mutant Q1/E1 channel complexes.

To determine whether the T6F mutation altered the biophysical properties of Q1/E1 channel complexes, we measured current elicited at various depolarizing voltages using perforated patch clamp of CHO-K1 cells co-expressing Q1 and either wild type E1 or T6F. Families of currents generated for Q1/E1 and Q1/T6F show no significant difference in current amplitude (Fig. 4.8A). Tail current analysis additionally revealed no change in the midpoint of activation ($V_{1/2}$) of Q1/T6F as compared to Q1/E1 channel complexes (Fig. 4.8B).

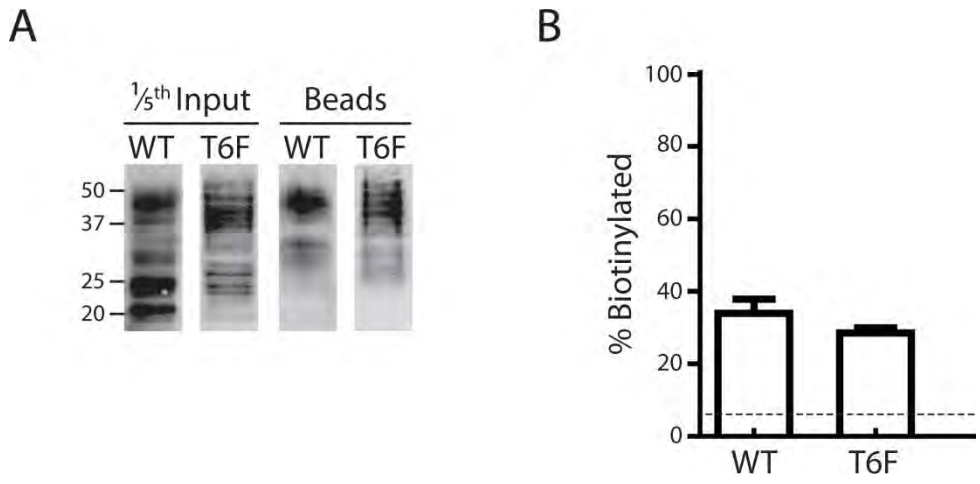

Figure 4.7 Cell surface distribution of wild type versus T6F mutant KCNE1 peptides. (A) A representative immunoblot of wild type and T6F mutant E1 peptides expressed in CHO cells with Q1 channel subunits. Transfected cells were labeled as described for CHO cells. (**B**) Quantification of the biotinylated E1 proteins. The percentage of biotinylated protein was calculated by dividing the band intensities in the biotinylated lane by the band intensities in the one-fifth total input lane, which were multiplied by five. The *error bars* are standard error measurement (S.E.M.) from three immunoblots. The *dotted line* indicates background biotinylation, which was calculated from calnexin staining (6 ± 1%).

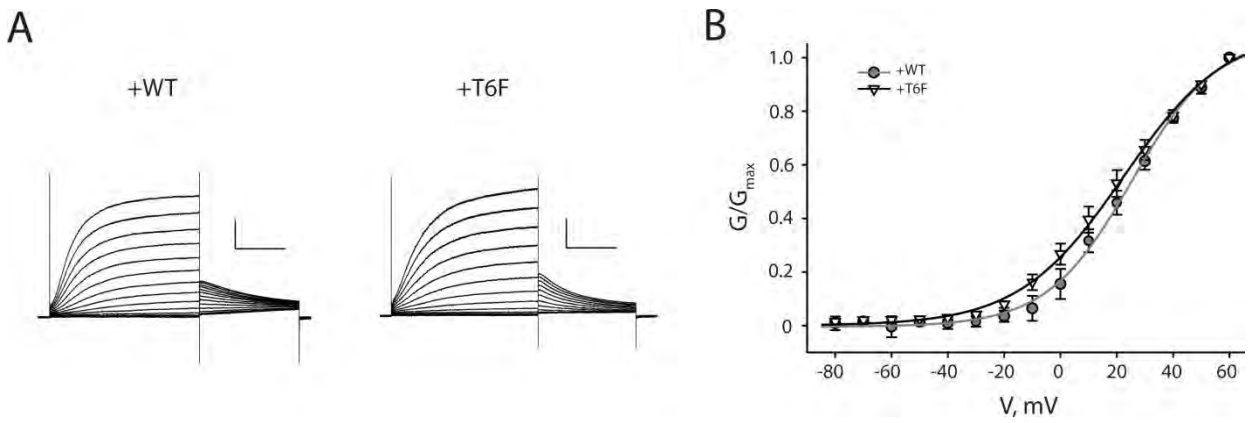

Figure 4.8 Electrophysiological properties of KCNQ1 channels co-expressed with wild type or T6F mutant KCNE1 peptides in CHO cells. (**A**) representative families of I_{Ks} current traces recorded from CHO cells using the following voltage protocol: membrane was held at –80 mV, subjected to 3-s depolarizing pulses ranging from –100 mV to +60 mV, followed by 1-s pulses at –30 mV. Cells were transfected with a Q1 partnered with either wt (+WT) or mutant (+T6F) E1 cDNA. T6F mutant I_{Ks} channels generated a typical slowly activating voltage-dependent current at depolarizing potentials above –40 mV. (**B**) Voltage dependence of activation: activation curves were obtained by plotting the normalized tail currents as a function of the pre-pulse potential. Values for the midpoint of activation ($V_{1/2}$) were obtained by fitting with the Boltzmann equation (solid lines). No significant difference was observed between the $V_{1/2}$ values of wild type and mutant I_{Ks} current.

DISCUSSION

We investigated the presence of an additional post-translational modification on E1 by the enzymatic removal of glycans from mature E1 peptides. Incomplete digestion products identified by PNGase F deglycosylation of E1 were observed to be sensitive to O-glycosidase treatment, indicating the presence of O-glycans on E1. We generated specific N-terminal chimeras of E1 and E3 and treated them with a deglycosylation enzyme cocktail of PNGase F, neuraminidase and O-glycosidase to determine specific regions of the E1 N-terminus where O-glycan attachment residues were located. Using predictions from the NetOGlyc3.1 algorithm and site-directed mutagenesis, we then determined that E1 acquires O-glycans at one or both threonine residues located within an N-glycosylation consensus site. O-linked glycosylation was only observed on mature E1 as PNGase F digestion of immature E1 does not yield any incomplete digested products (Fig. 2.2). Co-expression of E1 with Q1 is required to facilitate progression of E1 peptides through the biosynthetic pathway to the Golgi compartments where the mature modification of N-glycans and attachment of O-glycans are catalyzed (Roth et al. 1986).

Removal of mature N-glycans upon PNGase F digestion of E1 reveals the presence of additional modifications on E1 otherwise masked in the heterogeneous distribution of mature protein on an SDS-PAGE. Endo N-acetyl galactosaminidase is a specific O-glycosidase which catalyzes the removal of unsubstituted Gal β (1-3) GalNAc units from serine or threonine residues. As sialylated O-glycans are inefficient substrates for O-glycosidase digestion (Van den Steen et al. 1998), terminal sialic acid substituents

on O-glycans were removed with neuraminidase. Therefore, we created a deglycosylation enzyme cocktail of PNGase F, neuraminidase and O-glycosidase to determine whether there was a change in the mobility of the incomplete digested products. The susceptibility of E1 to endo N-acetyl galactosaminidase suggests the predominance of O-linked glycans that are sialylated with a core Gal β (1-3) GalNAc sugar unit.

The O-glycosidase used in the characterization of the O-glycan modifications on E1 is specific for unsubstituted N-acetyl galactosamine residues. We consistently observe that upon O-glycosidase treatment of E1 there are very faint residual bands that do not collapse even on prolonged enzyme treatment (Figs. 4.1 and 4.2). One possible explanation for the residual banding could be the presence of other substituents on the N-acetyl galactosamine core sugar that renders the O-glycosidase ineffective in hydrolyzing the O-glycan. The neuraminidase used to cleave the terminal sialic acid substituents preferentially removes α2-3 and α2-6 linkages over α2-8 linkages. As a result, any α2-8 sialic acid groups on O-glycans would reduce the efficiency of O-glycosidase hydrolysis resulting in the persistent residual bands observed upon enzyme digestion of E1.

The cellular distribution of glycosyl-transferases involved in O-glycan modification varies by cell-type (Roth et al. 1986). We routinely observed incomplete digestion products on PNGase F digestion of mature E1 in CHO, HEK and COS-7 cells (Chandrasekhar et al. 2006). In order to verify that O-glycosylation of E1 was not an artifact of the over-expression cell systems we used in biochemical investigation of E1 trafficking, we performed enzymatic deglycosylation on tissue lysates from transgenic

mouse hearts expressing the MK24 Q1/E1 fusion protein. The MK24 protein was used in functional studies of Q1/E1 assembly and stoichiometry and recapitulated the biophysical properties of naturally associating Q1/E1 channel complexes (Wang et al. 1998). On SDS-PAGE, the MK24 protein migrated at a combined molecular weight of each of the Q1 and E1 subunits it contains. However, multiple bands observed on the blot correspond to the various glycosylated forms of E1 in the fusion protein (Sampson et al. 2008). PNGase F digestion of N-glycans from the MK24 fusion protein resulted in a difference in distribution of the residual digestion products compared to CHO cells (Figs. 4.1 and 4.2). It is likely that this disparity in the migration of the digestion products was a result of the difference in the SDS-PAGE used (15% in Fig. 4.1 versus 6% in Fig. 4.2) making it harder to accurately resolve the small molecular weight variations in some of the residual digestion products. Another explanation for this observed difference could be the subtle variations in O-glycan modification that are unique to cardiac cells. It is also possible that the MK24 fusion protein does not acquire all the O-glycan modifications we observe in CHO cells. Through these observations, we established that O-glycosylation of E1 occurs in both over-expression systems and native cardiac tissues.

The relative location of O-linked glycosylation sites on E1 was determined by generating two chimeras of E1 with N-terminal regions substituted from the homologous peptide, E3. Enzymatic deglycosylation established that E3 acquires only N-glycans as a protein modification (Gage and Kobertz 2004). The systematic substitution of two regions of the N-terminus of E1 with E3 preserves the positioning of the N-glycan sites in wild type E1 which are important for E1 protein expression and trafficking. The chimera

proteins exhibit different migration patterns on SDS-PAGE in the absence and presence of Q1 channels. The chi1 chimera appears to acquire mature glycosylation even in the absence of Q1, unlike its wild type E1 counterpart. Unpublished results have shown that wild type E3 peptides acquire mature glycosylation even in the absence of Q1 channels (Fig. 4.4). It appears that the E3 N-terminal region substituted in chi1 allows the protein to retain some of the trafficking characteristics of E3. On the other hand, the chi2 mutant behaves similar to wild type E1 in that it acquires mature glycans only in the presence of Q1. Mature chi2 migrates faster than mature wild type E1, suggesting that chi2 may have impaired N-glycosylation as a result of the substitution of the N-terminal sequon in E1. Previous work shows that efficient co-translational N-glycosylation of E1 at the first sequon is an important determinant in subsequent post-translational N-glycosylation at the second sequon (Chapter III). Insertion of E3 N-terminal sequon may have reduced the overall efficiency of N-glycosylation of chi2. However, co-expression of Q1 channel results in an increased efficiency of chi1 and chi2 maturation and suggests there is otherwise normal biosynthetic processing of the chimera proteins.

Enzymatic deglycosylation of the E1/E3 chimera proteins place the O-linked glycosylation sites on E1 in the region contained within residues 1 through 25. Predictive sequence analysis of the residues using the NetOGlyc3.1 server revealed two potential O-linkage sites at T6 and T7 (Fig. 4.5). These residues form part of the N-glycosylation sequon at asparagine 5 (N5). T7 is implicated in LQTS and cannot be mutated because of its role in glycan transfer to N5. Analyzing efficient amino acid substitutions at T6 determined that a phenylalanine at T6 would most severely affect the O-linked

glycosylation at both T6 and T7. However, the downside to this mutation is the reduced efficiency of N-glycosylation of the T6F mutant as a result of an increase in the hydrophobic environment around N5. A hydrophobic environment around the N-terminal sequon has an adverse effect on the overall efficiency of E1 N-glycosylation (Chapter III) and is likely why T6F migrates as multiple mature N-glycosylated forms (Fig. 4.6).

Recent enzymatic deglycosylation characterization of a small single transmembrane spanning protein Opalin, revealed the presence of N- and O-glycans in close proximity to each other in the extracellular N-terminal domain of the protein (Yoshikawa et al. 2008). Using O-glycosidase in combination with PNGase F and neuraminidase, the authors identified the presence of small sialylated O-glycans attached to Opalin. In order to determine the exact sites of O-glycan attachment, the authors used alanine-substitution of specific threonine residues. One particular threonine to alanine substitution is located at the terminal position in a consensus site for N-glycosylation (N-T-T→N-T-A). In addition to preventing O-glycosylation, the alanine substitution disrupts N-glycosylation at the asparagine residue. E1 contains an identical N-glycan sequon at N5 (N-T-T). To circumvent the disruption of N-glycosylation at N5 by substitution of T7, we engineered the T6F mutation. The caveat to this approach is that the introduction of a hydrophobic residue within an N-glycan consensus site reduces the N-glycosylation efficiency of T6F peptides. This effect is evident in the presence of multiple mature glycosylated forms of T6F. Less severe hydrophobic mutations, T6A and T7A, prevent O-glycosylation only at T6 or T7 respectively (Hamby and Hirst 2008). We then used enzymatic deglycosylation of the T6A and T7A mutants to determine which site

specifically acquires O-glycans (Fig. 4.6). Enzymatic deglycosylation reveals that both T6 and T7 acquire O-glycans; however, T7 appears to be the predominately modified site. It is interesting to note the proximity of the N- and O-glycan attachment sites in E1. One of the two threonine residues considered to be involved in O-glycan linkage is also part of an N-glycosylation consensus sequence (T7). It appears that there is no spatial interference on the attachment of O-glycans in the presence of N-glycans as we observe that mature E1 peptides efficiently acquire O-glycans. Previous work done on the mouse hepatitis virus membrane protein showed that O-glycosylation occurs efficiently on the hydroxylamino acid of an exogenously introduced N-glycosylation site (de Haan et al. 1998). The prior addition of N-glycans to the protein does not impede subsequent addition of O-glycans. It is likely that the positioning of O-glycans within the conserved N-glycan sequon contributes to the structural integrity of the N-terminus of E1 peptide. O-glycans are also involved in proper cell surface expression of proteins like Glycophorin A (Remaley et al. 1991), so their presence might contribute to the overall protein stability and expression of E1 peptides.

The necessary desialylation of O-glycans on E1 to facilitate O-glycosidase hydrolysis establishes the predominance of sialic acid sugars on a majority of O-glycans on E1. The importance of sialic acid moieties in Na^+ channel function has been determined. Ufret-Vincenty et al. established that the glycosylation state of the cardiac sodium channel affected both the current density and voltage-dependence of channel conductance (Ufret-Vincenty et al. 2001). Neuraminidase digestion of terminal sialic

acids from N-glycans present on Na^+ channels reduced the overall measured current density and elicited a positive shift in the midpoint of activation.

Unlike Na^+ channels, Q1 channels do not acquire any kind of glycosylation. Therefore, any predicted effect of glycosylation on channel trafficking and function would be a result of changes to N- or O-glycans on E1. We then determined whether O-glycans on E1 had an effect on Q1/E1 channel trafficking by comparing the cell surface distribution of wild type Q1/E1 to Q1/T6F complexes (Fig. 4.7). We observed no significant difference in the percentage of biotinylated wild type or mutant E1 peptides. We also observed no significant effect from the lack of O-glycans on channel function by comparing biophysical parameters such as voltage sensitivity and midpoint of activation between the wild type and mutant channels. These observations strongly suggest that the O-glycans on E1 do not exert any effect on channel modulation. .

The discovery of a novel post-translational modification, O-linked glycosylation, on E1 peptides enhances our understanding of how glycosylation plays an important role in the stability and trafficking of E1 peptides. Since this modification has only been identified in E1 peptides so far, it would be interesting to determine whether other members of the KCNE peptide family acquire O-glycans. KCNE4 (E4) is the only other member of the KCNE family that possesses a hydroxylamino acid at the X-position within its N-terminal sequon. E4 transcripts are present in the heart and E4 peptides are thought to contribute to the generation of I_{Ks} currents (Lundquist et al. 2005; Morin and Kobertz 2007; Manderfield and George 2008). The presence of O-glycans on other

KCNE peptides would suggest a role for these glycans in the generation of assembly and trafficking-competent K^+ channel complexes that function in the heart.

EXPERIMENTAL PROCEDURES

MK24 cardiac lysates were generously provided by R. Kass. Lysates were prepared as previously described (Marx et al. 2002).

Plasmids and cDNAs—Human Q1 and E1 were subcloned into pcDNA3.1 (–) (Invitrogen). All E1 constructs (wild type and chimeras) contained a C-terminal HA (YPYDVPDYA) epitope tag attached to the C-terminus of E1 through an SGSG linker. Chimeras of E1 and E3 were generated by cassette mutagenesis. The T6A, T6F and T7A point mutations were introduced into E1 using QuikChange ® site-directed mutagenesis (Stratagene).

Cell Culture and Transfections—Chinese Hamster Ovary-K1 (CHO) cells were cultured in F-12K nutrient mixture (Invitrogen), supplemented with 10% fetal bovine serum (Hyclone) and 100 units/ml penicillin/streptomycin (Invitrogen). Cells were plated at 60–75% confluency in 35-mm dishes. After 24 h, the cells were transiently transfected at room temperature (RT) with Lipofectamine (Invitrogen) 8 μl per mL of Opti-MEM (Gibco-Invitrogen) and returned to fresh culture media after 6 h. DNA ratios (in μg): E1/empty pcDNA 3.1 plasmid: 1.5/0.75; Q1/E1, Q1/T6F or Q1/chimeras: 0.75/1.5. Cells were lysed 48 h post-transfection for Western Blot analysis.

Cell Lysis and Western Blot Analysis—The cells were washed in ice-cold PBS (3 x 2 ml) and lysed at 4°C in RIPKA lysis buffer (10 mM Tris·HCl, pH 7.4, 140 mM NaCl, 10 mM KCl, 1 mM EDTA, 1% Triton X-100, 0.1% SDS, 1% sodium deoxycholate), supplemented with protease inhibitors, 1 mM phenylmethylsulfonyl fluoride, and 1 μg/ml

each of leupeptin, pepstatin, and aprotinin. For expression gels, CHO cells were lysed in 250 µl of RIPKA buffer. Cell debris was pelleted in a microcentrifuge (16,100 x *g* for 10 min at room temperature). The supernatants were diluted with SDS-PAGE loading buffer containing 100 mM dithiothreitol, separated on a 15% SDS polyacrylamide gel, and transferred to nitrocellulose (0.2 µ; Schleicher & Schuell). The membranes were blocked in blocking buffer (5% nonfat dry milk in Tris-buffered saline containing 0.2% Tween-20 (TBS-T)) for 30 min at RT and then incubated with rat anti-HA (Roche Applied Science) (1:750) in blocking buffer overnight at 4°C. For MK24 lysates, blots were incubated with rabbit anti-Q1 (Sigma) (1:1000) in blocking buffer for 2 h at RT. The membranes were washed in TBS-T (4 x 5 min) and incubated with goat anti-rat horseradish peroxidase-conjugated antibody (Santa Cruz Biotechnology, Inc.) (1:2000) or goat anti-rabbit horseradish peroxidase-conjugated antibody (Cell Signaling Technology) (1:3000) in blocking buffer for 30 min at RT. The membranes were subsequently washed with TBS-T (4 x 5 min). Horseradish peroxidase-bound proteins were detected by chemiluminescence using SuperSignal West Dura Extended Duration Substrate (Pierce) and a Fujifilm LAS-3000 CCD camera.

Enzymatic Deglycosylation Analysis—Cell lysates (30 µl) were digested with Endo H_f (3 µl) or PNGase F (3 µl) (New England BioLabs, Inc.) or an enzyme cocktail containing PNGase F/neuraminidase/O-glycosidase (3 µl/3 µl/1 µl) for 1 h at 37°C (Neuraminidase; O-glycosidase: Roche). The samples were then raised to 100 mM dithiothreitol and 3.5% SDS before resolving by SDS-PAGE (15% gel) and analyzed by Western blot.

Enzymatic deglycosylation of MK24 cardiac lysates—MK24 lysates (20 μl) were digested with Endo H_f (5 μl) or PNGase F (5 μl) or an enzyme cocktail containing PNGase F/neuraminidase/O-glycosidase (5 μl/5 μl/5 μl) for 1 h at 37°C. Lysates were raised to 100 mM dithiothreitol and 5% SDS before resolving by SDS-PAGE (6% gel) and analyzed by Western blot.

Cell Surface Biotinylation—Cells were rinsed with ice cold PBS^{2+} buffer (four times with 2 ml; PBS containing 1 mM $MgCl_2$, 0.1 mM $CaCl_2$) at 4°C to arrest membrane internalization. The cells were then incubated with 1 mg/ml sulfo-NHS-SS-biotin (Pierce) in PBS^{2+} buffer twice for 15 min at 4°C. To quench the excess biotinylation reagent, the cells were washed quickly (three times with 2 ml) with quench solution (PBS^{2+} containing 100 mM glycine) and then incubated with quench solution twice for 15 min at 4°C. The cells were lysed in RIPKA buffer for 30 min at 4°C. Cell debris was removed by centrifugation (16,100 x *g* for 10 min at 4°C). Total protein in each sample was quantitated by BCA analysis. Of these samples, 75 μg of total protein was separated by affinity chromatography on 25 μl of Immunopure® immobilized streptavidin beads (Pierce) overnight at 4°C, whereas 15 μg was saved as an input control to determine the percentage of biotinylated proteins. The beads were washed (three times with 500 μl) in 0.1% SDS wash buffer (10 mM Tris·HCl, pH 7.4, 150 mM NaCl, 1 mM EDTA, 0.1% SDS). Biotinylated proteins were eluted from the beads using 2xSDS-PAGE loading buffer with 200 mM dithiothreitol for 15 min at 55°C. The inputs and eluted proteins were resolved by SDS-PAGE (15% gel) and analyzed by Western blot. The images of nonsaturated bands were captured on a Fujifilm LAS-3000 CCD camera, and the band

intensities were quantitated using MultiGauge V2.1 software (FujiFilm). An ER-resident protein, calnexin, was used as a control to determine the percentage of cell rupture that occurred during the labeling process. Background cell lysis was quantitated as a ratio of biotinylated calnexin protein to total input calnexin. The percentage of E1 protein on the cell surface was calculated from the ratio of avidin-bound protein to total input protein after background lysis subtraction.

Perforated Patch Whole-Cell Recordings—For electrophysiological experiments, CHO-K1 cells were transiently transfected (in μg per dish) with 0.75 Q1 (wt) and 1.5 E1 (wt or mutant) plus 0.25 pEGFP-C3. Cells were used 24-48 h post-transfection. Currents were recorded in the standard whole-cell perforated patch configuration as described (Lvov et al. 2010). Briefly, on the day of the experiment, cells were seeded onto glass coverslips and placed in a recording chamber filled with *extracellular solution* containing (in mM): 160 NaCl, 2.5 KCl, 2 $CaCl_2$, 1 $MgCl_2$, 8 glucose, and 10 HEPES (pH 7.5 with NaOH). For the perforated patch configuration, a glass electrode (pipette resistance: 2.5-3.5 MΩ) filled with *electrode solution* containing (in mM): 126 KCl, 1 $MgSO_2$, 0.5 $CaCl_2$, 5 EGTA, 4 K_2-ATP, 0.4 GTP, 25 HEPES (pH 7.5 with CsOH), and 60 μg/ml Amphotericin B (Sigma; prepared in DMSO) was attached to the transfected (eGFP-expressing) cell. Electrical access to the inside of the cell was monitored using 3-s depolarizing test pulse from the holding potential of -80 mV to +20 mV taken every 15 s. Once the access resistance was dropped to a level suitable to record the membrane potential (<10 MΩ), I_{Ks} currents were assayed for native-like function using a pulse protocol to generate a

family of traces as described in Figure legend 4.8. All measurements were performed at room temperature (24 ± 2°C).

CONCLUSIONS

The work presented in this thesis determined the significance of the correct assembly and trafficking of KCNQ1/KCNE1 (Q1/E1) channel complexes for their proper physiological function. Our observations explain how deficiencies in the biosynthesis of K^+ channel complexes, either by impaired assembly or aberrant trafficking, can be correlated to Long QT Syndrome. In Chapter II, we described how the forward trafficking and efficient cell surface expression of KCNE1 (E1) peptides was dependent on co-expression of KCNQ1 (Q1) channels. Our observations helped to explain conflicting observations about the trafficking of E1 peptides and confirmed the endoplasmic reticulum (ER) as the cellular location for Q1/E1 complex formation (Krumerman et al. 2004; Chandrasekhar et al. 2006).

Glycosylation has been shown to be important in the expression, stability and trafficking of K^+ ion channels such as Shaker and hERG (Petrecca et al. 1999; Gong et al. 2002; Khanna et al. 2004). N-glycosylation of these channels increases the overall stability of individual subunits promoting efficient folding and assembly into functional channels that traffic to the cell surface. Since Q1 does not acquire glycosylation, any predicted effects of glycosylation on channel function would be due to the presence of glycans on the KCNE β-subunits. In Chapter III, we determined the importance of the conserved N-terminal glycosylation sites in E1 peptides in generating correctly functioning Q1/E1 channel complexes. Glycosylation did not significantly impact protein stability of E1 peptides as measured by the kinetics of decay of wild type and

glycosylation-deficient E1 peptides. However, glycosylation of E1 did influence the forward trafficking of Q1/E1 complexes and their function at the cell surface. Our observations in Chapter III suggest a novel mechanism by which glycosylation deficiency promotes Q1/E1 channel dysfunction. These findings can be applied to investigate the mechanism of co- and post-translational glycosylation of other KCNE peptides. For instance, since KCNE3 has three putative sequons, which sites acquire N-glycans co- or post-translationally? In contrast, KCNE4 (E4) has only one putative sequon. Does interruption of N-glycosylation of E4 affect its stability and ability to associate efficiently with K^+ channels?

The presence of O-glycan modifications on E1 is a novel discovery for ion channel proteins. In Chapter IV, we determined potential O-glycan linkage sites at two threonine residues (T6 and T7) located within a highly conserved N-glycan sequon. Other studies have demonstrated the functional importance of sialylated glycans on cardiac Na_v ion channels and their associated β1 subunits (Ufret-Vincenty et al. 2001; Johnson et al. 2004). Biochemical and electrophysiological studies were used to determine whether O-glycan deficiency impairs efficient Q1/E1 complex trafficking and plasma membrane localization. The proximity of N- and O-glycans could imply a cooperative effect by both modifications on the stability and trafficking of Q1/E1 complexes. Similar to E1, sequence analysis of the KCNE family revealed that E4 contains hydroxylamino acids within its N-terminal sequon that are predicted to acquire O-glycans. RT-PCR analysis shows that E4 transcripts are abundantly expressed in the human heart (Bendahhou et al. 2005; Lundquist et al. 2005). E4 peptides can also associate with Q1/E1 channel

complexes to contribute to I_{Ks} currents (Morin and Kobertz 2007). Taken together, these observations suggest a potential role for sialylated O-glycans on KCNE peptides in the maintenance of cardiac rhythm.

FUTURE DIRECTIONS

Does the processing and trafficking of KCNE peptides in native cells mimic our observations in over-expression systems?

While we have used epitope-tagged constructs in over-expression cell systems for the biochemical characterization of KCNE1 (E1) peptides, it would be advantageous to examine the trafficking and biosynthetic processing of K^+ channel complexes in their native environments. The lack of good-quality commercially-available native antibodies presents a challenge to the investigation of KCNE peptides in native cells.

One alternative approach could be to use the presence of glycan modifications on KCNE peptides to investigate their glycosylation states, cell surface expression and association with K^+ channel partners. Previous work in the lab has shown the feasibility of incorporating non-native sugars into N-glycans on KCNE peptides. Using thiol-derivatized acylated sialic acid as precursors, we can exploit the native cellular processing of sugars to guide the incorporation of this non-native sugar into N- and possibly O-glycans attached to KCNE peptides. The incorporation would introduce a thiol group on the sugar that can be chemically modified by labeling with different probes specific for K^+ channel/KCNE complexes.

Are other KCNE peptides glycosylated co- or post-translationally?

N-glycosylation is a post-translational modification common to all members of the KCNE family, particularly at the conserved N-terminal sequon. The study of co- and post-translational glycosylation of E1 in Chapter III prompts the question of whether other KCNE peptides acquire co- and post-translational N-glycosylation and the relevance to disease. How does the T8A mutation in KCNE2 (E2) impact assembly and trafficking of the peptide in a channel complex? Does the T8A mutation impact glycosylation of the other site in E2? We could examine these questions using kinetic analyses similar to those in Chapter III.

Since transcripts for all the KCNEs have been identified in the heart, we could determine the impact of glycosylation deficiency on the efficiency of channel complex assembly. Does the interruption of glycosylation of KCNE1 peptides improve KCNQ1 channel assembly with other KCNEs? This could have serious implications in cardiac tissue where generation of I_{Ks} current is important.

Are O-glycan modifications present on other KCNE peptides? Is there a functional role for O-glycans in K^+ channel modulation?

Preliminary electrophysiological recordings of O-glycan deficient Q1/E1 channel complexes showed no significant change in currents compared to wild type Q1/E1 channel complexes. Additionally, biochemical analysis by cell surface biotinylation of

Q1/E1 complexes revealed that there is no trafficking defect associated with O-glycan deficiency.

Similar to E1, KCNE4 (E4) possesses hydroxylamino residues within its N-terminal sequon. We could determine whether O-glycans are present on E4 peptides. Using biochemical and electrophysiological techniques, we could determine the role of O-glycans in the assembly, trafficking and function of E4/K^+ channel complexes, particularly the heteromeric complex of Q1/E1/E4 which has been shown to generate I_{Ks} currents (Morin and Kobertz 2007). We could investigate functional effects of O-glycans by the enzymatic deglycosylation of CHO cells expressing Q1/E1/E4 channel complexes and subsequent patch clamp of the cells. It would also be interesting to determine whether the presence of wild type E4 had an effect on the assembly of O-glycan deficient E1 (T6F) in a heteromeric complex with Q1 channels and could rescue the reduction in current that we observe with Q1/T6F complexes. The presence of O-glycans on E4 peptides could suggest a potential role for sialic acid modifications in the proper trafficking and function of K^+ channel/KCNE complexes in the heart.

In all, the work done in this thesis examining the assembly and trafficking of a specific K^+ channel/KCNE complex extends the understanding of how the efficient biosynthetic processing of ion channel complexes is important in their proper physiological function. Additionally, the post-translational modifications on KCNE peptides have been implicated in disease and suggest novel mechanisms for ion channel dysfunction. Our biochemical investigation of KCNQ1/KCNE1 K^+ channel complexes

prompts questions that can enhance our understanding of the mechanisms responsible for ion channel disease.

BIBLIOGRAPHY

Ackerman, M. J. and D. E. Clapham (1997). "Ion channels--basic science and clinical disease." N Engl J Med **336**(22): 1575-86.

Ackerman, M. J., D. J. Tester, et al. (2003). "Ethnic differences in cardiac potassium channel variants: implications for genetic susceptibility to sudden cardiac death and genetic testing for congenital long QT syndrome." Mayo Clin Proc **78**(12): 1479-87.

Angelo, K., T. Jespersen, et al. (2002). "KCNE5 induces time- and voltage-dependent modulation of the KCNQ1 current." Biophys J **83**(4): 1997-2006.

Bal, M., J. Zhang, et al. (2008). "Homomeric and heteromeric assembly of KCNQ (Kv7) K+ channels assayed by total internal reflection fluorescence/fluorescence resonance energy transfer and patch clamp analysis." J Biol Chem **283**(45): 30668-76.

Barhanin, J., F. Lesage, et al. (1996). "K(V)LQT1 and lsK (minK) proteins associate to form the I(Ks) cardiac potassium current." Nature **384**(6604): 78-80.

Bause, E. (1983). "Structural requirements of N-glycosylation of proteins. Studies with proline peptides as conformational probes." Biochem J **209**(2): 331-6.

Ben-Dor, S., N. Esterman, et al. (2004). "Biases and complex patterns in the residues flanking protein N-glycosylation sites." Glycobiology **14**(2): 95-101.

Bendahhou, S., C. Marionneau, et al. (2005). "In vitro molecular interactions and distribution of KCNE family with KCNQ1 in the human heart." Cardiovasc Res **67**(3): 529-38.

Bianchi, L., S. M. Kwok, et al. (2003). "A potassium channel-MiRP complex controls neurosensory function in Caenorhabditis elegans." J Biol Chem **278**(14): 12415-24.

Bianchi, L., Z. Shen, et al. (1999). "Cellular dysfunction of LQT5-minK mutants: abnormalities of IKs, IKr and trafficking in long QT syndrome." Hum Mol Genet **8**(8): 1499-507.

Bolt, G., C. Kristensen, et al. (2005). "Posttranslational N-glycosylation takes place during the normal processing of human coagulation factor VII." Glycobiology **15**(5): 541-7.

Burda, P. and M. Aebi (1999). "The dolichol pathway of N-linked glycosylation." Biochim Biophys Acta **1426**(2): 239-57.

Casimiro, M. C., B. C. Knollmann, et al. (2001). "Targeted disruption of the Kcnq1 gene produces a mouse model of Jervell and Lange-Nielsen Syndrome." Proc Natl Acad Sci U S A **98**(5): 2526-31.

Chandrasekhar, K. D., T. Bas, et al. (2006). "KCNE1 subunits require co-assembly with K+ channels for efficient trafficking and cell surface expression." J Biol Chem **281**(52): 40015-23.

Charlier, C., N. A. Singh, et al. (1998). "A pore mutation in a novel KQT-like potassium channel gene in an idiopathic epilepsy family." Nat Genet **18**(1): 53-5.

Chen, H., L. A. Kim, et al. (2003). "Charybdotoxin binding in the I(Ks) pore demonstrates two MinK subunits in each channel complex." Neuron **40**(1): 15-23.

Cheung, J. C. and R. A. Reithmeier (2007). "Scanning N-glycosylation mutagenesis of membrane proteins." Methods **41**(4): 451-9.

Chiang, C. E. and D. M. Roden (2000). "The long QT syndromes: genetic basis and clinical implications." J Am Coll Cardiol **36**(1): 1-12.

Chouabe, C., N. Neyroud, et al. (1997). "Properties of KvLQT1 K+ channel mutations in Romano-Ward and Jervell and Lange-Nielsen inherited cardiac arrhythmias." EMBO J **16**(17): 5472-9.

Cooper, E. C. and L. Y. Jan (2003). "M-channels: neurological diseases, neuromodulation, and drug development." Arch Neurol **60**(4): 496-500.

de Haan, C. A., P. Roestenberg, et al. (1998). "Structural requirements for O-glycosylation of the mouse hepatitis virus membrane protein." J Biol Chem **273**(45): 29905-14.

Deschenes, I. and G. F. Tomaselli (2002). "Modulation of Kv4.3 current by accessory subunits." FEBS Lett **528**(1-3): 183-8.

Dilly, K. W., J. Kurokawa, et al. (2004). "Overexpression of beta2-adrenergic receptors cAMP-dependent protein kinase phosphorylates and modulates slow delayed rectifier potassium channels expressed in murine heart: evidence for receptor/channel co-localization." J Biol Chem **279**(39): 40778-87.

Do, H., D. Falcone, et al. (1996). "The cotranslational integration of membrane proteins into the phospholipid bilayer is a multistep process." Cell **85**(3): 369-78.

Duggal, P., M. R. Vesely, et al. (1998). "Mutation of the gene for IsK associated with both Jervell and Lange-Nielsen and Romano-Ward forms of Long-QT syndrome." Circulation **97**(2): 142-6.

Duvet, S., A. Op De Beeck, et al. (2002). "Glycosylation of the hepatitis C virus envelope protein E1 occurs posttranslationally in a mannosylphosphoryldolichol-deficient CHO mutant cell line." Glycobiology **12**(2): 95-101.

Ellgaard, L. and A. Helenius (2001). "ER quality control: towards an understanding at the molecular level." Curr Opin Cell Biol **13**(4): 431-7.

Ellgaard, L. and A. Helenius (2003). "Quality control in the endoplasmic reticulum." Nat Rev Mol Cell Biol **4**(3): 181-91.

Finley, M. R., Y. Li, et al. (2002). "Expression and coassociation of ERG1, KCNQ1, and KCNE1 potassium channel proteins in horse heart." Am J Physiol Heart Circ Physiol **283**(1): H126-38.

Folander, K., J. S. Smith, et al. (1990). "Cloning and expression of the delayed-rectifier IsK channel from neonatal rat heart and diethylstilbestrol-primed rat uterus." Proc Natl Acad Sci U S A **87**(8): 2975-9.

Franqueza, L., M. Lin, et al. (1999). "Long QT syndrome-associated mutations in the S4-S5 linker of KvLQT1 potassium channels modify gating and interaction with minK subunits." J Biol Chem **274**(30): 21063-70.

Gage, S. D. and W. R. Kobertz (2004). "KCNE3 truncation mutants reveal a bipartite modulation of KCNQ1 K+ channels." J Gen Physiol **124**(6): 759-71.

Gavel, Y. and G. von Heijne (1990). "Sequence differences between glycosylated and non-glycosylated Asn-X-Thr/Ser acceptor sites: implications for protein engineering." Protein Eng **3**(5): 433-42.

Gomez, M., S. J. Scales, et al. (2000). "Membrane recruitment of coatomer and binding to dilysine signals are separate events." J Biol Chem **275**(37): 29162-9.

Gong, Q., C. L. Anderson, et al. (2002). "Role of glycosylation in cell surface expression and stability of HERG potassium channels." Am J Physiol Heart Circ Physiol **283**(1): H77-84.

Gouas, L., C. Bellocq, et al. (2004). "New KCNQ1 mutations leading to haploinsufficiency in a general population; Defective trafficking of a KvLQT1 mutant." Cardiovasc Res **63**(1): 60-8.

Green, W. N. and O. S. Andersen (1991). "Surface charges and ion channel function." Annu Rev Physiol **53**: 341-59.

Grunnet, M., T. Jespersen, et al. (2002). "KCNE4 is an inhibitory subunit to the KCNQ1 channel." J Physiol **542**(Pt 1): 119-30.

Hamby, S. E. and J. D. Hirst (2008). "Prediction of glycosylation sites using random forests." BMC Bioinformatics **9**: 500.

Harmer, S. C., A. J. Wilson, et al. (2010). "Mechanisms of disease pathogenesis in long QT syndrome type 5." Am J Physiol Cell Physiol **298**(2): C263-73.

Heinrich, S. U., W. Mothes, et al. (2000). "The Sec61p complex mediates the integration of a membrane protein by allowing lipid partitioning of the transmembrane domain." Cell **102**(2): 233-44.

Helenius, A. and M. Aebi (2001). "Intracellular functions of N-linked glycans." Science **291**(5512): 2364-9.

Helenius, A. and M. Aebi (2004). "Roles of N-linked glycans in the endoplasmic reticulum." Annu Rev Biochem **73**: 1019-49.

Hershey, J. W. (1991). "Translational control in mammalian cells." Annu Rev Biochem **60**: 717-55.

Hirschberg, C. B., P. W. Robbins, et al. (1998). "Transporters of nucleotide sugars, ATP, and nucleotide sulfate in the endoplasmic reticulum and Golgi apparatus." Annu Rev Biochem **67**: 49-69.

Hoppe, U. C., E. Marban, et al. (2001). "Distinct gene-specific mechanisms of arrhythmia revealed by cardiac gene transfer of two long QT disease genes, HERG and KCNE1." Proc Natl Acad Sci U S A **98**(9): 5335-40.

Jervell, A. and F. Lange-Nielsen (1957). "Congenital deaf-mutism, functional heart disease with prolongation of the Q-T interval and sudden death." Am Heart J **54**(1): 59-68.

Jespersen, T., M. Grunnet, et al. (2005). "The KCNQ1 potassium channel: from gene to physiological function." Physiology (Bethesda) **20**: 408-16.

Jiang, B., X. Sun, et al. (2002). "Endogenous Kv channels in human embryonic kidney (HEK-293) cells." Mol Cell Biochem **238**(1-2): 69-79.

Johnson, D., M. L. Montpetit, et al. (2004). "The sialic acid component of the beta1 subunit modulates voltage-gated sodium channel function." J Biol Chem **279**(43): 44303-10.

Julenius, K., A. Molgaard, et al. (2005). "Prediction, conservation analysis, and structural characterization of mammalian mucin-type O-glycosylation sites." Glycobiology **15**(2): 153-64.

Kang, C., C. Tian, et al. (2008). "Structure of KCNE1 and implications for how it modulates the KCNQ1 potassium channel." Biochemistry **47**(31): 7999-8006.

Kasturi, L., H. Chen, et al. (1997). "Regulation of N-linked core glycosylation: use of a site-directed mutagenesis approach to identify Asn-Xaa-Ser/Thr sequons that are poor oligosaccharide acceptors." Biochem J **323 (Pt 2)**: 415-9.

Khanna, R., E. J. Lee, et al. (2004). "Transient calnexin interaction confers long-term stability on folded K+ channel protein in the ER." J Cell Sci **117**(Pt 14): 2897-908.

Khanna, R., M. P. Myers, et al. (2001). "Glycosylation increases potassium channel stability and surface expression in mammalian cells." J Biol Chem **276**(36): 34028-34.

Kolhekar, A. S., A. S. Quon, et al. (1998). "Post-translational N-glycosylation of a truncated form of a peptide processing enzyme." J Biol Chem **273**(36): 23012-8.

Krumerman, A., X. Gao, et al. (2004). "An LQT mutant minK alters KvLQT1 trafficking." Am J Physiol Cell Physiol **286**(6): C1453-63.

Kubisch, C., B. C. Schroeder, et al. (1999). "KCNQ4, a novel potassium channel expressed in sensory outer hair cells, is mutated in dominant deafness." Cell **96**(3): 437-46.

Lai, L. P., Y. N. Su, et al. (2005). "Denaturing high-performance liquid chromatography screening of the long QT syndrome-related cardiac sodium and potassium channel genes and identification of novel mutations and single nucleotide polymorphisms." J Hum Genet **50**(9): 490-6.

Lambert, C. and R. Prange (2007). "Posttranslational N-glycosylation of the hepatitis B virus large envelope protein." Virol J **4**: 45.

Larsen, L. A., P. S. Andersen, et al. (2001). "Screening for mutations and polymorphisms in the genes KCNH2 and KCNE2 encoding the cardiac HERG/MiRP1 ion channel: implications for acquired and congenital long Q-T syndrome." Clin Chem **47**(8): 1390-5.

Lee, M. P., J. D. Ravenel, et al. (2000). "Targeted disruption of the Kvlqt1 gene causes deafness and gastric hyperplasia in mice." J Clin Invest **106**(12): 1447-55.

Lemp, D., A. Haselbeck, et al. (1990). "Molecular cloning and heterologous expression of N-glycosidase F from Flavobacterium meningosepticum." J Biol Chem **265**(26): 15606-10.

Lerche, C., C. R. Scherer, et al. (2000). "Molecular cloning and functional expression of KCNQ5, a potassium channel subunit that may contribute to neuronal M-current diversity." J Biol Chem **275**(29): 22395-400.

Letts, V. A., A. Valenzuela, et al. (2000). "A new spontaneous mouse mutation in the Kcne1 gene." Mamm Genome **11**(10): 831-5.

Lewis, A., Z. A. McCrossan, et al. (2004). "MinK, MiRP1, and MiRP2 diversify Kv3.1 and Kv3.2 potassium channel gating." J Biol Chem **279**(9): 7884-92.

Lu, Y., M. P. Mahaut-Smith, et al. (2003). "Mutant MiRP1 subunits modulate HERG K+ channel gating: a mechanism for pro-arrhythmia in long QT syndrome type 6." J Physiol **551**(Pt 1): 253-62.

Lundquist, A. L., L. J. Manderfield, et al. (2005). "Expression of multiple KCNE genes in human heart may enable variable modulation of I(Ks)." J Mol Cell Cardiol **38**(2): 277-87.

Lvov, A., S. D. Gage, et al. (2010). "Identification of a protein-protein interaction between KCNE1 and the activation gate machinery of KCNQ1." J Gen Physiol **135**(6): 607-18.

MacKinnon, R. (1991). "Determination of the subunit stoichiometry of a voltage-activated potassium channel." Nature **350**(6315): 232-5.

Manderfield, L. J. and A. L. George, Jr. (2008). "KCNE4 can co-associate with the I(Ks) (KCNQ1-KCNE1) channel complex." FEBS J **275**(6): 1336-49.

Marban, E. (2002). "Cardiac channelopathies." Nature **415**(6868): 213-8.

Marshall, R. D. (1972). "Glycoproteins." Annu Rev Biochem **41**: 673-702.

Marx, S. O., J. Kurokawa, et al. (2002). "Requirement of a macromolecular signaling complex for beta adrenergic receptor modulation of the KCNQ1-KCNE1 potassium channel." Science **295**(5554): 496-9.

McCormick, P. J., Y. Miao, et al. (2003). "Cotranslational protein integration into the ER membrane is mediated by the binding of nascent chains to translocon proteins." Mol Cell **12**(2): 329-41.

McCrossan, Z. A. and G. W. Abbott (2004). "The MinK-related peptides." Neuropharmacology **47**(6): 787-821.

McDonald, T. V., Z. Yu, et al. (1997). "A minK-HERG complex regulates the cardiac potassium current I(Kr)." Nature **388**(6639): 289-92.

Melman, Y. F., A. Domenech, et al. (2001). "Structural determinants of KvLQT1 control by the KCNE family of proteins." J Biol Chem **276**(9): 6439-44.

Melman, Y. F., S. Y. Um, et al. (2004). "KCNE1 binds to the KCNQ1 pore to regulate potassium channel activity." Neuron **42**(6): 927-37.

Morin, T. J. and W. R. Kobertz (2007). "A derivatized scorpion toxin reveals the functional output of heteromeric KCNQ1-KCNE K+ channel complexes." ACS Chem Biol **2**(7): 469-73.

Morin, T. J. and W. R. Kobertz (2008). "Counting membrane-embedded KCNE beta-subunits in functioning K+ channel complexes." Proc Natl Acad Sci U S A **105**(5): 1478-82.

Napolitano, C., S. G. Priori, et al. (2005). "Genetic testing in the long QT syndrome: development and validation of an efficient approach to genotyping in clinical practice." JAMA **294**(23): 2975-80.

Neyroud, N., F. Tesson, et al. (1997). "A novel mutation in the potassium channel gene KVLQT1 causes the Jervell and Lange-Nielsen cardioauditory syndrome." Nat Genet **15**(2): 186-9.

Nicolas, M., D. Dememes, et al. (2001). "KCNQ1/KCNE1 potassium channels in mammalian vestibular dark cells." Hear Res **153**(1-2): 132-45.

Nilsson, I. and G. von Heijne (2000). "Glycosylation efficiency of Asn-Xaa-Thr sequons depends both on the distance from the C terminus and on the presence of a downstream transmembrane segment." J Biol Chem **275**(23): 17338-43.

Nilsson, I. M. and G. von Heijne (1993). "Determination of the distance between the oligosaccharyltransferase active site and the endoplasmic reticulum membrane." J Biol Chem **268**(8): 5798-801.

Palmer, D. J., J. B. Helms, et al. (1993). "Binding of coatomer to Golgi membranes requires ADP-ribosylation factor." J Biol Chem **268**(16): 12083-9.

Papazian, D. M. (1999). "Potassium channels: some assembly required." Neuron **23**(1): 7-10.

Papazian, D. M., T. L. Schwarz, et al. (1987). "Cloning of genomic and complementary DNA from Shaker, a putative potassium channel gene from Drosophila." Science **237**(4816): 749-53.

Park, K. H., S. M. Kwok, et al. (2003). "N-Glycosylation-dependent block is a novel mechanism for drug-induced cardiac arrhythmia." FASEB J **17**(15): 2308-9.

Petrecca, K., R. Atanasiu, et al. (1999). "N-linked glycosylation sites determine HERG channel surface membrane expression." J Physiol **515 (Pt 1)**: 41-8.

Pusch, M., R. Magrassi, et al. (1998). "Activation and inactivation of homomeric KvLQT1 potassium channels." Biophys J **75**(2): 785-92.

Remaley, A. T., M. Ugorski, et al. (1991). "Expression of human glycophorin A in wild type and glycosylation-deficient Chinese hamster ovary cells. Role of N- and O-linked glycosylation in cell surface expression." J Biol Chem **266**(35): 24176-83.

Roden, D. M., J. R. Balser, et al. (2002). "Cardiac ion channels." Annu Rev Physiol **64**: 431-75.

Romano, C., G. Gemme, et al. (1963). "[Rare Cardiac Arrythmias of the Pediatric Age. Ii. Syncopal Attacks Due to Paroxysmal Ventricular Fibrillation. (Presentation of 1st Case in Italian Pediatric Literature)]." Clin Pediatr (Bologna) **45**: 656-83.

Romey, G., B. Attali, et al. (1997). "Molecular mechanism and functional significance of the MinK control of the KvLQT1 channel activity." J Biol Chem **272**(27): 16713-6.

Roth, J., D. J. Taatjes, et al. (1986). "Differential subcompartmentation of terminal glycosylation in the Golgi apparatus of intestinal absorptive and goblet cells." J Biol Chem **261**(30): 14307-12.

Ruiz-Canada, C., D. J. Kelleher, et al. (2009). "Cotranslational and posttranslational N-glycosylation of polypeptides by distinct mammalian OST isoforms." Cell **136**(2): 272-83.

Sampson, K. J., C. Terrenoire, et al. (2008). "Adrenergic regulation of a key cardiac potassium channel can contribute to atrial fibrillation: evidence from an I Ks transgenic mouse." J Physiol **586**(2): 627-37.

Sanguinetti, M. C. (1999). "Dysfunction of delayed rectifier potassium channels in an inherited cardiac arrhythmia." Ann N Y Acad Sci **868**: 406-13.

Sanguinetti, M. C., M. E. Curran, et al. (1996). "Coassembly of K(V)LQT1 and minK (IsK) proteins to form cardiac I(Ks) potassium channel." Nature **384**(6604): 80-3.

Sanguinetti, M. C. and P. S. Spector (1997). "Potassium channelopathies." Neuropharmacology **36**(6): 755-62.

Schroeder, B. C., M. Hechenberger, et al. (2000). "KCNQ5, a novel potassium channel broadly expressed in brain, mediates M-type currents." J Biol Chem **275**(31): 24089-95.

Schroeder, B. C., C. Kubisch, et al. (1998). "Moderate loss of function of cyclic-AMP-modulated KCNQ2/KCNQ3 K+ channels causes epilepsy." Nature **396**(6712): 687-90.

Schroeder, B. C., S. Waldegger, et al. (2000). "A constitutively open potassium channel formed by KCNQ1 and KCNE3." Nature **403**(6766): 196-9.

Schulze-Bahr, E., Q. Wang, et al. (1997). "KCNE1 mutations cause jervell and Lange-Nielsen syndrome." Nat Genet **17**(3): 267-8.

Sesti, F., G. W. Abbott, et al. (2000). "A common polymorphism associated with antibiotic-induced cardiac arrhythmia." Proc Natl Acad Sci U S A **97**(19): 10613-8.

Shakin-Eshleman, S. H., S. L. Spitalnik, et al. (1996). "The amino acid at the X position of an Asn-X-Ser sequon is an important determinant of N-linked core-glycosylation efficiency." J Biol Chem **271**(11): 6363-6.

Shikano, S. and M. Li (2003). "Membrane receptor trafficking: evidence of proximal and distal zones conferred by two independent endoplasmic reticulum localization signals." Proc Natl Acad Sci U S A **100**(10): 5783-8.

Shim, S. H., M. Ito, et al. (2005). "Gene sequencing in neonates and infants with the long QT syndrome." Genet Test **9**(4): 281-4.

Silberstein, S. and R. Gilmore (1996). "Biochemistry, molecular biology, and genetics of the oligosaccharyltransferase." FASEB J **10**(8): 849-58.

Singh, N. A., C. Charlier, et al. (1998). "A novel potassium channel gene, KCNQ2, is mutated in an inherited epilepsy of newborns." Nat Genet **18**(1): 25-9.

Splawski, I., J. Shen, et al. (2000). "Spectrum of mutations in long-QT syndrome genes. KVLQT1, HERG, SCN5A, KCNE1, and KCNE2." Circulation **102**(10): 1178-85.

Splawski, I., K. W. Timothy, et al. (1997). "Molecular basis of the long-QT syndrome associated with deafness." N Engl J Med **336**(22): 1562-7.

Splawski, I., M. Tristani-Firouzi, et al. (1997). "Mutations in the hminK gene cause long QT syndrome and suppress IKs function." Nat Genet **17**(3): 338-40.

Takumi, T., K. Moriyoshi, et al. (1991). "Alteration of channel activities and gating by mutations of slow ISK potassium channel." J Biol Chem **266**(33): 22192-8.

Takumi, T., H. Ohkubo, et al. (1988). "Cloning of a membrane protein that induces a slow voltage-gated potassium current." Science **242**(4881): 1042-5.

Teixeira, M., S. Viengchareun, et al. (2006). "Functional IsK/KvLQT1 potassium channel in a new corticosteroid-sensitive cell line derived from the inner ear." J Biol Chem **281**(15): 10496-507.

Tempel, B. L., D. M. Papazian, et al. (1987). "Sequence of a probable potassium channel component encoded at Shaker locus of Drosophila." Science **237**(4816): 770-5.

Tinel, N., S. Diochot, et al. (2000). "KCNE2 confers background current characteristics to the cardiac KCNQ1 potassium channel." EMBO J **19**(23): 6326-30.

Tyson, J., L. Tranebjaerg, et al. (2000). "Mutational spectrum in the cardioauditory syndrome of Jervell and Lange-Nielsen." Hum Genet **107**(5): 499-503.

Ufret-Vincenty, C. A., D. J. Baro, et al. (2001). "Role of sodium channel deglycosylation in the genesis of cardiac arrhythmias in heart failure." J Biol Chem **276**(30): 28197-203.

Ufret-Vincenty, C. A., D. J. Baro, et al. (2001). "Differential contribution of sialic acid to the function of repolarizing K(+) currents in ventricular myocytes." Am J Physiol Cell Physiol **281**(2): C464-74.

Van den Steen, P., P. M. Rudd, et al. (1998). "Concepts and principles of O-linked glycosylation." Crit Rev Biochem Mol Biol **33**(3): 151-208.

Vetter, D. E., J. R. Mann, et al. (1996). "Inner ear defects induced by null mutation of the isk gene." Neuron **17**(6): 1251-64.

Wang, H. S., Z. Pan, et al. (1998). "KCNQ2 and KCNQ3 potassium channel subunits: molecular correlates of the M-channel." Science **282**(5395): 1890-3.

Wang, K. W. and S. A. Goldstein (1995). "Subunit composition of minK potassium channels." Neuron **14**(6): 1303-9.

Wang, Q., M. E. Curran, et al. (1996). "Positional cloning of a novel potassium channel gene: KVLQT1 mutations cause cardiac arrhythmias." Nat Genet **12**(1): 17-23.

Wang, W., J. Xia, et al. (1998). "MinK-KvLQT1 fusion proteins, evidence for multiple stoichiometries of the assembled IsK channel." J Biol Chem **273**(51): 34069-74.

Wangemann, P. (2002). "K+ cycling and the endocochlear potential." Hear Res **165**(1-2): 1-9.

Ward, O. C. (1964). "A New Familial Cardiac Syndrome in Children." J Ir Med Assoc **54**: 103-6.

Weerapana, E. and B. Imperiali (2006). "Asparagine-linked protein glycosylation: from eukaryotic to prokaryotic systems." Glycobiology **16**(6): 91R-101R.

Wilson, A. J., K. V. Quinn, et al. (2005). "Abnormal KCNQ1 trafficking influences disease pathogenesis in hereditary long QT syndromes (LQT1)." Cardiovasc Res **67**(3): 476-86.

Wu, D. M., M. Jiang, et al. (2006). "KCNE2 is colocalized with KCNQ1 and KCNE1 in cardiac myocytes and may function as a negative modulator of I(Ks) current amplitude in the heart." Heart Rhythm **3**(12): 1469-80.

Wulff, H., N. A. Castle, et al. (2009). "Voltage-gated potassium channels as therapeutic targets." Nat Rev Drug Discov **8**(12): 982-1001.

Yamashita, F., M. Horie, et al. (2001). "Characterization and subcellular localization of KCNQ1 with a heterozygous mutation in the C terminus." J Mol Cell Cardiol **33**(2): 197-207.

Yang, W. P., P. C. Levesque, et al. (1998). "Functional expression of two KvLQT1-related potassium channels responsible for an inherited idiopathic epilepsy." J Biol Chem **273**(31): 19419-23.

Yoshikawa, F., Y. Sato, et al. (2008). "Opalin, a transmembrane sialylglycoprotein located in the central nervous system myelin paranodal loop membrane." J Biol Chem **283**(30): 20830-40.

Zerangue, N., B. Schwappach, et al. (1999). "A new ER trafficking signal regulates the subunit stoichiometry of plasma membrane K(ATP) channels." Neuron **22**(3): 537-48.

Zhang, M., M. Jiang, et al. (2001). "minK-related peptide 1 associates with Kv4.2 and modulates its gating function: potential role as beta subunit of cardiac transient outward channel?" Circ Res **88**(10): 1012-9.